Dottorato Industriale in “Tecnologie e Scienze per la Salute dell’Uomo”
Dipartimento Biomedico di Medicina Interna e Specialistica DIBIMIS
Settore Scientifico Disciplinare FIS/07

Advanced characterization of a fully human IgG1 therapeutic monoclonal antibody by structure-activity relationship studies

IL DOTTORE
Enrico Mazzarella

IL COORDINATORE
Ch.mo Prof. Maurizio Leone

IL TUTOR
Prof.ssa Valeria Vetri

IL TUTOR INDUSTRIALE
Dott. Cosimo - Walter D’Acunto

CICLO XXXIII
ANNO CONSEGUIMENTO TITOLO 2020/2021

Ph.D. Thesis

Ph.D. thesis by Enrico Mazzarella under the Industrial PhD programme. Supervised by Valeria Vetri (University of Palermo) and Cosimo Walter D'acunto (Merck Serono S.p.A., Rome, Italy; an affiliate of Merck KGaA, Darmstadt, Germany).

Contacts:

E.M.[1] +39 0774 350-527 enrico.mazzarella@merckgroup.com

V.V.[2] +39.091.23891782 valeria.vetri@unipa.it

W.D.[1] +39 0774 350389 walter.dacunto@merckgroup.com

[1] Analytical Development Biotech Department (ADB) Merck Serono S.p.A., Rome, Italy; an affiliate of Merck KGaA, Darmstadt, Germany. Via Luigi Einaudi 11, 00012 Guidonia Montecelio (Rome) - Italy

[2] Department of Physics and Chemistry, University of Palermo, Viale Delle Scienze ed. 18, 90128 Palermo - Italy

Table of contents

Table of figures

Abbreviations

ADCC	Antibody-Dependent Cell-mediated Cytotoxicity
ASN 1,2,3,4	Conventional code given to 4 Asparagine sites monitored in the study
CE/SDS	Capillary Electrophoresis – Sodium Dodecyl Sulfate
CMC	Chemical Manufacturing Control
CQA	Critical Quality Attribute
CV	Coefficient of Variation
DP	Drug product
DS	Drug Substance
EMA	European Medicine Agency
Fab	Fragment antigen-binding
FcRn	Neonatal Fc Receptor (PK indicator)
FDA	Food and Drug Administration agency
FLR	Fluorescence
GMP	Good Manufacturing Practices
HC	Heavy Chain
HMW	High Molecular Weight
IgG1	Immunoglobulin isotype G subclass 1
IP	Inflection Point
KD	Affinity Constant at equilibrium
kDa	kilo-Dalton
LC-MS	Liquid Chromatography – Mass Spectrometry
LC-MS/MS	Liquid Chromatography coupled to tandem Mass Spectrometry
LC	Light Chain
LMW	Low Molecular Weight
MALLS	Multi Angle Laser Light-scattering
MET 1,2,3,4	Conventional code given to 4 methionine sites monitored in the study
MoA	Mechanism of Action
MS	Mass Spectrometry
MW	Molecular Weight
Nano DSF	Differential Scanning Fluorimetry
NGHC	Non-Glycosylated Heavy Chain

NRED	Non-Reducing Conditions
OD	Optical Density
PD-1	Programmed Death protein-1
PD-L1	Programmed Death ligand-1
PMDA	Pharmaceutical and Medical Device Agency
RGA	Reporter gene assay
SAR	Structure-Activity Relationship

Preface and acknowledgments

This thesis highlights the work done from September 1st, 2017 to January 15th, 2021 by Enrico Mazzarella. The thesis is submitted to university of Palermo in fulfillment of the requirements for the Ph.D. degree. The work was done under the Industrial PhD programme in collaboration with Merck Serono S.p.A., Rome, Italy; an affiliate of Merck KGaA, Darmstadt, Germany.

The main part of the work was carried out at Analytical Development Biotech (Merck Serono S.p.A., Rome, Italy) where I really appreciated the help of my colleagues and managers from mine and other departments, since part of the project is also based on supportive data generated in their laboratories.

My academic tutor Prof. Valeria Vetri and my industrial supervisor Cosimo Walter D'Acunto are gratefully acknowledged for their support, in particular for the dedicated supervision I have received for writing this document. Also, I am obliged to my former managers Anna Rita Pezzotti and Mariagrazia Terlizzese for giving me the opportunity to apply for this Ph.D. programme.

Last but not least, I am very grateful to my family and to Serena, for their continuous support and for encouraging me to embark on this journey.

Rome, January 15th, 2021

Enrico Mazzarella

1 Summary

The scope of this Ph.D. thesis is the extended biological characterization of a therapeutic monoclonal antibody (mAb) directed against the programmed death ligand 1 (anti–PD-L1 mAb). The work is performed in the framework of an Industrial PhD program conducted by the University of Palermo and Merck Serono S.p.A., Rome, Italy; an affiliate of Merck KGaA, Darmstadt, Germany.

Programmed cell death protein-1 (PD-1; CD274) and its ligand Programmed death ligand-1 PD-L1 (PD-L1; CD274; B7-H1), are two transmembrane glycoproteins that play a physiological role in regulating the human immune response (1). However, under certain conditions, many cancer cells overexpressing PD-L1 exploit this biological axis as a strategy for eluding immune system and form tumors (2).

Anti–PD-L1 mAb belongs to the immune checkpoint inhibitors, a class of compounds that find application in the immune-oncology field. Being an IgG-based drug, it is a far more complex than a classical small molecule and a deep characterization is a key requirement for the maintenance of its structural and biological features. Such characteristics are commonly known as Critical Quality Attributes (CQAs). CQAs are defined as physical, chemical, biological or microbiological properties of the molecule that determine its quality profile, which are a result of product itself or dependent on manufacturing process (3). These properties must be guaranteed and kept under control throughout the entire biotechnological development program. However, since each lead compound is characterized by a unique quality profile, the latter must be first explored and then being monitored in routine.

In view of these premises, through the development of a tailored analytical panel and leveraging ad-hoc structure-activity relationship studies, here is proposed a strategy applicable to the in-depth biological characterization of a therapeutic Anti–PD-L1 mAb and, potentially, to similar new biological entities (NBEs).

Throughout this work, dedicated studies for the generation of Anti–PD-L1 specific variants and degraded products have been carried out. Then, orthogonal bioassay platforms have been exploited to evaluate the impact of these species on the anti–PD-L1 functional profile, biological behaviour and therapeutic efficacy. Among all the potential molecule functions, the following have been mainly investigated in this study: the ability of Anti–PD-L1 to bind its target PD-L1 and block the PD-1/PD-L1 interaction, the binding affinity towards the

main fragment crystallizable gamma receptors (FcγRs) (4), the affinity to the *in-vitro* Pharmacokinetic (PK) predictive indicator FcRn (5) and the Antibody-Dependent Cell-mediated Cytotoxicity (ADCC). At the same time, in order to support biological data, physico-chemical analysis has been also performed for the detection of molecule's structural elements.

The outcome of this work is a relevant information package concerning the Anti–PD-L1 mAb functional profile, reached by bridging biological data with detected structural characteristics. The consequence is an increased scientific knowledge with an impact on product value. Furthermore, the set-up of a proper analytical strategy shortens the times for submissions and market authorization, which translates into an ethical other than economic impact.

The main activities and results obtained in this work are:

1. Anti–PD-L1 mAb was confirmed to exert its activity through two main biological functions: it is able to bind its target PD-L1 while enhancing an ADCC activity via its Fc moiety. Furthermore, it was demonstrated that two typical IgG effector functions, antibody mediated cellular phagocytosis (ADCP) and complement dependent cytotoxicity (CDC), are not part of Anti-PD-L1 mAb mechanism of action (MoA).

   A forced degradation study performed at earlier stages of development, led to the definition of the main degradation pathways and to the preliminary assessment of Anti–PD-L1 CQAs. In this instance, the exposure of the antibody at 50° C for 2 and 4 weeks resulted considerably detrimental on its structure, leading to an overall increase of deamidation and oxidation of several residues together with the formation of high and low molecular weight species (HMW/LMW). Consequently, antibody functionality in terms of binding to the target PD-L1, FcγRIIIa (V158) and FcRn resulted affected. In the frame of this study, high pH and oxidative treatments were carried out as well. While these conditions did not extensively affect Anti–PD-L1 Fab binding towards its target PD-L1, Fc portion affinity for FcγRIIIa and FcRn, together with ADCC activity, resulted moderately impacted.
2. A critical asparagine site particularly prone to deamidation was identified. In order to elucidate its role on Anti–PD-L1 biological functions, a site-specific variant was obtained by substituting an asparagine (Asn, N) with an aspartic acid (Asp, D). This residue was located in one of the antibody's CDRs (complementary-determining regions) of the LC (light chain) loop. This sample showed similar biological properties

in terms of binding to the target PD-L1 and FcRn receptor when compared to an anti–PD-L1 mAb reference material. On the other hand, despite the antibody Fc portion affinity toward the FcγRIIIa resulted unmutated, the ADCC activity (generally enhanced following Fc-FcγRIIIa interaction) was slightly decreased, an event probably due to the overall structural stability.

3. During a biotechnological production process, HMWs (high molecule weights) and LMWs (low molecular weights) must be kept under control as these species may affect antibody functions. In order to study the effect of these degraded forms on Anti–PD-L1 mAb ability to block the PD-1/PD-L1 interaction, these species were isolated and purified from manufacturing. Then, samples containing different amounts of HMWs/LMWs were prepared and tested via cell-based blockade assay. Results proved that the presence of small amounts of both degraded forms were negatively correlated to the Anti–PD-L1 Fab functionality.
4. Finally, the effect of different N-Glycosylation patterns characterizing the biological properties of the Anti–PD-L1 Fc portion were also assessed. More specifically, binding affinity to the FcγRIIIa and ADCC activity were monitored via SPR and a cell-based reporter gene assay, respectively. Both activities resulted strongly enhanced in highly A-fucosylated and mannosylated samples. Moreover, through a dedicated correlation study, samples at different % of these forms were analyzed and threshold values at which these structural modifications significantly affected Anti–PD-L1 biological activity have been set up.

2 Introduction

2.1 Monoclonal antibodies as biotherapeutics

Monoclonal antibodies (mAbs) are immunoglobulins (Igs) produced from an identical immune cell derived from a single parental clone (6). Such molecules take advantage of their ability to recognize through the Fab portion a single epitope on an antigen (7), and such a characteristic make them appropriate therapeutic candidates.

MAbs for therapeutic purposes were first developed during the '70s from Hybridoma cell lines (8) and during last decades the plethora of published manuscripts and clinical studies have corroborated their application in medicine. Nowadays, many classes of chimeric humanized and fully humanized mAbs can be produced by recombinant DNA engineering technologies (9). As a result, mAbs are already representing a quarter of all drugs developed by biotech companies.

From a biochemical point of view, immunoglobulins are glycoproteins physiologically produced by activated B-cells. Among the different isotypes, immunoglobulin G (IgG) is the most abundant in human serum (10). In particular, subclass IgG1 is the most commonly used for medical treatments, due to its stability, less propensity to aggregate and for triggering several Fc-mediated effector functions such as ADCC, ADCP and CDC (11), (12). The architecture of a typical IgG1 together with representative examples of engineered mAbs are shown in Figure 1. In panel A, it is represented a typical IgG1 type mAb. It is composed of two light chains (CL; lambda or kappa) and two heavy chains (CH) of ca. 25 kDa and ca. 50 kDa respectively. These are connected by a disulfide bond, forming two heterodimers. Light chain contains a constant (CL) and a variable (VL) subdomains, while heavy chain one variable (VH) and three constant domains (CH1, CH2, CH3) (11). A central and flexible region containing two disulfide bonds, named “hinge”, crosslinks the CH1 and CH2 domains, leading to the typical “Y-shape” antibody conformation. A further subdivision is into two functional areas: two fragment antigen binding ($F(ab')_2$) domains, structurally subdivided as 3 complementarity determining regions (CDR1, CDR2 and CDR3) and one fragment crystallizable (Fc). In Panel B, examples of different engineered therapeutic mAbs are sketched. As well known, human anti-mouse antibody (HAMA) response (13), is an adverse reaction of host organism toward injected Abs. HAMA is triggered by immune cells following their interaction with non-human sequences and T cell epitopes contained in the injected mAb. Molecular engineering practices such as

chimerization, humanization and de-immunization are routinely performed to reduce this event. However, a fair compromise between a reduced immunogenicity and drug efficacy should be reached (14).

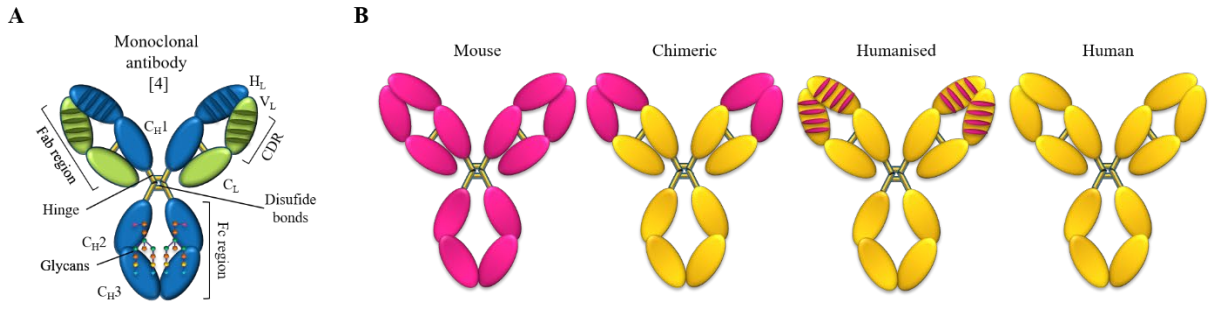

Figure 1 **Outline of an immunoglobulin structure and examples of engineered IgG-based mAbs.**

A. Schematic drawing of structural and functional areas of a typical IgG1 isotype **B.** Representative examples of different engineered therapeutic IgG-based mAbs.

Nowadays, therapeutic mAbs are largely used to treat a wide range of diseases and importantly, during last years, new encouraging research results together with a more thorough structural and functional characterization, led many pharmaceutical companies to develop more complex and potent bioproteins (Figure 2). Panel A shows a typical monoclonal antibody (mAb) that represent the ancestors of new generation Ig-based biotherapeutics (9), (11). In 2019, at least 570 therapeutic mAbs have been investigated in clinical trials (15), and 79 drug products have been approved by the United States Food and Drug Administration (US FDA) (16). Bi-specific and tri-specific mAbs (Figure 2 B, C), are a subclass of mAbs designed to recognize specific epitopes of the same, two or three different antigens. Their implementation is intended to improve both target specificity and therapeutic efficacy. Another emerging class of Ig-based therapeutics are represented by the Antibody-drug conjugates (ADCs) (Figure 2 D), which is currently one of the most complex, potent and promising class of drugs in the oncology field (8). Their structure consists of a classic mAb conjugated through a linker to a highly potent drug substance (payload). Following epitope recognition and subsequent internalization into targeted cell, the ADC is transported to the lysosome and processed, so that the pharmacologically active drug can be released to exert its cytotoxic effects on host cell. Recombinant fusion proteins (Figure 2 E), are proteins consisting of two or more moieties

encoded by different genes. These genes are previously joined, then transcribed and translated to produce a single polypeptide (17). Those intended for therapeutic purposes, are generally composed by a functional moiety directed against a specific target and an Ig-Fc portion triggering effector functions. Beyond these "classical" antibodies based on a typical Ig structure, alternative strategies have been designed with the aim of optimizing several therapeutic features such as stability, target accessibility and efficacy as well as reducing production costs. For example, Nanobodies (Figure 2 F) , also known as heavy-chain antibodies (hcAb), are a class of compounds firstly discovered in the sera of Camelidae (18). Being antibody fragments, the antigen-binding portion is reduced to a single variable domain (VHH). These are easier and cheaper to produce compared to large mAbs, and generally show high stability under different harsh conditions. Finally, another novel class of biotherapeutics to be mentioned are the Bi-specific and Tri-specific T-cell engager (BiTEs and TriTEs) (Figure 2 G), recombinant proteins formed by different single-chain variable fragments (scFvs) of individual antibodies. From a functional point of view, a moiety is able to target a cell-surface molecule on NK or T cells, while other portions, target antigens on the surface of malignant cells (19)

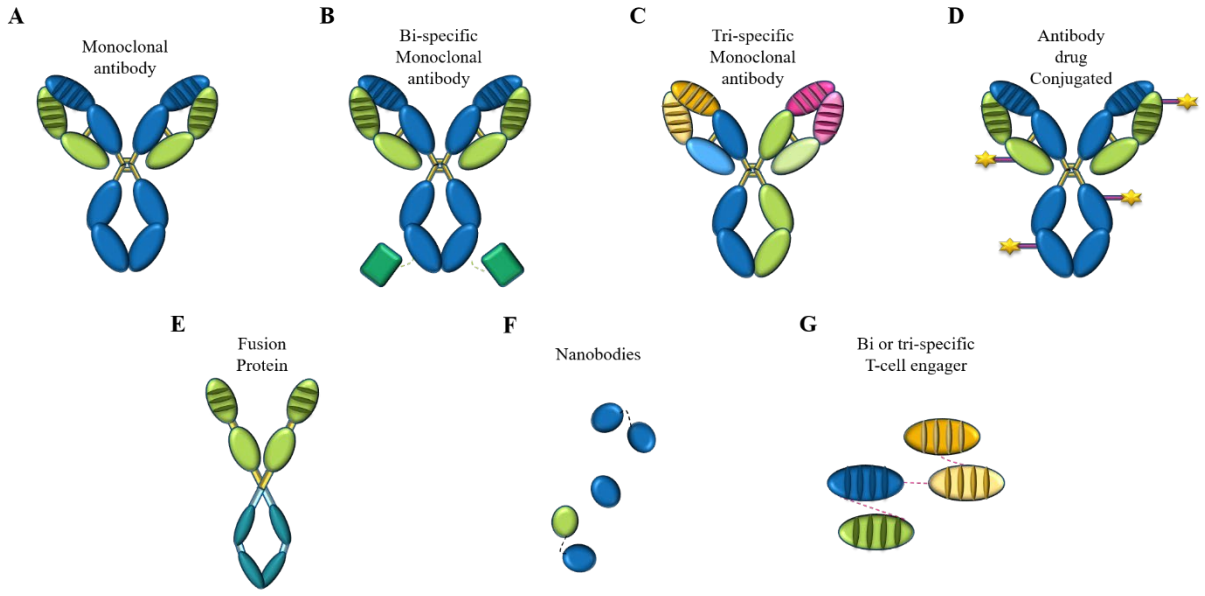

Figure 2 Representative classes of Ig-based biotherapeutics

The figure shows the structure of main classes of Ig-based biotherapeutics currently developed in pharmaceutical industry **A.** Monoclonal antibodies (mAbs), represent the wider class of antibody-based drugs currently marketed and ancestors of new generation compounds belonging to this class. **B, C.** Bi-specific and tri-specific mAbs, are specifically designed to recognize multiple epitopes of the same or different antigens. **D.** Antibody-drug conjugates (ADCs), are based on a typical mAb structure at which is attached a highly potent payload exerting cytotoxic effect on targeted cells **E.** Recombinant fusion proteins are generally composed by different functional moieties, and among these, specific Ig-Fc portions are responsible for triggering efficacious effector functions **F.** Nanobodies, are a sort of antibody fragments whose take advantage from their structure for improving their stability. These are easier and cheaper to produce compared to large mAbs, and generally show high stability under different harsh conditions **G.** Bi-specific and Tri-specific T-cell engager (BiTEs and TriTEs) are recombinant proteins formed by different single-chain variable fragments (scFvs) of individual antibodies. From a functional point of view, a moiety is able to target a cell-surface molecule on NK or T cells while other portions target antigens on the surface of malignant cells (19).

These molecules are characterized by different mechanism of actions (MoA). Shining a light on common mAbs, besides antigen or receptor blocking, they also play a crucial role in triggering powerful effector functions against targeted host cells. Indeed, the concurrent binding of Fab and Fc portions to the Fc gamma receptors (FcγRs) widely distributed on the cells of immune system, lead to the activation of typical innate and adaptive cell mediated immune responses. (*Figure 3*). Antibodies belonging to the class of immune checkpoints

inhibitors, have been shown to release the suppression of the T cell-mediated antitumor immune response by direct blocking a target antigen overexpressed on tumor surface (20) (Figure 3 A). Together with antigen binding, therapeutic efficacy of this class of compounds is amplified by several effector functions carried out through the interaction between antibody Fc portion and Fcγ receptors expressed on several immune cells. For example, the antibody-dependent cellular phagocytosis ADCP is a mechanism of elimination of antibody-opsonized target cells, which is activated following the interaction of antibody Fc portion with FcγRIIa receptors (CD32, FcγRIIa-131H/R, arginine or histidine polymorphic variants) expressed on the surface of macrophages. As a result, target cells are phagocytized and degraded into a phagosome (21) (Figure 3 B). Also, mAbs trigger an antibody-dependent cell-mediated cytotoxicity (ADCC), mostly attributed to Natural Killer cells (NK) (22) (Figure 3 C). Typically, this mechanism is elicited upon FcγRs such as the FcγIIIa (CD16, FcγRIIIa-158 V/F, Valine or phenylalanine polymorphism) is recognized by the Fc fragment of IgGs (23). Moreover, the binding between the first subcomponent of the C1 complement complex (C1q) and Fc region of a cell-bound antibody, triggers the CDC activity. As a consequence, a series of complement proteins are recruited, leading to the formation of a membrane attack complex (MAC) that causes the lysis of targeted cells (24). (Figure 3 D).

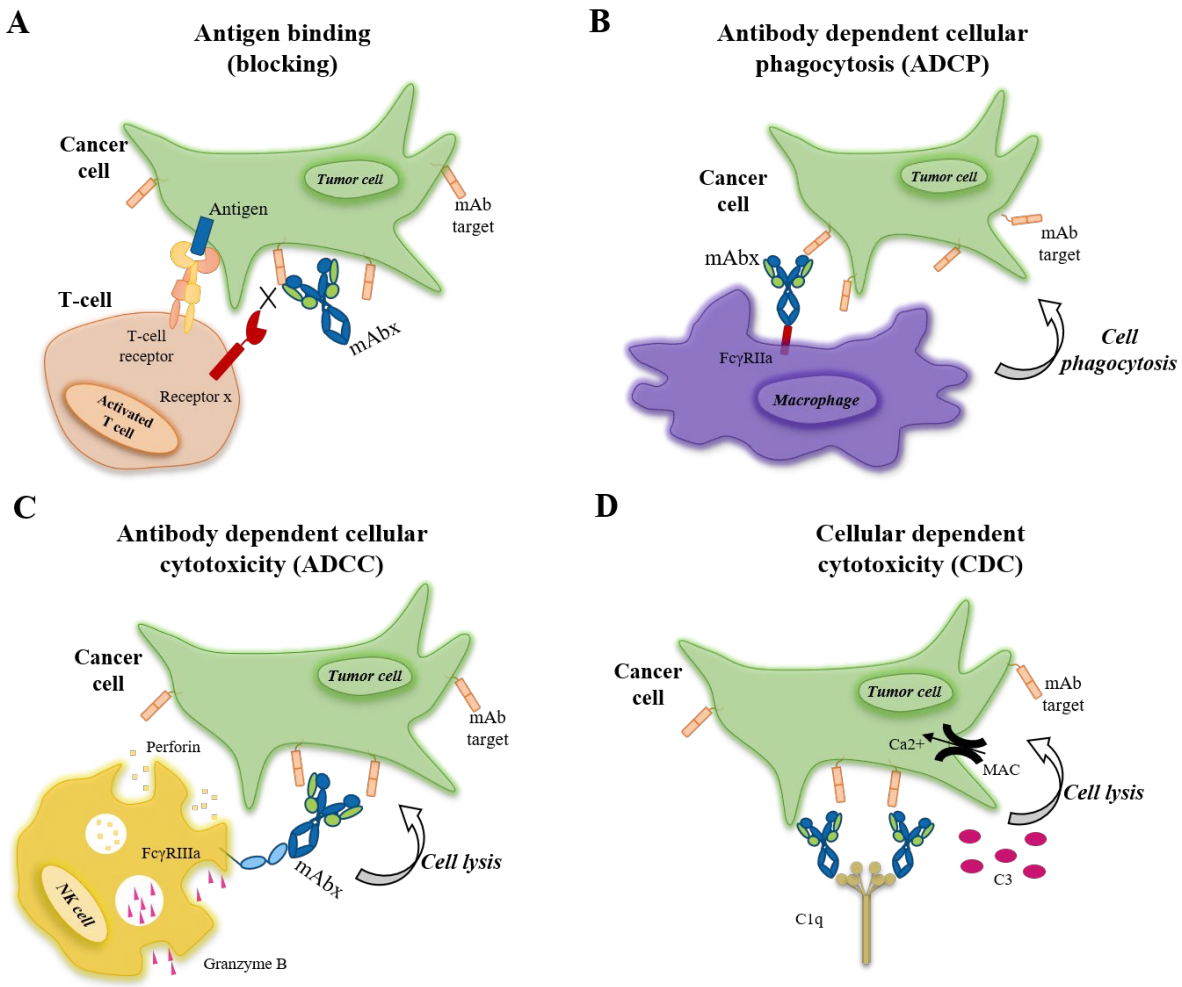

Figure 3 **IgG-based mAb Fab and Fc-mediated biological functions**

A. The binding to a specific epitope of a targeted antigen is the major mechanism of action of antibody-based drugs and it basically represents the main purpose for which mAbs are designed. **B-C.** Antibody-dependent cellular phagocytosis (ADCP) and antibody-dependent cellular cytotoxicity (ADCC) are two fc-mediated effector functions which are part of the mAbs' therapeutic armory. Both mechanisms are triggered following both antigen recognition and fc interaction with specific types of Fcγ receptors expressed on several immune cells. As a consequence, two potent cell-mediated immune response like phagocytosis and cell cytotoxicity are enhanced, resulting in the elimination of targeted cells (21), (22). **D.** Complement-dependent cytotoxicity (CDC) is another physiological immune response which is exploited by therapeutic mAbs for killing host cells. In this case the Fc portion interacts with the C1 complement complex (C1q) and activate a protein cascade leading to the formation of a membrane attach complex (MAC) and consequently to the cell lysis (24).

2.2 PD-1/PD-L1 immune checkpoint

The design and development of mAbs, together with the rise of complex next-generation antibodies, marked the beginning of a new era in immuno-oncology. Immuno-oncology represents a branch of Science that studies and develop specific immunotherapies (therapies based on the natural response of host's immune system) to fight cancer. In recent years, important progresses have been made toward a deeper understanding of the molecular pathways involved in cancer cell resistance to host anti-tumor immunity. Among these, the PD-1/PD-L1 (Programmed cell Death protein-1, CD279/PCDC1; Programmed Death Ligand-1, CD274/B7-H1) pathway has emerged as a key checkpoint for the suppression of the immune anti-tumor activity and as an important adaptive immune resistance mechanism exerted by tumor cells.

Physiologically, PD-L1 is a glycoprotein which interacts with receptor PD-1 expressed on activated T cells, forming an immunomodulatory checkpoint that ensures the immune system activation only at appropriate time to avoid chronical responses. The PD1/PD-L1 binding delivers inhibitory signals such as inhibition of T lymphocyte proliferation, survival and effector functions (cytokine release, cytotoxicity, phagocytosis, complement system activation), all mechanisms that allow tumor immune escape (25) (Figure 4A, left-panel side). Blocking the PD-1/PD-L1 pathway by anti–PD-L1 antibodies, promotes the proliferation of T-effector cells and the inhibition of T-cell mediated regulatory mechanisms, events that lead to tumor rejection. (Figure 4, right-panel side).

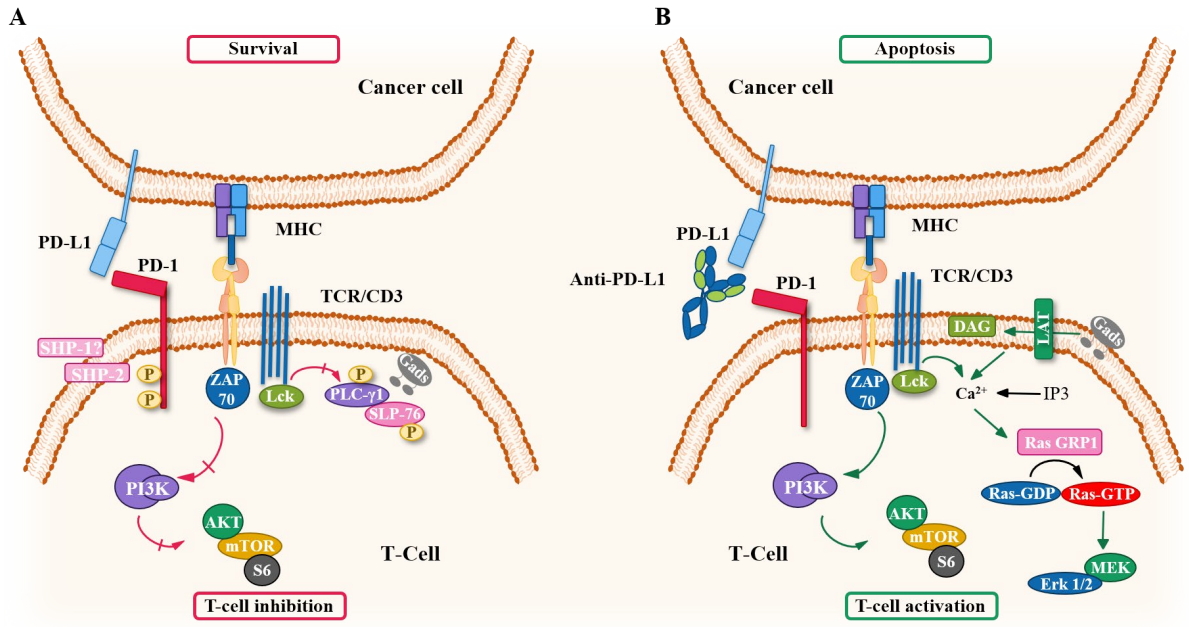

Figure 4 **PD-1/PD-L1 blockade releases PD-L1 mediated T-cell suppression leading to tumor regression.**

Under physiological conditions, PD-1/PD-L1 axes represents an immune checkpoint. Their interaction promotes cellular and molecular regulatory mechanisms such as inhibition of T effector and memory cells proliferation while enhancing differentiation of T-exhausted and T-regulatory cells. The sum of these events avoids a chronical activation of the immune response. **A.** However, several types of cancers, exploit this mechanism by overexpressing PD-L1 on their surface to elude human body defenses. **B.** The employment of mAbs directed against PD-L1 interrupts PD-1/PD-L1 interaction and restores T-effectors and T-memory functions. Inspired and adapted from reference (25).

Anti–PD-L1 mAb is a therapeutic monoclonal IgG1-based antibody that specifically targets the transmembrane protein PD-L1, found constitutively over-expressed in certain tumors besides host immune cells. Anti–PD-L1 mAb has been shown to release the suppression of the T-cell mediated immune response by blocking PD-L1/PD-1 interaction and induce the innate immunity via ADCC mechanism. (*Figure 5*):

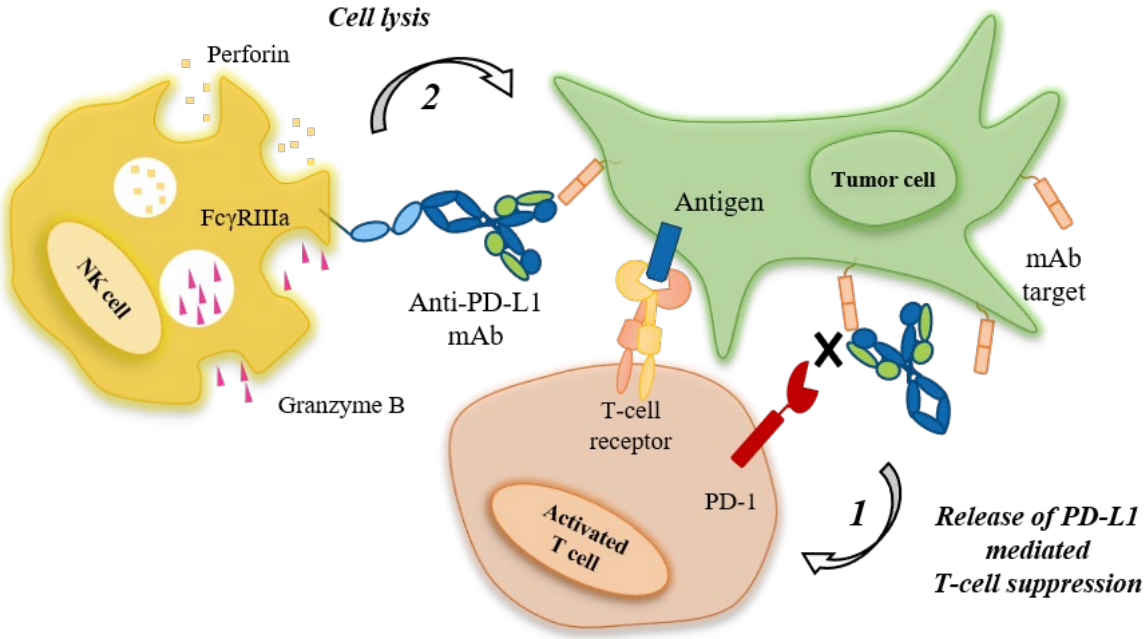

Figure 5 **Anti–PD-L1 mAb MoA**

1. Blockade of PD-1/PD-L1 interaction releases T cell from immune-suppression enhancing anti-tumor activity. **2.** ADCC activity is carried out by engaging immune effector cells (typically natural killer cells) against a targeted cell.

2.3 Principles of pharmaceutical development and analytical control strategies

In pharmaceutical industry, the process that from initial drug discovery leads to the commercialization of a lead compound takes from 10 to up to 15 years (26). Before becoming "real" drug and prior to their test in human clinical trials, these candidates must be well characterized in terms of pharmacodynamic (PD), pharmacokinetic (PK) and toxicological proprieties through both an *in-vivo* and an *in-vitro* pre-clinical phase. In Figure 6 the workflow of a typical pharmaceutical program is described. As already seen above, pharmaceutical development of a new biological entity lasts approximately a decade from drug discovery to market authorization. Typically, drug discovery begins with the selection of a specific target responsible for a disease condition. Then, thousands drug candidates are screened to test their

ability to interact with the target. Among these, only a few molecules are selected and proceed with further steps. Once the best candidate is chosen, this proceeds with pre-clinical experimentations during which the toxicological and pharmacokinetics/pharmacodynamics profiles are assessed. If pre-preclinical data demonstrated a high grade of safety and efficacy on these models, it is allowed to enter in clinical phase I, also defined "First in man", where the first GMP batch is manufactured and tested on a small group of human voluntaries. Clinical experimentation requires several years, and during this time, the manufacturing process is developed, optimized and qualified to be ready for the massive production and administration in advanced clinical phases. Finally, if regulatory package is complete and the requests made by the different health authorities are fulfilled in all clinical stages, it is possible to proceed with the launch of a drug product. However, even after the commercialization, the control of all product quality attributes must be continuously monitored by a validated analytical panel. In this regards, *in-vitro* assays are usually preferred over the *in-vivo* approach (which requests a massive animal employment) because of their high reproducibility and applicability on laboratory scale, cost-effectiveness, minor ethical impact and greater convenience to test many samples. Through all clinical phases of drug development, laboratory tests are requested to evaluate and monitor drug efficacy and stability. Physico-chemical and biological assays are the main approaches used to assess the quality, efficacy and stability of a drug during pre-clinical and clinical stages of development.

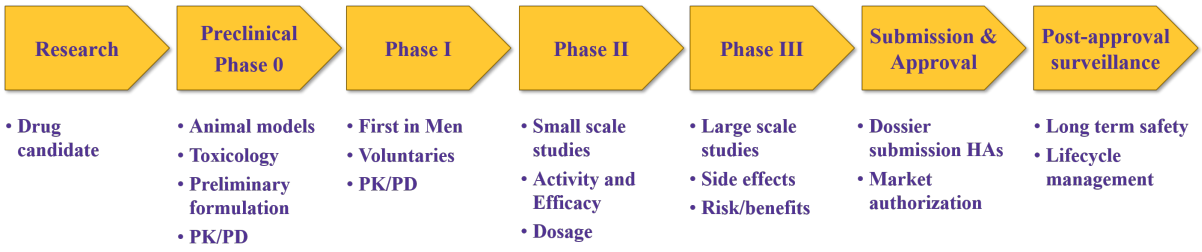

Figure 6 Simplified flowchart of a typical pharmaceutical development program

Representation of the main R&D, preclinical and clinical phases before market authorization of a candidate compound.

With the advent of the high-throughput technologies, there has been a significant improvement in terms of screening capability and scientific knowledge of selected candidate compounds. (27). Specifically, concerning the determination of efficacy and biological

behaviour, bioassays such as cell-based or ligand binding assays are routinely performed in order to ensure the quality and consistency of a given product. The outcome of a bioassay is generally a relative value obtained by comparing the result of a tested sample to that of a reference material (e.g. International Standard or Internal Standard). For being suitable for drug testing, a bioassay should meet some requirements that are reported in international guidelines: it has to be specific for the tested product and fulfil strict criteria of linearity, accuracy, precision and robustness (27). Also, an assay fit for purpose, should be user-friendly for routinely use, as well as stability indicating for regulatory purposes. In this regard, health authorities and regulatory agencies (e.g. EMA, FDA, PMDA), which are responsible for approving drugs for clinical trials, require assays that reflect as much as possible the mechanism of action of the molecule and that serve as a tool to perform an extensive characterization of any potential degradation (28). Finally, the need for orthogonal methods is made explicit in the EMA/FDA guidelines, which require cross-validation with independent but complementary or orthogonal approaches to prove and strengthen the reliability of results.

2.4 Structure-Activity relationship studies (SAR) and biological characterization in support of CQAs assessment

The definition of pharmaceutical operations includes all the activities needed for the production, distribution and control of medicinal products. Throughout the clinical experimentation, these series of practices are aimed at assuring the appropriate level of product quality before being administered. The Quality by Design (QbD) is a regulatory concept introduced in the pharmaceutical field by ICH and USP during last decades. The basic "tenet" of QbD implemented in pharmaceutical industry is to design the quality of the final product instead of testing it (29). It represents a systematic approach for drug development which emphasizes the product.

As a starting point of QbD approach, the guideline ICH Q8(R2) provides the definition of quality target product profile (QTPP): it is "*a prospective summary of the quality characteristics of a drug product that ideally will be achieved to ensure the desired quality, taking into account safety and efficacy* (30). Basically, it describes all essential qualitative characteristics to be maintained in order to assure a defined quality standard. Typical examples are dosage strength and form, container system, distribution, stability etc. and some of these parameters are usually defined critical for product quality.

A critical quality attribute (CQA) is defined as "*a physical, chemical, biological or microbiological property or characteristic that should be within an appropriate limit, range, or distribution to ensure the desired product quality"* (31), in other words a CQA defines a variety of molecular features that could potentially affect its quality profile in terms of efficacy, safety, PK and immunogenicity. For complex biotechnological products like mAbs, three representative categories of CQAs have been identified: product specific variants (i.e. post-translational modifications, glycans, aggregates, fragments), process-related impurities (i.e. host cell proteins, residual DNA) and mandatory attributes (to be monitored regardless of criticality).

In this work, the first category of attributes will be treated and the magnitude of their effects on product quality will be assessed through dedicated Structure-Activity Relationship studies (SAR). This kind of analysis is proposed and carried out as part of bioanalytical characterization studies normally required for the deep analysis of the critical attributes of a new therapeutic candidate. This approach is even more useful if applied for molecules characterized by a high degree of complexity as mAbs. It is indeed not always immediate to find a direct cause-effect relationship on how antibody's structural elements (usually characterized by different % and complexity grade) can impact biological functions. Under certain circumstances, these structural features may potentially lead to complex assemblies, causing different or even overlapping biological effects. The deployment of advanced bioanalytical platforms based on different principles, complemental or orthogonal among them, in some cases allow to figure out these relationships. Furthermore, for certain attributes that are well-known to affect antibody's biological functions (e.g. aggregation, fragmentation, glycans modifications etc.), the establishment of a theoretical functional threshold at which an effect is expected or abolished, results highly supportive for the development of a tailored analytical strategy able to control specific attributes.

SAR studies have been here integrated in the frame of the classical process development and validation workflow summarized in figure 7. This task requires many years and during this time a well product and process understanding must be reached. The purpose of process validation indeed, is to demonstrate that such process is capable to deliver a therapeutic molecule maintaining all its quality attributes within defined limits, namely "product specifications". As reported by several Food and Drug Administration (FDA) guidelines, a typical biotech manufacturing process is grossly divided into a development, validation and continuous verification stages. At each step, a CQAs assessment is performed on the basis of literature information, prior knowledge and experimental data. Regarding the latter,

considerations are made by leveraging dedicated SAR studies aimed at determining the impact of structural elements (impurities, degraded products and sequence variants) on biological activity and behaviour. The outcome of these studies are collected and included into regulatory modules and then submitted to Health Authorities at the end of each clinical phase. As per FDA nomenclature, these "checkpoints" are defined as Investigational New Drug Application (IND) and Biologics License Applications (BLA) and represent the milestones to be achieved before launching on market a new drug product.

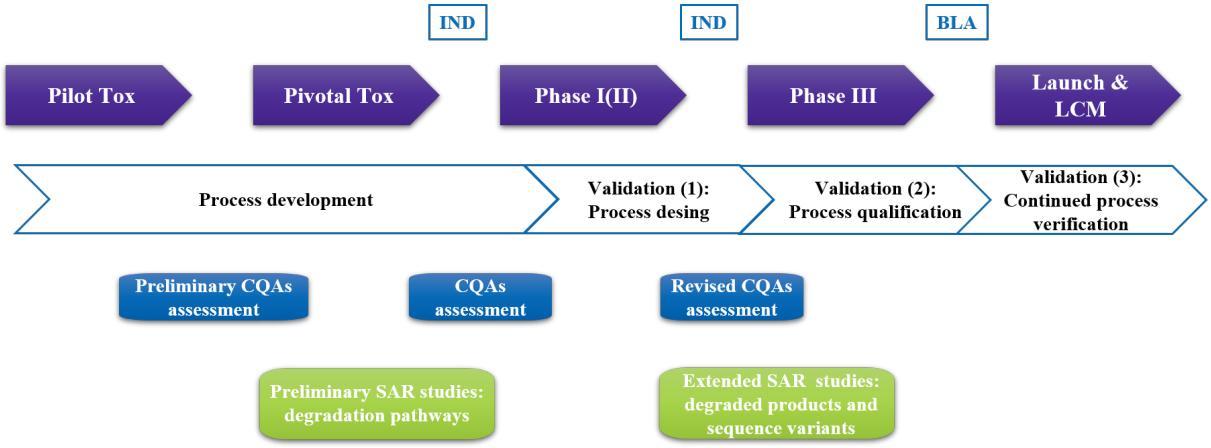

Figure 7 A typical process development and validation flowchart

In the figure are summarized the several steps of a typical development and validation process, together with the CQAs assessments and SAR studies to be performed.

The CQAs assessment is an essential part of process development (blue rectangles in Figure 7); a common practice carried out to assess criticality of a specific quality attribute is the application of a risk scoring system (graded from very low to very high). This scoring system, however, might change based on the internal organization of different companies and their strategic decisions (32). Starting from prior knowledge and information found in literature at the beginning of a development programme, this assessment evolves being repeated several times throughout the project, supported by accumulated experimental evidences. However, since early stages of development, the availability of experimental results obtained via physico-chemical and biological assays provide relevant information for the early understanding of the manufacturing process and for improving the overall product knowledge. In this regard structure-activity relationship (SAR) studies, if well-designed, represent a valid bioanalytical approach to explore the relationship between the drug's biological activities and its physico-

chemical modifications, which support the assignment of criticality scores (green rectangles in Figure 7) (33). During dedicated characterization studies, it would be recommendable the application of this analytical strategy to highlight potential differences in the product quality profile, as such differences could affect molecule's safety and efficacy (34). The fundamental premise is that the structure of a molecule implicitly determines its physico-chemical properties and reactivities, which, interacting with a biological system, determine its biological/toxicological properties. For example, it is well-known that the presence of antibody aggregates and fragments, commonly generated during prolonged thermal stress exposure, affect biological properties such as antigen-binding affinity and some of the Fc-mediated functions (35). Also, it is widely documented in literature that different glycosylation patterns occurring at certain levels during several manufacturing steps, significantly impact antibody effector functions, in particular the antibody dependent cell-mediated cytotoxicity (36).

2.5 Influence of glycosylation pattern on biological properties of mAbs

As already mentioned in the previous paragraph, specific post-translational modifications or other degradation profiles could affect the biological activities of antibody-based molecules. Among these, glycosylation is one of the most complex. The attachment of different sugar moieties lead to the generation of different patterns potentially impacting the biological activity of the antibody, especially those carried out through its Fc portion (37).

From a biochemical point of view, glycosylation can be described as a post-translational modification process which leads to the attachment of simple sugars or an oligosaccharide chain (glycan) to proteins. This is a multi-step process carried out by several enzymes, and in eukaryotes occurs among endoplasmic reticulum and Golgi apparatus.

Glycans, are generally divided into two main categories based on their chemical structure: linear and branched. The first class is composed by repeated disaccharide units, mostly O-linked to serine and threonine residues of a peptide chain. Branched chains instead can be O-linked and N-linked to aminoacidic residues. The latest, forms an amidic bound with the nitrogen of asparagine residues in different antibody's regions. The type and abundance of specific N-linked glycans mainly depends on the organisms where they are expressed, the type of proteins they are attached and the cells in which they are synthetized. The most abundant IgG branched N-linked glycans are represented in Figure 8:

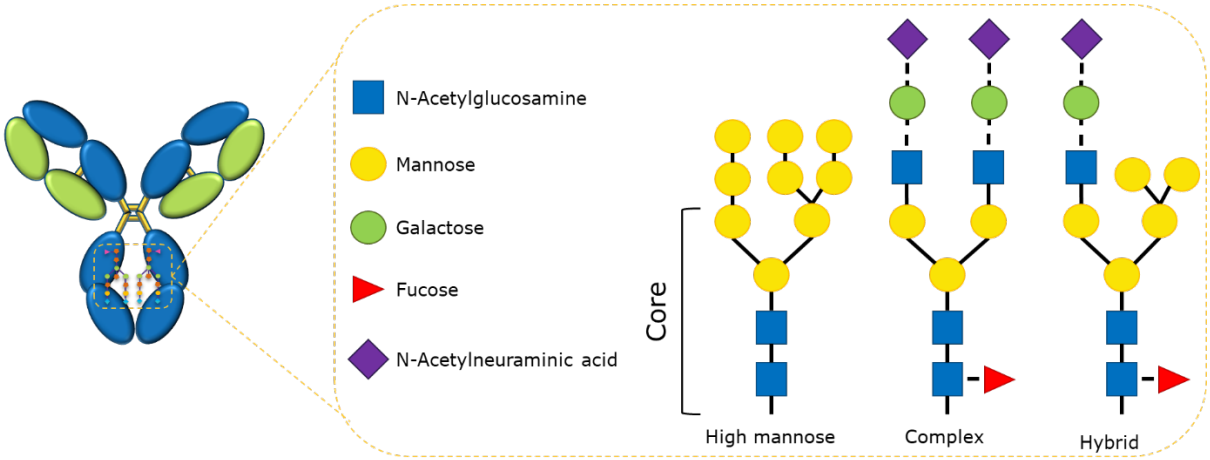

Figure 8 Representative examples of IgG N-linked glycans

The most common N-glycan types attached to the conserved N-glycosylation site on the two IgG heavy chains are complex di-antennary N-linked glycans. There are many possible combinations of these glycans which share a common core. In this image, as representative examples, are drawn a highly mannosylated, a typical G2F complex and a hybrid form.

Branched N-linked glycans present in IgG are complex di-antennary type and are typically bound to Asn297 in CH2 domain (38). These oligosaccharides are composed of a combination of the following sugars: mannose (Man), N-acetylglucosamine (NAcGlc), galactose (Gal), fucose (Fuc) and sialic acid or N-acetylneuraminic acid (S). Broadly, oligosaccharides are defined as G0, G1 and G2 based on the numbers of galactose residues brought. If the fucose is present, the nomenclature changes in G0F, G1F and G2F. Similarly, G0BF indicates the bisection at N-acetylglucosamine level. To the pentasaccharide core can be added variable combinations of the aforementioned sugars. The generation of complex combinations of branched glycan chains (i.e. high mannose) as well as hybrids forms are also possible and four different monosaccharides can be combined to form 35,560 unique oligosaccharides (39), most of which may impact molecule functionality beyond structure and stability.

Glycomics, is the science that studies and links glycans' structural heterogeneity to protein functions (40). These functions are usually influenced by the presence of several oligosaccharides' combinations that can affect or enhance IgG's biological functions in dependence of their type or complexity degree. Beyond putative binding properties for which therapeutic antibodies are designed for (typically the binding towards a specific target), other

effector functions are usually part of their mechanism of action. These functions are triggered by the interaction of specific sites on Fc portion and the Fcγ receptors exposed on different cells of immune system (41). A great variety of studies demonstrated that there are many reasons why oligosaccharide structures influence the pharmaceutical properties of mAbs, such as impairing their structural stability, creating steric hindrance for the Fc-Fcγ receptors binding or reducing their bioavailability in serum (42). In some circumstances for instance, different N-glycans types stabilize and hold CH_2 domains apart to providing an open state of the Fc fragment, which favorites the binding to different Fcγ receptors (43). Fab glycosylation is only found in ~15-25% of serum IgGs and its effect in modulating antigen binding can vary case by case (44). Similarly, there are not clear evidences pointing out a univocal effect of these species on affinity towards the FcRn (45). Moreover, immune effector functions may considerably change. In fact, the presence of such forms at certain levels can significantly impact both safety and biological activity of the therapeutic antibodies. Specifically, on one side safety can be impacted in terms of immunogenic effects (46), which is influenced by the type, complexity and amount of these forms; on the other, a not well fine-tuned glycosylation activity may lead to an excessive response in terms of antibody-mediated effector functions, resulting in an over activation of the host immune system. Among these effects, typical antibody effector functions triggered by antibody Fc portion are ADCC, ADCP and CDC, whose can be affected or enhanced by the presence of different glycans species.

In biotechnological industry, attention is placed in studying and monitoring the impact of glycans on ADCC activity whenever a new biological entity exerting this mechanism is developed. Specifically, during the upstream steps of manufacturing, several parameters inherent the cellular model chosen must be monitored as they result critical for the glycosylation levels of the nascent mAb. Indeed, if not well controlled, it is not unusual to observe slight variation in the level of several glycosylation patterns of different batches. These differences whether compared to a reference value are relatively small, but the resulting biological effect may increase exponentially. This is the reason why such levels must be kept under control through the establishment of a well-defined analytical strategy and an appropriate setting of product specifications is mandatory. In this way, during last decades, great efforts have been made towards the monitoring of these patterns during process development and validation, through the design of dedicated characterization studies and the application of orthogonal platforms able to monitor antibodies biological activities. Among these approaches, dedicated structure-activity relationship studies (SAR) represent an effective strategy to carried out thorough analysis and in-depth characterize a new biological entity.

3 Results

As stated by the European Medicine Agency through its Guideline ICH guideline Q8 (R2) (3) on pharmaceutical development: *"A greater understanding of the product and its manufacturing process can create a basis for more flexible regulatory approaches. The degree of regulatory flexibility is predicated on the level of relevant scientific knowledge provided in the registration application. It is the knowledge gained and submitted to the authorities, and not the volume of data collected, that forms the basis for science- and risk-based submissions and regulatory evaluations. Nevertheless, appropriate data demonstrating that this knowledge is based on sound scientific principles should be presented with each application".*

In this thesis an analytical strategy for the extended biological characterization of a therapeutic Anti–PD-L1 mAb, is reported. This experimental platform with selected experiments and defined CQAs is potentially applicable to similar new biological entities (NBEs). The presented approach is based on the employment of a series of functional methods as cell-based and SPR technologies supported by structural and physico-chemical data. The analysis of a single quality attribute was performed by using a set of orthogonal techniques which allowed the design of a tailored strategy used for the extended characterization of an Anti–PD-L1 mAb. The rationale of the experimental choices is based on the idea of bridging critical structural elements like post translational modifications, aggregation, fragmentation and several fc-glycans patterns to the Anti–PD-L1 mAb biological activity. In addition to that, whenever possible, a theoretical functional threshold at which the level of an attribute affects molecule's functionality is proposed as well. The scope is reaching a deep molecule knowledge and overcome the possible gaps related to the data obtained applying a single technique per attribute. The set-up of such a strategy leads to an improved product value besides shortening times for submissions and market authorization.

3.1 Forced degradation studies and Anti–PD-L1 mAb main degradation pathways

During both earlier and then later stages of drug development, the determination of product-specific degradation pathways is an essential part of the characterization process of a new biological entity. In the case of earlier phases, such assessment is mainly based on literature data, in-silico structural predictions as well as prior knowledge gained with compounds belonging to similar pharmaceutical class. Based on these preliminary considerations, a list of critical aminoacidic residues on which modification may occur are identified. After that, several experimental activities are designed, and the first characterization begins. During these kinds of studies, as soon as these "artificially-induced" modifications are detected by physico-chemical analytical methods, the impact of such modifications on safety, efficacy and immunogenicity are also assessed. Based on the outcome of this assessment, a specific attribute can be "scored" as critical and monitored during routine. Typical examples of common structural elements or chemical modifications that generally affect the biological properties of IgG-based drugs are deamidation, oxidation and presence of high molecular weights (HMWs) and low molecular weights LMWs species.

There is common agreement among different regulatory agencies and Health authorities, that such attributes must be checked and then monitored during routine, regardless of the fact they significantly affect the antibody biological functions. Indeed, as these modifications are generally considered critical for the majority of mAbs and have an impact on immunogenicity and safety beyond efficacy and pharmacokinetics, these are anyhow included in a typical product specification document. In this regard, in order to detect these species, forced degradation studies represent a useful tool applied to explore the main degradation pathways of a molecule and provides an opportunity to gain in-depth understanding of its biological behavior in relation to structural features. In particular, when employed at earlier stages, a rough assessment of the impact of such modifications is performed, which contributes to build the initial information package. Then, it is set up a proper analytical strategy for controlling process parameters that may affect molecule's attributes during routine manufacturing. Regarding the latest consideration, during the development of bioanalytical methods, degraded products are also used to challenge the method capability to be stability indicating. In this regard, an analytical method should have such sensitivity to be able to detect a small number of degraded products in order to evaluate their impact on drug's biological properties.

The scope of a forced degradation study is to figure out what may happen to a molecule in terms of structural changes and biological activity under specific stressing conditions. For example, extended incubation at high temperature is known to compromise the structural stability of almost all IgG based therapeutics.

Since during long term and accelerated stability studies, months if not years are needed to detect any appreciable effects on the molecule, these kinds of studies are performed under extreme conditions in order to accelerate degradation pathways. However, although the evident advantages in carrying out forced degradation studies, a consideration must be made to draw proper conclusions. The degradation performed under harsh conditions indeed, offers the opportunity for an adequate characterization of drug product, which considerably shorten times for defining critical hot spots of mutation. However, it is worth to note that such a practice leads to the generation of degraded species which may not be fully representative of what happens during conventional stability studies performed over months or years.

3.2 Effects of intensive stress conditions on Anti–PD-L1 mAb structure

In this work, a dedicated forced degradation study has been performed to explore the most relevant structural attributes affecting Anti–PD-L1 mAb activity. Starting from an Anti–PD-L1 mAb representative batch, different harsh conditions have been applied to induce the generation of degraded products. The stress study started with a thermal stress exposure of the antibody, where it was incubated at 50°C for 2 and 4 weeks. Temperature is a physical parameter that can accelerate several degradation pathways and generally leads to the formation of antibody fragments and aggregates (47). In some cases, deamidation of asparagine and glutamine residues, methionine oxidation or isomerization of other residues are also observed (48). The fact that all these species may potentially impact molecule structure and stability, depends on their concentration in the sample, the criticality of the aminoacidic residue modified or species generated, and finally the specific antibody function involved.

Samples were prior characterized applying a physico-chemical panel. All relevant data regarding the main degraded products generated after forced thermal stress at 50° C for 2 and 4 weeks are reported in Figure 9. For the main post translational modifications monitored such as deamidation and oxidation, in the graph bar are only reported the % of modification of those residues which are believed being most susceptible to these stress condition and mainly affecting Anti–PD-L1 mAb functions in terms of fab-binding ability (49), PK (50) and ADCC

activity (51). Anti–PD-L1 mAb size variants were also monitored as three main populations based on their molecular weight: total high molecular weights species (HMWs), dimers and total low molecular weights species (LMWs).

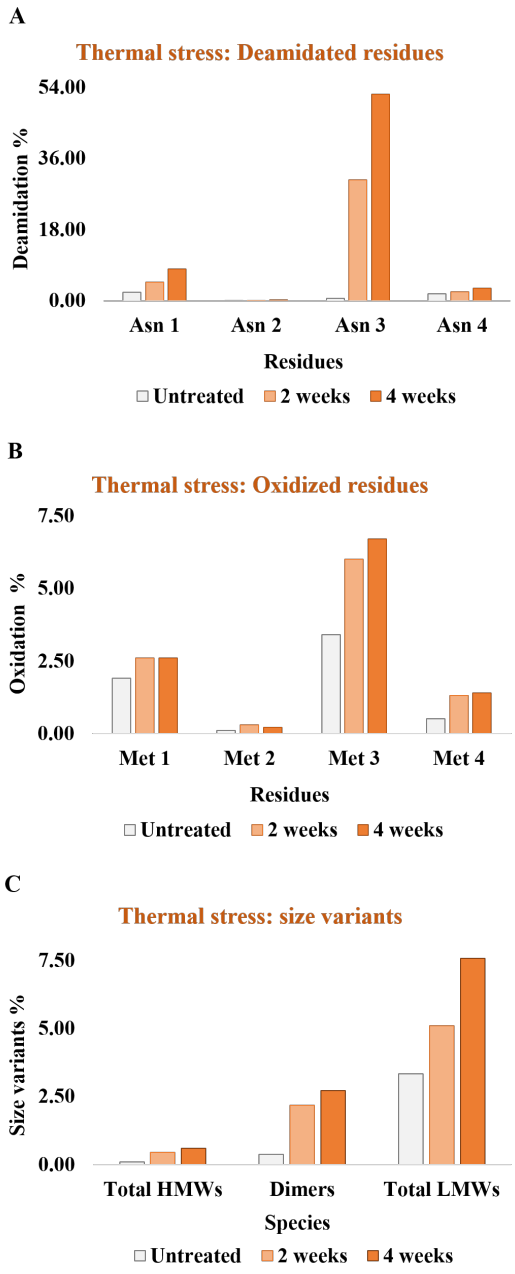

Figure 9 Determination of the Anti–PD-L1 mAb degradation profile following a forced thermal stress

A representative batch of Anti–PD-L1 mAb was exposed at 50°C for 2 and 4 weeks to characterize its main degradation pathways. Results come from a single analysis for the sole purpose of providing the levels of each species. Therefore, no statistical analysis was performed **(A–B)** Reducing Peptide Mapping by LC-MS/MS was used to quantify the main deamidated and oxidized sites (4 asparagine and 4 methionine residues respectively). **(C)** On the other hand, size variants were detected and quantified by CE-SDS in non-reducing conditions for total LMWs while SEC-MALLS was exploited for detecting dimers and total HMWs.

Degraded products and modified aminoacidic residues were quantified and expressed as absolute % respect to the total amount of detected species. Post translational modifications occurred in the Anti–PD-L1 mAb structure such as deamidation and oxidation were monitored through four asparagine residues (Asn 1-4) and four methionine residues (Met 1-4) respectively, chosen on the basis of their criticality for antibody functions (Fab functionality, ADCC activity and PK). While Asn 1-2 and Met 1-2 are located on the CDRs and mainly involved in the Fab-antigen recognition, Asn 3-4 and Met 3-4 are in the Fc region and mediate the FcγRIIIa and FcRn bindings respectively. However, it should further be noted that Asn 1-2 are just marginal mediators of the Anti–PD-L1 mAb binding to its target, as they are located relatively far form sites interacting with PD-L1. In addition to that, it is evident from the antibody structure (not shown) that there are no critical asparagine sites prone to deamidation on the three antibody's CDRs.

The amount of deamidated species in untreated and treated Anti–PD-L1 mAb were detected and quantified by Reducing Peptide Mapping by LC-MS/MS. As expected, the deamidation % resulted increased in all the Asn sites after 2 and 4 weeks at 50°C. Such increase was particularly evident on Asn 3 (30.6 % after 2 weeks and 52.2 % after 4 weeks), which is located in proximity of an asparagine known in literature for being a critical site for the binding to FcγIIIa receptor and, consequently, for ADCC activity (51). Furthermore, also the Asn 1 located in one of the CDR regions and mainly involved in the Fab function, was particularly affected by the stress as its starting level of deamidation was 2.10 % and dropped to 8.00 % after 4 weeks. In the same analysis, it was also demonstrated that thermal stress did not cause relevant changes in the oxidation profile of Anti–PD-L1 mAb. The only remarkable change in terms of oxidation is the enrichment at Met 3 level, which is a residue located in proximity of the area recognizing the neonatal fc receptor (FcRn). The % of oxidation on such site was more than doubled if compared to that of untreated sample. On the other hand, the total amount of HMWs and dimeric species in the untreated and stressed sample were detected and quantified by SEC-MALLS analysis. Overall, the treatment at high temperature induced only a very slight raising of Anti–PD-L1 mAb HMWs species after 2 and 4 weeks of exposure at 50°C, while dimeric species were found to be increased of about 2.5 times. Furthermore, non-reducing sodium dodecyl sulfate-polyacrylamide capillary gel electrophoresis (non-Red-CGE-SDS) was able to detect a moderate increase of total LMWs species, indicating that the incubation of the sample at high temperature leads to antibody fragmentation. Regarding size variants species, it has to be mentioned that when such structural elements populate the sample, it is not always immediate to create a correlation among these structural elements and biological functions, so

that all the considerations for this relationship have to be contextualized and revised case by case.

After thermal stress exposure, another study was performed to figure out the effect of extreme pH on anti–PD-L1 mAb structure and activity. As seen for the exposure at high temperature, events like pH variations may occur during several steps of antibody production and storage. A typical condition applied during forced degradation studies is the incubation of tested molecule at low and high pH. Following this approach, Anti–PD-L1 mAb was incubated with 1.2M Ammonium bicarbonate (pH 9.2) at room temperature for 5 days and with 0.5 M sodium citrate (pH 4.0) at 37°C for 3 days.

The same physico-chemical analytical panel was applied for the detection of Anti–PD-L1 mAb degradation products under certain conditions and most relevant results are shown in Figure 10:

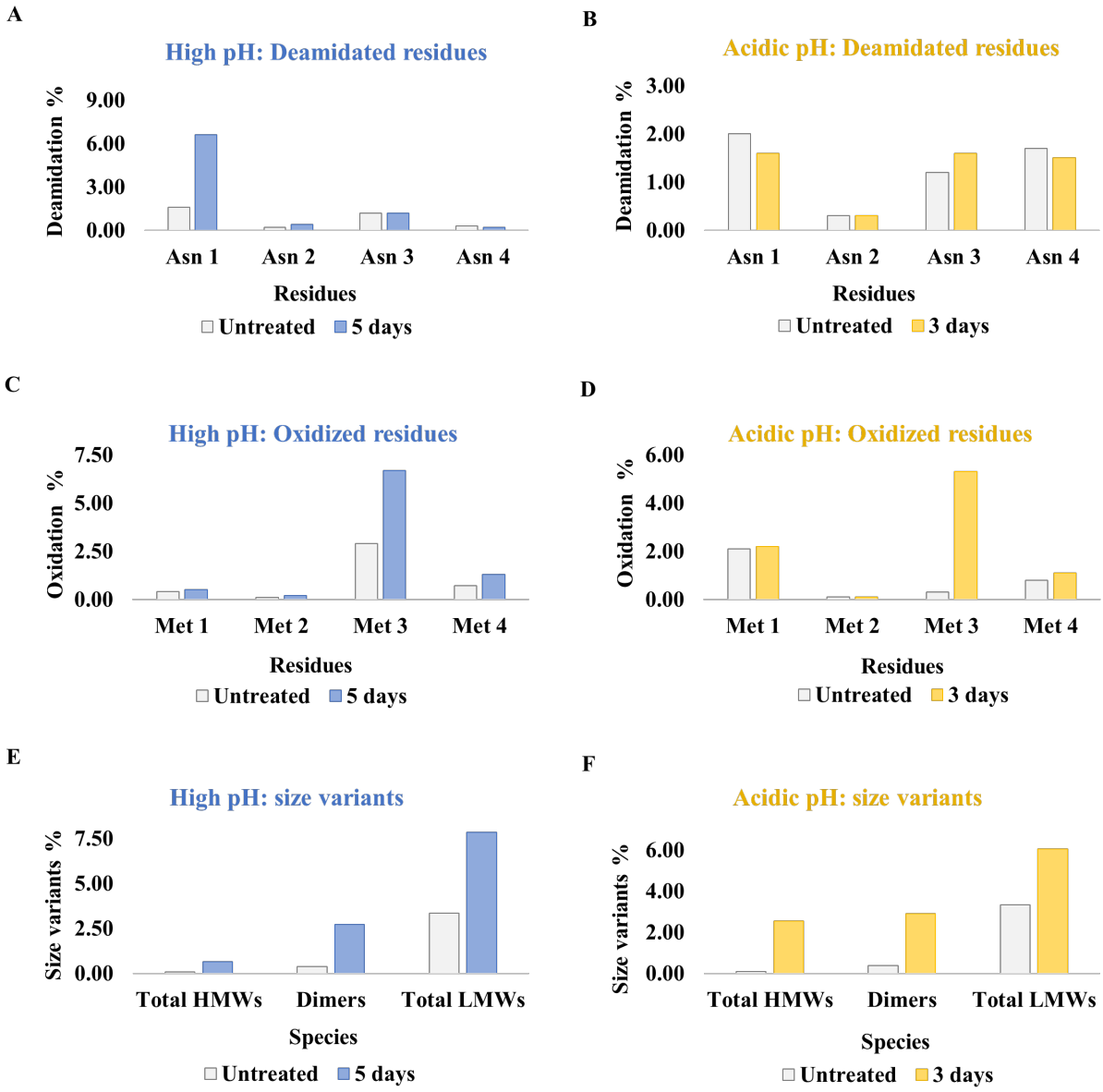

Figure 10 **Determination of the Anti–PD-L1 mAb degradation profile following the exposure at high and low pH**

A representative batch of Anti–PD-L1 mAb was incubated at high and low pH with 1.2 M Ammonium bicarbonate (pH 9.2) for 5 days and with 0.5 M sodium citrate (pH 4.0) at 37°C for 3 days. In order to highlight potential degradation pathways following these treatments, samples were initially characterized from a physico-chemical point of view. Results come from a single analysis for the sole purpose of providing the levels of each species. Therefore, no statistical analysis was performed. Reducing Peptide Mapping by LC-MS/MS were used to quantify the main deamidated **(A-B)** and oxidized sites **(C-D)** (4 asparagine and 4 methionine residues respectively). On the other hand, size variants **(E-F)** were detected and quantified by CE-SDS in non-reducing conditions for total LMWs while SEC-MALLS was exploited for detecting dimers and total HMWs.

The basic pH treatment at 1.2 M Ammonium bicarbonate (pH 9.2) for 5 days, resulted in an overall deamidation as main degradation pathway, involving Asn residues on both LC and HC. However, only Asn 1 showed major differences in comparison with the untreated levels (1.60 % vs 6.60 %) (Figure 10). Moreover, minor changes in oxidation were detected, with a consistent increase in the oxidation of Met 3. High pH exposure also led to an increase of aggregation, mainly in forms of dimeric species and small fragments, which was already evident in the starting material. Similar effects were observed following the treatment at acidic pH (0.5 M sodium citrate pH 4.0 at 37°C for 3 days). While an overall deamidation was not expected, a similar increase of the levels of oxidation on Met 3 was noticed. Also, all three subpopulation of size variants were considerably increased. In particular, high pH exposure mainly led to the fragmentation of the antibody; on the other hand, the incubation under acidic conditions provoked the formation of high molecular weights species.

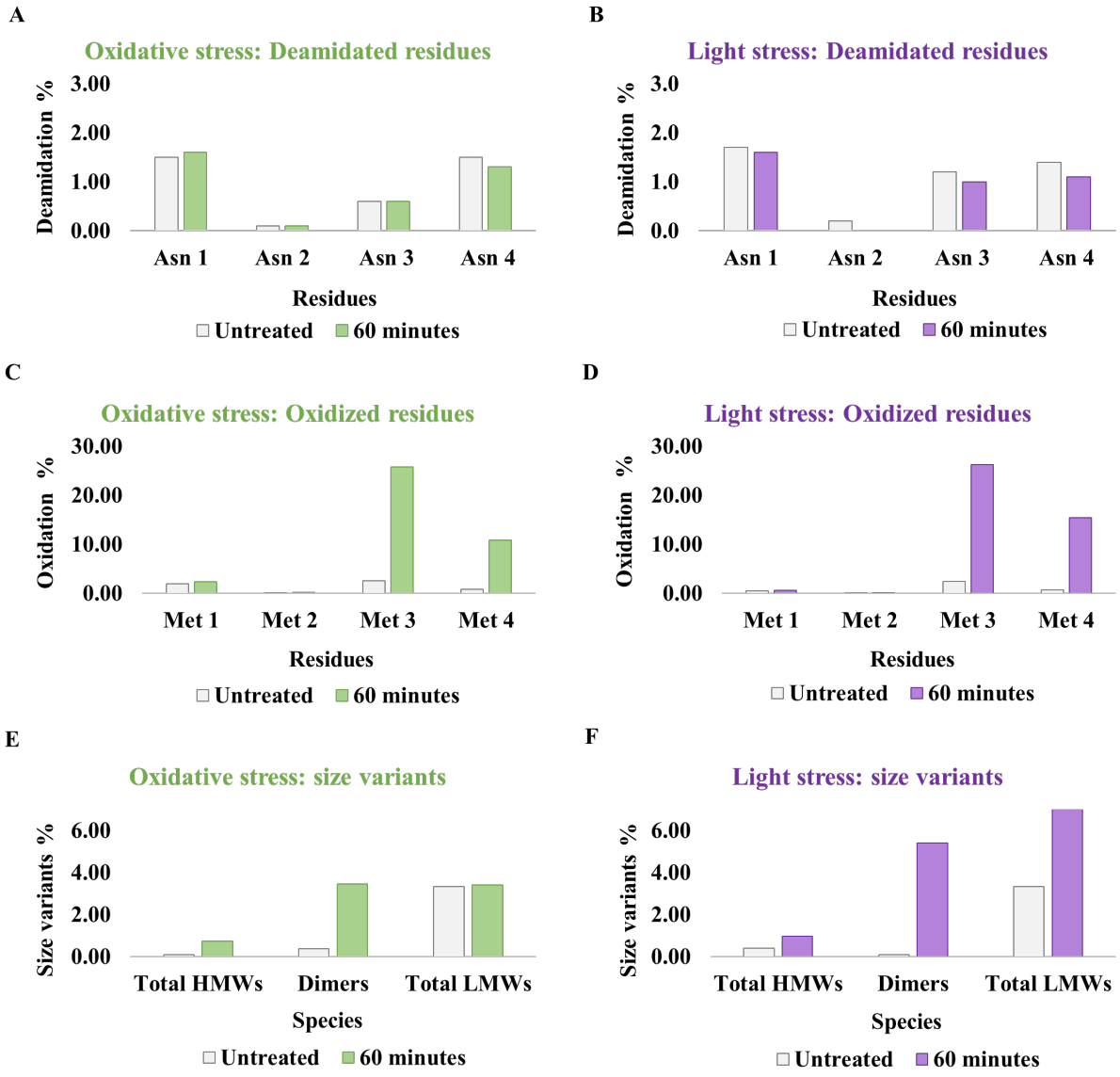

Figure 11 Determination of the Anti–PD-L1 mAb degradation profile following an oxidative treatment and light exposure

A representative batch of Anti–PD-L1 mAb was incubated under an intensive oxidative condition with 0.1% H_2O_2 for 60 minutes at room temperature and exposed at 765 W/m^2 for 24 hours. After the stress, these samples were analyzed by reducing Peptide Mapping by LC-MS/MS to quantify the main deamidated **(A-B)** and oxidized sites **(C-D)** (4 asparagine and 4 methionine residues respectively). In addition to that, also size variants produced by the forced conditions were detected and quantified **(E-F)**. CE-SDS in non-reducing conditions was applied for detecting total LMWs forms while SEC-MALLS was exploited for dimers and total HMWs species. Results come from a single analysis for the sole purpose of providing the levels of each species. Therefore, no statistical analysis was performed

Finally, two further studies typically used for exploring antibody degradation profiles were carried out: an incubation under oxidative conditions (0.1% H_2O_2 for 60 minutes at room temperature) and a light exposure (at 765 W/m2 for 24 hours), whose provided quite similar results regarding the Anti–PD-L1 mAb degradation profiles. These forced treatments had two main effects on antibody structure: the increase of size variants abundance and the oxidation of met 3 and met 4 residues. Indeed, oxidation mainly occurred on HC (met 3-4) and minor changes were observed on LC. A certain aggregation degree was observed as well, with a noticeable increase of dimeric species (greatly increased if compared to that of untreated material). On the other hand, while LMWs increased to a minor extent in the case of oxidative stress (3.34 % of the untreated vs 3.39 % of treated sample), these species were found moderately increased after light exposure (about 2.5 times respect to untreated sample).

3.3 Relationship between Anti–PD-L1 mAb degraded products and its biological properties

Looking at previous physico-chemical characterization data, it can be noted that Anti–PD-L1 mAb was prone to be modified under certain conditions. Forced conditions undergone by the antibody indeed, led to the formation of several degraded products causing post translation modifications of several aminoacidic residues, which in turn, might potentially affect Anti–PD-L1 mAb functions. In order to understand whether specific antibody's biological activities were impaired by these degradation products and establish the magnitude of their effect, a series of bioanalytical methods were developed and qualified. Together with structural methods, biological assays (Bioassays) are routinely developed and validated as part of a typical characterization panel and applied to determine mAb's biological functions based on their peculiar MoA (52).

During last decades, bioanalytical field has emerged as a discipline exploited for analyzing data of other branches of research. Nowadays, it has become a true and independent scientific sector particularly relevant in the pharmaceutical industry environment. The advent of high-throughput technologies together with great advancements in terms of sensitivity, precision and accuracy of such platforms, allowed the establishment of this scientific branch in many strictly regulated manufacturing areas. Biological assays can be broadly classified on the basis of their format and the scope they are developed for. For example, cell-based assays mimicking the *in-vivo* mechanism of action of a new candidate, are generally developed and validated for assessing with a high degree of reliability the biological efficacy of batches to be

administrated in clinics. For the same purposes, in certain circumstances cell-free ligand binding assays, like ELISA-based methods, can be also developed if they reflect the drug's mode of action (e.g. for the mere binding to a ligand or receptor without any activation of intracellular pathways). However, in addition to their application for the release of clinical batches, these two assay formats are also used for characterization studies, providing relevant information concerning the product functional profile. Other two well-known platforms primarily used for characterization purposes and in support of manufacturing process are the Biacore technology, which is based on the surface plasmon resonance (SPR) phenomenon and Bio-layer interferometry (BLI), which analyzes the interference pattern of white light reflected from two surfaces. Both techniques, leveraging different principles, provide similar information on biomolecular interactions.

Going more in-depth into technical matter, in Figure 12 is reported a typical bioassay workflow. The example illustrates a high-throughput assay format in which is carried out a common cell-binding experiment, where it is tested the ability of an antibody in binding its target expressed on a cellular model. The experiment is usually conducted by performing several step dilution points of the antibody, while the dose of other reagents and cells concentration are fixed to a determined value. The aim of this type of analysis, is the generation of a dose-response curve that is elaborated by a mathematical model. The 4PL (parameter logistic regression) nonlinear fitting model, is one of the most used as it is appropriate for the elaboration of a dose-response curve describing a drug's biological behavior. Once elaborated, the curve is analyzed from both a qualitative and quantitative point of view. Generally, a biological efficacy result is expressed as EC_{50}, described as the concentration required to obtain a 50 % of the biological effect (53) or, alternatively, in a relative manner like potency %, given by the ratio between the EC_{50} of a sample and its reference material. Similarly, in the case of Biacore results, data are formally expressed as absolute equilibrium dissociation constant (K_D) or relative K_D % respect to a reference material, representing a measure of the antibody binding affinity. Moreover, some considerations on the kinetics of the binding can be made by analyzing the two rate constants k_a and k_d, which describe the kinetics of ligand-analyte complex formation.

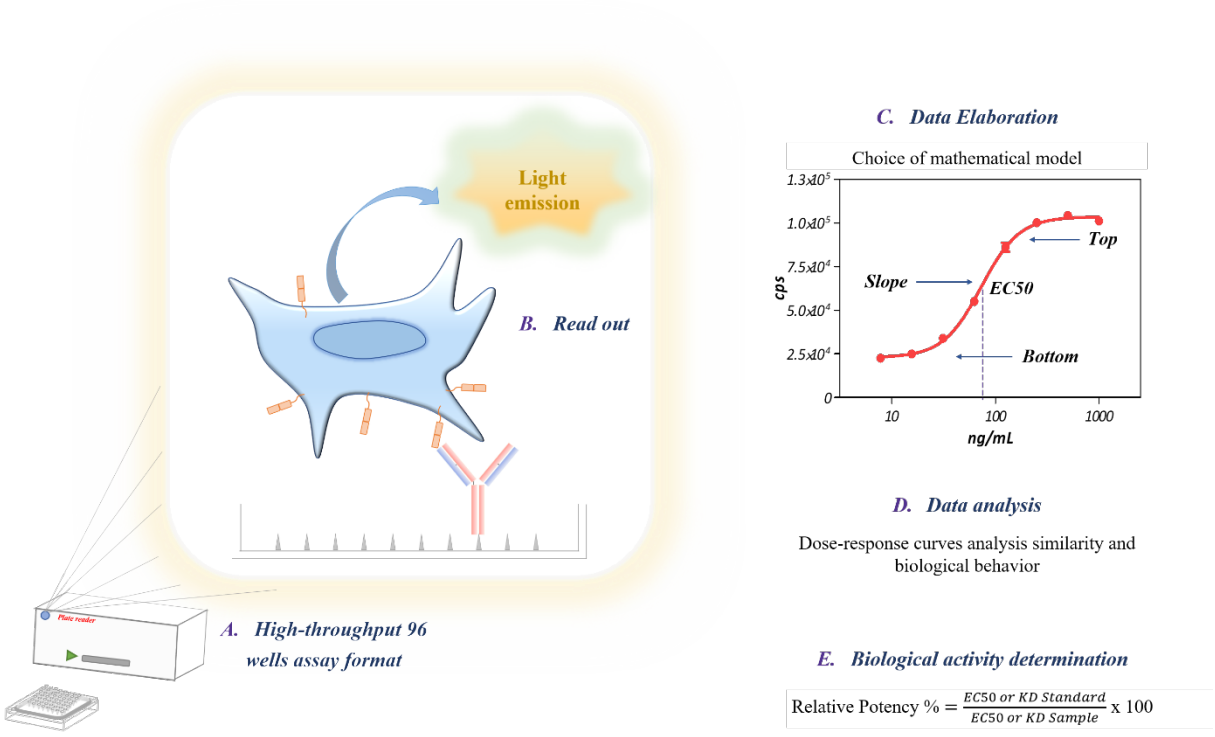

Figure 12 A typical bioassay workflow

In this figure is described a typical ligand-receptor dose-response curve, generated by performing a cell-based bioassay in a high-throughput format. **(A)** The experiment is usually performed in a 96-wells plate, where the set of reagents and the drug of interest are plated. **(B)** After a proper incubation time, each well is incubated with a read-out reagent and derived signal is read by a plate reader. **(C)** The dose-response curve generated is elaborated with a specific mathematical model **(D)** and analyzed from a qualitative point of view respect to a reference material. **(E)** Finally, a quantitative data is also provided by calculating a relative potency %, given by the ratio between EC_{50} of reference material on the EC_{50} of the analyzed samples.

As already described in the introductory chapter, Anti–PD-L1 mAb exerts its therapeutic effects through two different mechanisms of action: the binding against its main target protein PD-L1, which is commonly found overexpressed on a variety of tumors, and the antibody dependent cell cytotoxicity (ADCC), triggered by antibody Fc portion following the binding to FcγRIIIa receptor exposed on several cellular types of immune system. Furthermore, like many other classes of therapeutics based on an Ig structure, its pharmacokinetic properties are generally monitored via Fc-FcRn binding.

Starting from these premises, a tailored analytical panel was developed in order to elucidate the effect of the main degradation pathways and structural modifications induced by

the forced degradation study on Anti–PD-L1 mAb biological functions. Once assessed, at each attribute has been assigned a score for defining its criticality in terms of biological activity and pharmacokinetics. Such biological assays are essentially based on different cell based and SPR platforms. Briefly, a schematic representation of methods' layouts used in this study is provided in Figure 13:

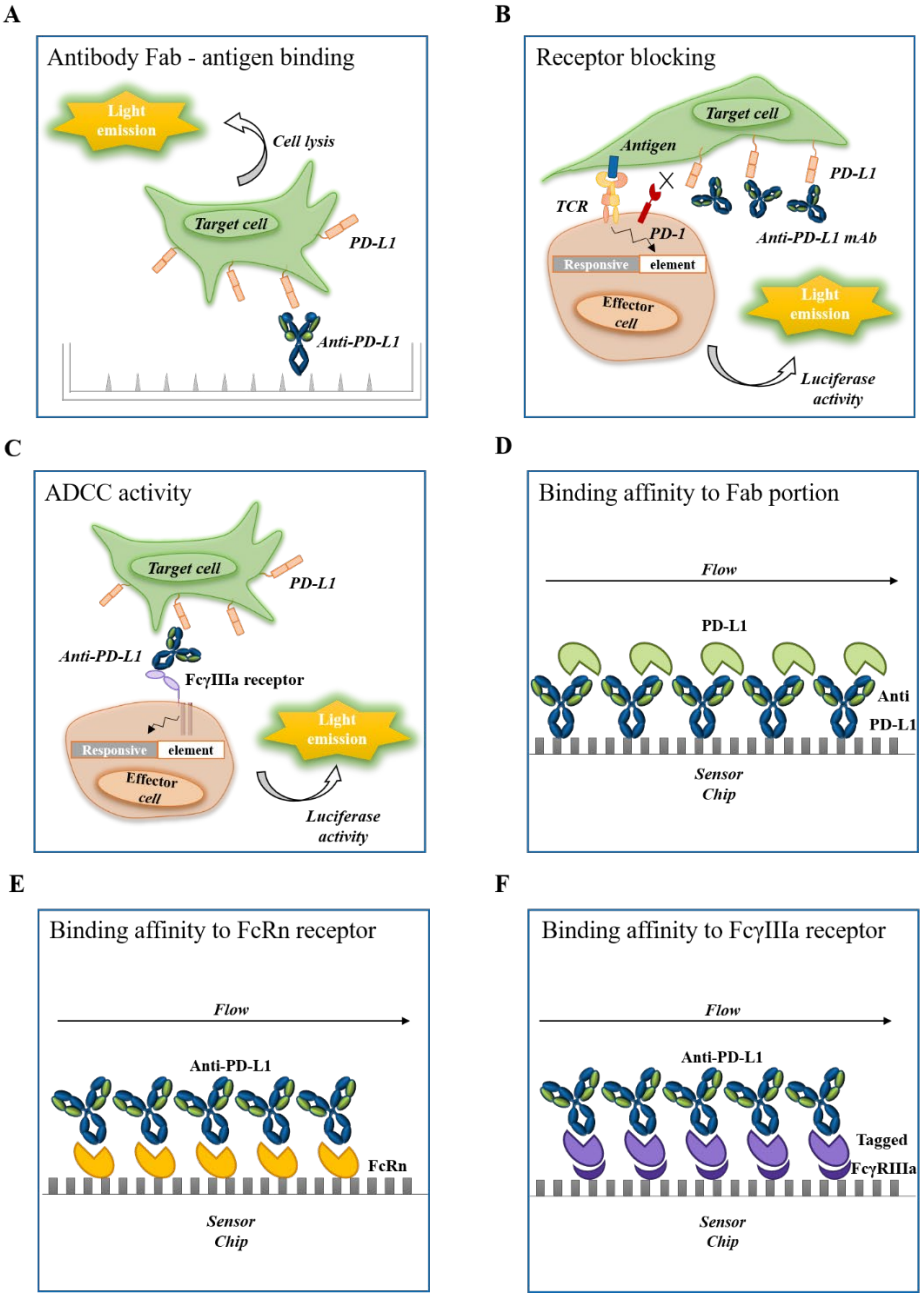

Figure 13 Schematic representation of the biological tests performed in the study

In this figure a series of biological assays are represented. In **A-B-C** panels are described three cell-based methods monitoring the direct binding of Anti–PD-L1 mAb to PD-L1, the blocking of PD-L1/PD-1 interaction and ADCC activity. On the other side, **D-E-F** panels are described three SPR-based methods. The first SPR method represents an orthogonal assay respect to the cell-based one, which monitors the binding to the PD-L1. The other two instead, are used to detect the interaction to the FcRn and FcγRIIIa, which respectively, represent a tool for measuring the *in-vitro* predictive PK and an orthogonal way to characterize the ADCC activity.

The first set of methods, characterized by the presence of living cells, are typical assays that should be always included into a bioanalytical panel during a pharmaceutical development program. Their implementation indeed is strongly recommended by several guidelines and in most cases such assays are used to determine the efficacy of drug's clinical batches as well as for characterization purposes. SPR technology instead is basically applied in the frame of characterization studies and provides complementary data to those already obtained with other biological methods. In this work, the binding to PD-L1 was firstly assessed via cell-based assays, closely representing *in-vivo* mechanism of action of the antibody of interest (Figure 13 A-B, see also Material and methods section). Then, when necessary, binding affinity was further investigated by SPR. SPR analysis was carried out to determine the kinetics and binding affinity of the interaction between Anti–PD-L1 mAb and its specific ligand (Figure 13 D, see also Material and methods section). Adopting the same criteria, ADCC activity (Figure 13 C, see also Material and methods section), FcγRIIIa binding (Figure 13 E, see also Material and methods section) and FcRn binding representing the pharmacokinetic properties (Figure 13 F, see also Material and methods section) were also assessed. As shown in Figure 14, samples exposed at 50°C for several weeks were the most affected if compared to the degraded products and modifications occurred applying other stress conditions. Thermally stressed Anti–PD-L1 mAb samples indeed, showed a decreased binding affinity towards the PD-L1 and a reduced activity in blocking PD-1/PD-L1 interaction. From the analysis of association (ka) and dissociation (kd) rate constants (data not shown), while the first was basically unaltered, the latter resulted considerably increased under both stress conditions, meaning that the overall decreased affinity of the Anti–PD-L1mAb/PD-L1 complex was mainly determined by an increased dissociation rate.

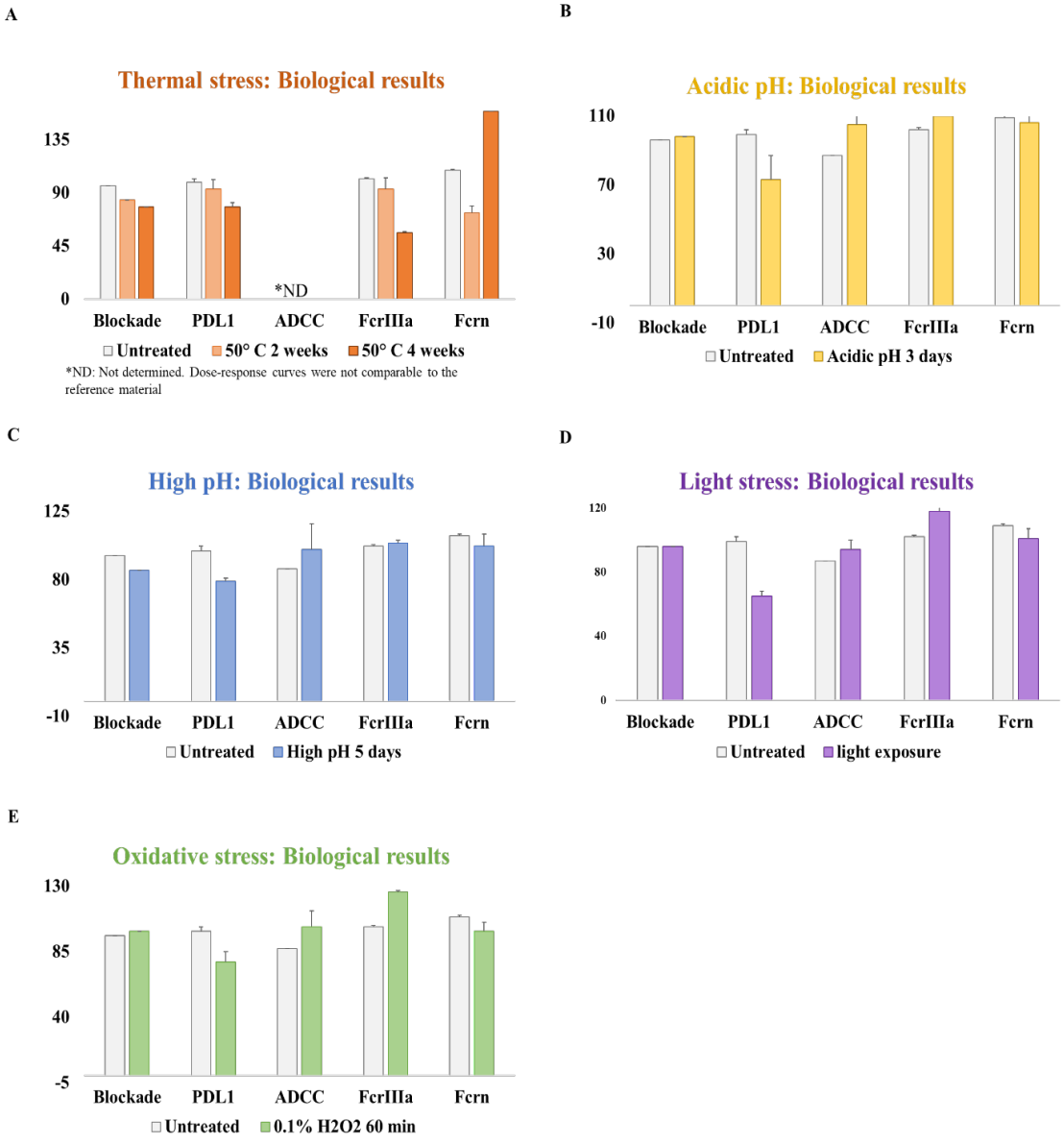

Figure 14 Effect of forced thermal stress on Anti–PD-L1 biological properties

Relative potency and relative K_D % data were obtained comparing each sample EC_{50} or absolute K_D values with respect to an internal reference material and were then represented on a graph bar. Biological results were obtained by exposing the tested batch under the following conditions: **(A)** thermal stress conducted at 50°C for 2 and 4 weeks, **(B)** acidic pH incubation with 0.5 M sodium citrate pH 4.0 at 37°C for 3 days, **(C)** high pH exposure with 1.2M Ammonium bicarbonate (pH 9.2) at room temperature for 5 days, **(D)** light stress exposure at 765 W/m^2 for 24 hours **(E)** incubation with 0.1 % of H_2O_2 for 60 minutes at room temperature. The error bars represent the coefficient of variance of technical replicates calculated on 3 and 2 independent runs for bioassay and SPR respectively. One exception concerned the results of blockade assay that was performed in a single run. Each sample was loaded on a 96-wells plate as a technical triplicate, following a plate layout that ensure a sufficient level of analytical variability and prevent potential plate effects due to the loading mode.

Representative bioassay dose-response curves are reported in Figure 15. Looking at graphs, it was highlighted a clear shift of curve to the right of *x*-axis (towards higher EC_{50} values), an event that is directly related to a decreased antibody efficacy in relation to the increased exposure time at high temperature.

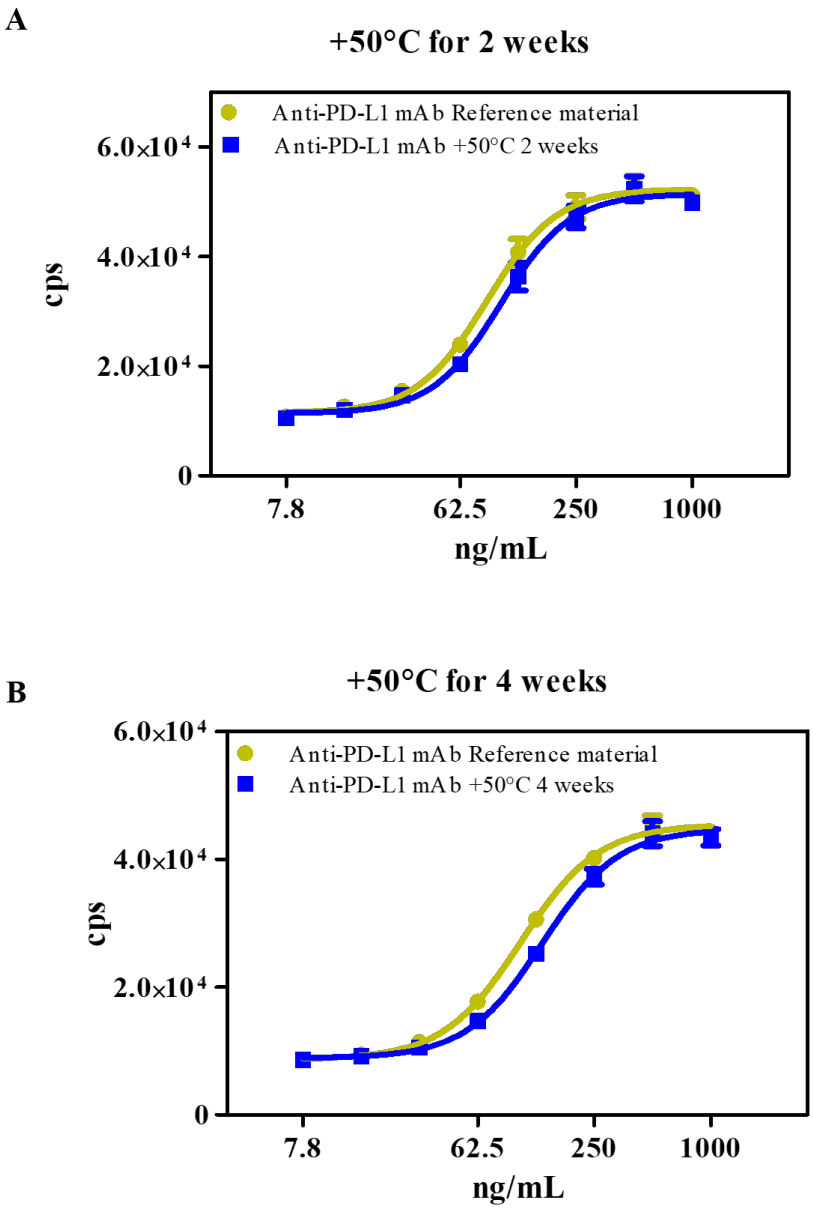

Figure 15 Representative dose-response curves of Anti–PD-L1 mAb at +50°C (2-4 weeks)

A-B Representative dose-response curves obtained by cell-based blockade assay of samples exposed at 2 and 4 weeks at +50°C, respectively. Curves similarity were firstly evaluated by F-test before the determination of potency results. All curves showed similar behaviors compared to the reference material (p-value 0,05).

Even if not immediately appreciable like dose-response curves, also the sensorgrams obtained by Biacore analysis (Figure 16, Figure 17) indicated a different affinity of stressed Anti–PD-L1 mAb towards its target.

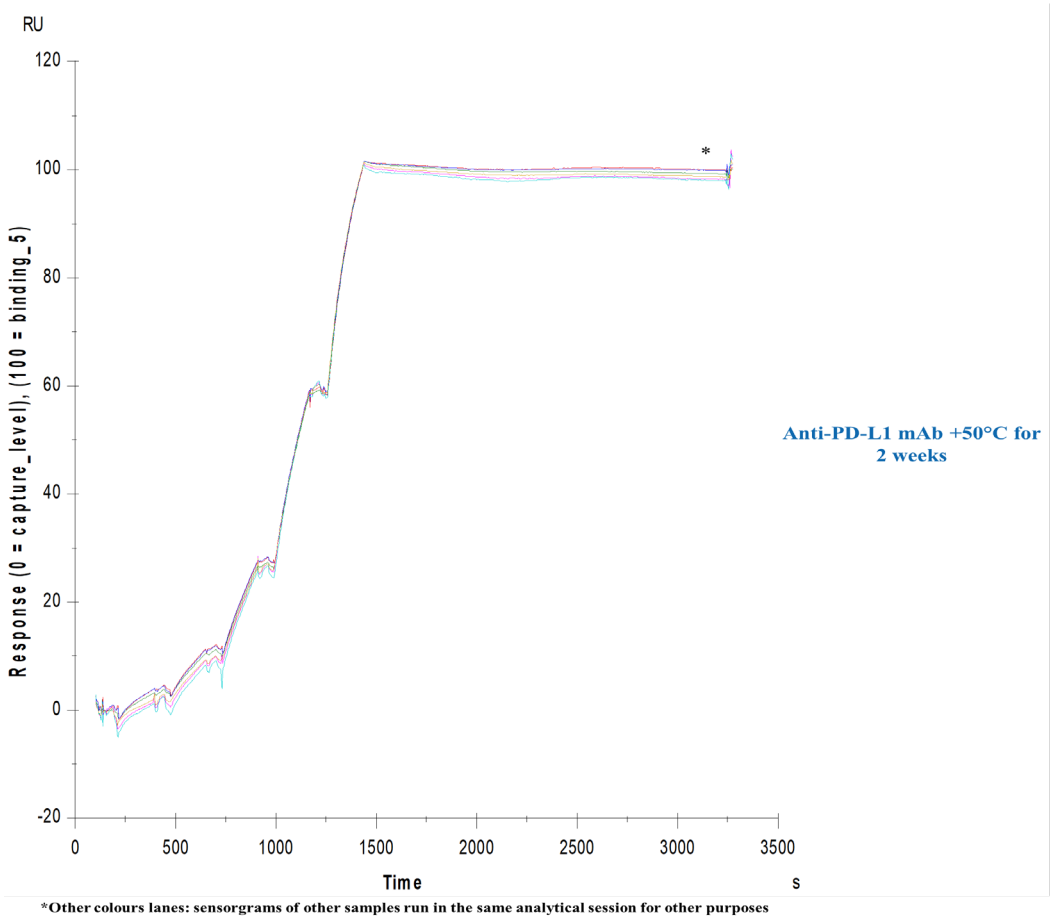

Figure 16 Representative sensorgrams of Anti–PD-L1 mAb at +50°C (2 weeks)

A Representative sensorgram of Anti–PD-L1 sample exposed at +50°C for 2 weeks. Data were analyzed by single cycle kinetic (SCK) model using a Biacore T200 evaluation software to determine the equilibrium dissociation constants (K_D) of binding.

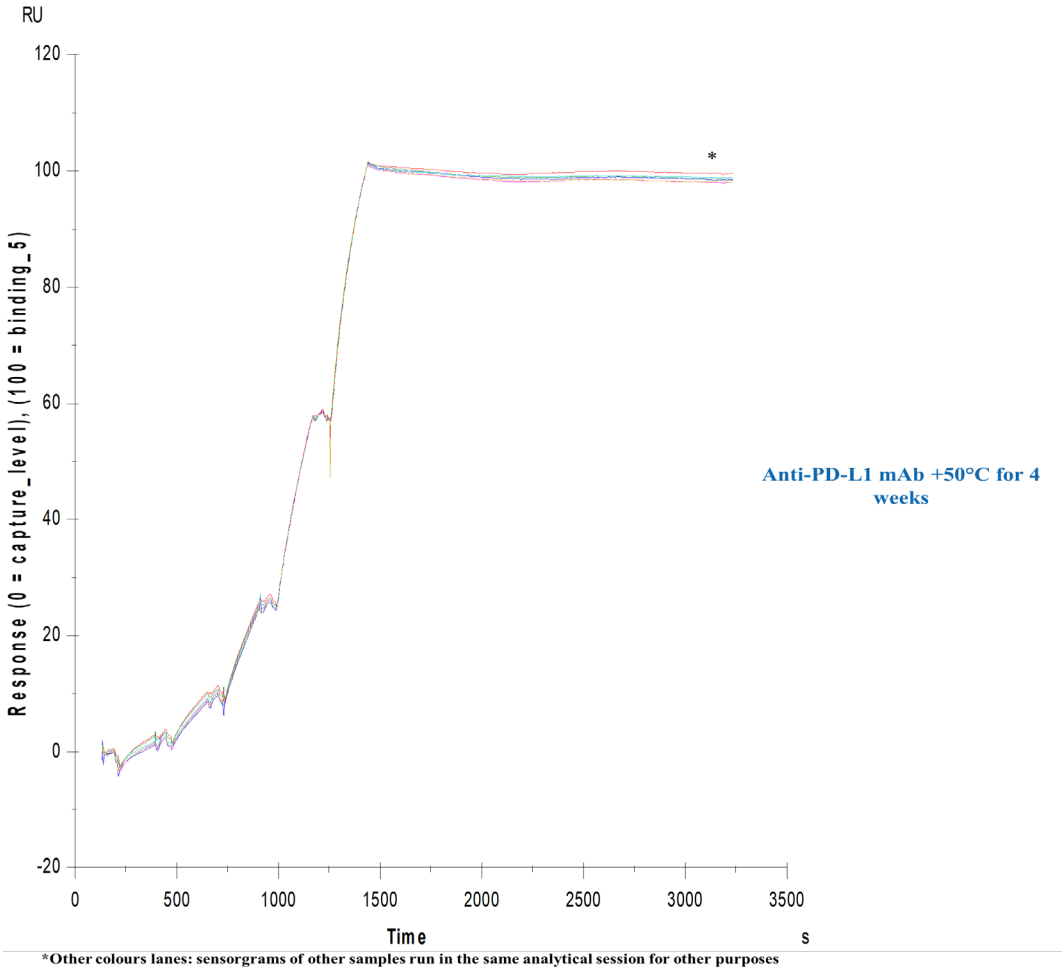

Figure 17 Representative sensorgrams of Anti–PD-L1 mAb at +50°C (4 weeks)

A Representative sensorgram of Anti–PD-L1 sample exposed at +50°C for 4 weeks. Data were analyzed by single cycle kinetic (SCK) model using a Biacore T200 evaluation software to determine the equilibrium dissociation constants (K_D) of binding.

Similarly, Fab-PD/L1 binding and Fc capability to bind FcγRIIIa receptor were consistently reduced respect to untreated samples. Accordingly, ADCC activity was even not determinable as dose-response curves of treated samples were not comparable to that of reference material. Regarding the latter result, in order to clearly show such evidence, representative dose-response curves of Anti–PD-L1 mAb reference material and after thermal treatment for 2 and 4 weeks are shown in Figure 18:

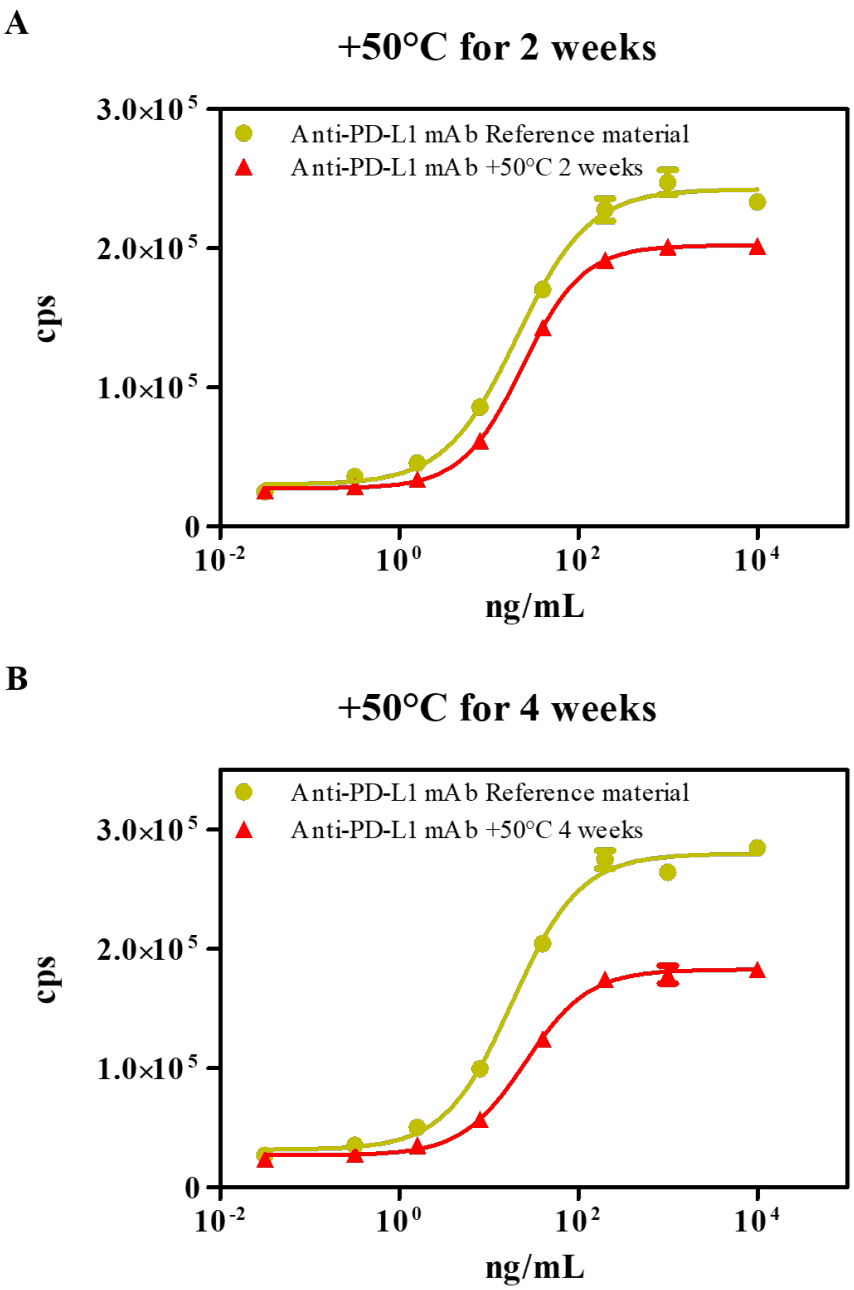

Figure 18 Representative dose-response curves of untreated and heat stressed Anti–PD-L1 mAb

Dose-response curves of the samples treated for 2 and 4 weeks at +50°C, showed a different profile respect to that of reference material, which indicates a different biological behavior of these samples. This aspect is particularly evident on the top of curves, where the maximal effect is not comparable to that of reference material.

Heat-stressed Anti–PD-L1 mAb after 2 and 4 weeks of exposure at 50°C, was compared in terms of similarity to that of reference material. Specifically, the top, bottom and slope

parameters describing a biological dose-response curve, was compared head-to-head to that of reference material. Despite both curves were well-described, it was highlighted that treated samples were not comparable in terms of similarity to that of reference material. It was also noticed that, the major difference between the curves was found at the top level, which is a direct expression of the maximal efficacy. Therefore, due to these differences, it was not possible to calculate a relative potency % value, that represents the measure through which the antibody biological activity is formally expressed. The only possible consideration is based on the qualitative interpretation of treated samples and reference material curves. The different behavior of these samples respect to reference material is associated to the presence of degraded products generated following the heat exposure. Furthermore, it has to be considered also the high % of deamidation on the Asn 3 reported in Figure 9, which is a residue known to be close to FcγRIIIa binding site (51). This post translational modification together with the presence of other degraded products, contributed to the anomalous biological behavior in terms of ADCC activity. However, considering that all samples tested showed similar profiles, the two processes are considered comparable. Finally, also FcRn binding seemed to be affected by this stress condition after 2 weeks of thermal stress. Biacore results indeed, which ability to bind the FcRn receptor is expressed as K_D %, was considerably decreased respect to the untreated sample (109 % vs 73 %). This result is in according to the fact that samples resulted particularly degraded under such conditions and oxidation levels on Met 3 residue were slightly increased. Unexpectedly, the results obtained by testing samples incubated for 4 weeks at 50°C showed a K_D % of about 159 %, meaning that the binding to the FcRn receptor was significantly increased respect to the untreated sample and the time-point 2 weeks. Despite the sample was grated affected at this time point, this result could be more related to the presence of different species generated by the thermal stress at 4 weeks such as aggregates, that can affect in a conversely way the binding to the receptor (54).

Concerning the Anti–PD-L1 mAb incubated at low and high pH, it was not highlighted significantly changes from both a physico-chemical and biological point of view. Overall, only PD-L1 binding results slightly decreased after both incubations (99 % vs 79 % following high pH incubation and 99 % vs 73 % at acidic pH), which anyhow did not cause any significant effect on the Anti–PD-L1 mAb efficacy in blocking PD-1/PD-L1 interaction pathway. Similarly, the moderate increase of Asn 1 deamidation % and Met 3 oxidation % (Figure 10), were not sufficiently enriched to such an extent to affect any biological function. Furthermore, as concluded for thermally stressed samples, the presence of even small amount of size variants,

may lead in some cases to a modification of the molecule functionality in dependence of size and amount of such species (54), (55).

Finally, as expected, oxidative stress and light exposure conditions, led to a strong increase of Met 3 and Met 4 oxidation %, which are known being two mutational hot spot residues located in the Fc portion, prone to be oxidized. While the affinity for PD-L1 resulted slightly decreased, according to the other stress conditions showing similar degraded size variants distributions (Figure 14 D-E), the antibody FcγRIIIa and ADCC functions resulted not affected. Furthermore, as seen for the previous conditions, FcRn binding was found not particularly impaired by the oxidations detected on met 3 and met 4 residues. As already mentioned, this result could be explained as a balance of two effects: on one hand a decreased FcRn binding activity and on the other a higher binding affinity of total aggregated species (HMWs + dimers). Indeed, from the analysis of rate constants (data not shown), it was noticed that the overall improved affinity of the complex was mainly due to an increased kinetics in association phase. In addition to that, Bajardi-Taccioli Et al demonstrated and confirmed previous results from other studies, that very high oxidation levels (above 40%) of met 3 are required in order to see a significant decrease in FcRn binding (54), (56), an event which is anyhow unlikely occurring during a routinely and well-defined common manufacturing process.

3.4 In-depth evaluation of oxidation and deamidation biological effect on Anti–PD-L1 mAb binding properties

The analysis of the main Anti–PD-L1 mAb degradation profiles brought out that the most frequent post translational modifications occurring on critical residues close to functional binding sites, did not significantly affect the biological properties of the antibody. However, although the overall potency and efficacy of the antibody was maintained, for some stressed samples the Biacore analysis showed a slight decreased affinity in the binding to PD-L1. In this regard, it was not fully clarified if the lower affinity was due to changes in the molecule structure or to the presence of size variants generated following the forced stress. In addition to the expected aminoacidic modifications, it was also observed that several degradation pathways following harsh incubations carried out during the study, led to the generation of small or moderate amounts of “undesired” antibody size variants. Forced degradation studies indeed, do not selectively address a desired modification to the molecule, or at least, it is not the only one occurring. The generation of several degradation products besides those expected from a well-

planned stress condition is an event that commonly happens. Indeed, the main aim of these studies is shortening times to investigate unknown degradation pathways, but under the condition of accepting that sometimes it is not possible to specifically ascribe a biological function to a structural attribute. Furthermore, the presence of several types of size variants beyond a certain threshold, may affect assays' performances in terms of specificity, selectivity, accuracy and precision.

In view of this and in order to answer the initial question that is whether the slight impact on Fab binding activity was mostly due to modifications occurring on binding sites or to the presence of size variants, the role of oxidation and deamidation have been analyzed more in depth.

An evaluation of the impact of oxidation on the biological function of Anti–PD-L1 mAb was conducted by testing an artificially oxidized sample treated under milder conditions respect to those carried out in the present study. This sample showed almost the same degradation profile as the samples described in this work, but lesser amount of aggregates and fragments. Moreover, it was used an alternative cell binding assay for the testing of this sample. This assay is a complemental cell-based method compared to the receptor blocking assay, which is usually used for characterization purposes in order to complete the information package on PD-L1 binding. The potency determined through this method was expressed as the Anti–PD-L1 mAb ability to directly bind its target PD-L1, overexpressed on a stably transfected HEK-293 cell line. Therefore, while receptor blocking assay provided information regarding the ability of Anti–PD-L1 mAb to block the PD-1/PD-L1 interaction, this assay is able to monitor the direct binding of the antibody to PD-L1 expressed on a cellular model, providing a complemental data concerning Fab activity. As shown in Figure 19 A, the oxidized sample showed a biological behavior similar to that of reference material and biological activity, provided as EC_{50} value, resulted not affected. Furthermore, it is known from Anti–PD-L1 mAb primary structure, that there are two methionine residues on the CDRs of heavy chain and one on light chain. However, in Figure 19 B, an in-silico analysis of the molecule structure showed that these residues are partially or not exposed to the external environment, being located in the inner part of the structure, without any direct interaction with the target. Consequently, it was overall concluded that the oxidation may just marginally or not affect at all the Anti–PD-L1 mAb ability to bind its target PD-L1.

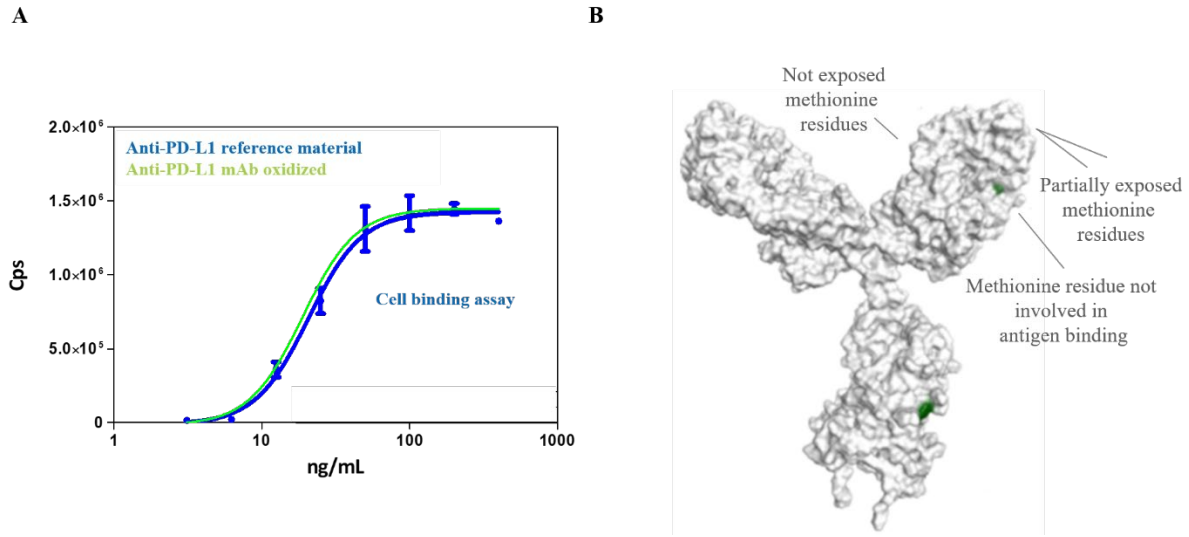

Figure 19 In-Silico analysis and cell binding assay confirmed that Fab activity was not affected by oxidation

Data provided by structural analyses and literature were used to assess the criticality of some methionine residues prone to oxidation, whose were located in the Anti–PD-L1 mAb CDRs. Moreover, an alternative cell-binding assay was run in order to complement the information package obtained with previous biological methods.

Adopting a similar "holistic" approach, the role of deamidation on Fab functionality was also elucidated. At this aim, an Anti–PD-L1 mAb variant characterized by the fully deamidation of Asn 1 located on one of the CDRs of light chain and potentially involved in the binding to the target, was generated by site-direct mutagenesis. Specifically, an asparagine residue was completely substituted by an aspartic acid, which is the classic residue in which the asparagine is converted. In this regard, the generation of specific sequence variants is a common practice conducted during later stages of a drug development program, as it is a costly and time-consuming practice. As this variant brought a sequence mutation, an impact on the entire structure cannot be excluded. For this reason, the sample have been analyzed by an extended characterization panel constituted by an *in-silico* analysis (data not shown) and different functional assays.

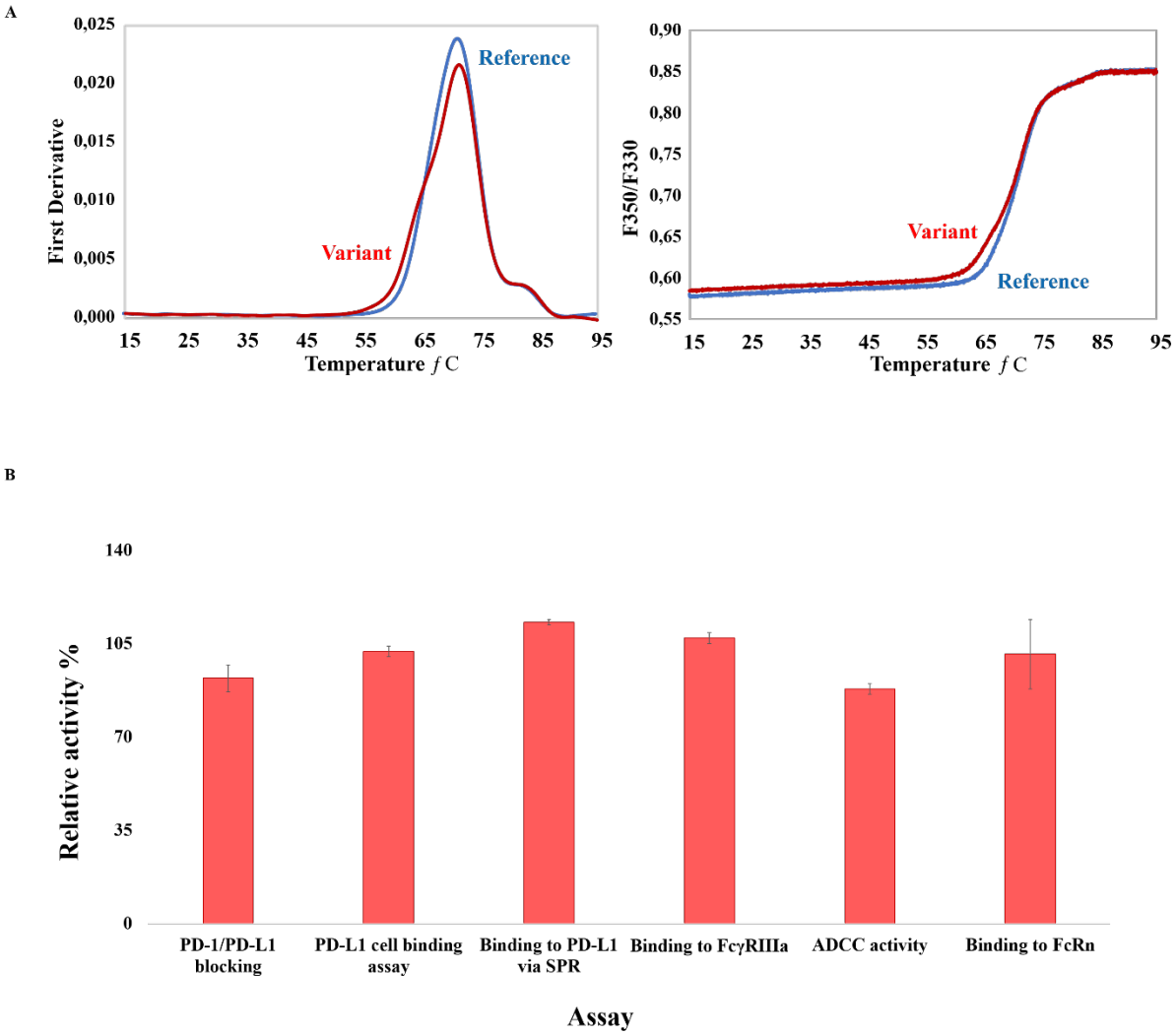

Figure 20 Site-specific deamidation mutant and its role on Anti–PD-L1 biological properties

As already done for the oxidation assessment on the CDRs, the role of deamidation on Fab portion biological activity was further assessed as well. In this case, it has been induced a site-specific mutation on an Asn site located in one of CDRs loops. This residue was fully converted to an aspartate residue. Then, the mutant was analyzed by the panel above, in order to assess its structural stability and biological properties**. A.** Nano DSF analysis of the stability profile of wild-type and variant Asn/Asp **B.** Functional analysis of Asn/Asp variant**.**

The Asn interaction network looked slightly changed compared to wild type, but the new interactions seemed in any case preserve the secondary structure (structure not shown).

As a consequence of such modification, the nano differential scanning fluorimetry (nano DSF) analysis Figure 20 B provided useful information regarding the overall molecule stability, which seemed to be moderately affected following the substitution event. Nano DSF indeed,

leverages the intrinsic fluorescence of tryptophan and tyrosine residues, whose may change in relation to their exposure to the external environment, indicating whether the antibody results unfolded in comparison to its reference standard. The fluorescence ratio (F350/F330) is measured respect to the increment of temperature and it monitors changes in fluorescence intensity as well as tryptophan specific shift of the fluorescence emission maximum. In Figure 20 B the Asn variant is drawn in red, while the reference material in blue.

Looking at ratio of F350/330, it was noticed that the variant shows the same three thermal transition typical of the reference material, probably associated to a different structural stability of the domains where the mutation is located. Moreover, focusing on the several T_{onset} (temperature at which unfolding begins) it was noticed that the variant sample showed a reduction of about 5°C then reference material (55.8°C vs 60.8°C.). From the 1st derivative transformation, the profile results of easier interpretation. In conclusion, the thermodynamic stability of this variant seems to be slightly decreased if compared to that of reference material. However, despite this data, the results shown in Figure 20 C indicated that all the antibody functional properties monitored on both Fab and Fc portions were preserved. Indeed, neither Fab binding nor Fc-mediated effector functions resulted affected by the mutation. Finally, from the analysis of dose-response curves (not shown), it was confirmed that both mutant and reference material were comparable also from behavioral point of view.

In conclusion, these results indicate that the Anti–PD-L1 mAb deamidation occurring on critical asparagine residues on the Fab portion, alone, does not significantly affect its biological activity to bind the ligand PD-L1; also, the presence of secondary degraded products like large or small aggregates and antibody fragments, may have a relevant role in reducing this binding by enhancing the small effect carried out by some post translational modification occurring on critical sites.

3.5 Isolated High molecular weight and low molecular weight species significantly affect Anti–PD-L1 mAb ability to bind its target PD-L1

Starting from assumptions made in the previous paragraph and following the approach of isolating specific antibody degraded products to be analyzed by a functional point of view, the same was made for HMWs and LMWs forms.

Generally, it is reported that HMW species have a negative effect on the biological activity, both in terms of binding to the target and antibody-mediated effector functions. Data from literature show that multimeric self-assembled recombinant proteins activity was decreased by FACS and ELISA analysis and responses were lower when HMWs % rose up (57). In order to confirm or deny this hypothesis, it was conducted a dedicated structure-activity study to explore the relationship between the presence of these species and the ability of Anti–PD-L1 mAb in binding its target PD-L1. At this aim, Anti–PD-L1 mAb HMWs and LMWs native forms were isolated and purified by SEC-LC starting from the intermediate bulk of a production batch. The procedure followed is described in "materials and methods" section. These materials were then used to generate four different levels of enriched HMW and LMW samples respectively, by diluting the native-HWMs (85.1%) and native-LMWs (97.9%) enriched fractions, with an anti–PD-L1 mAb control batch having a measured level of HMW species of 0.53% and of LMW species of 3.80%. The two series of mixtures were then analyzed by blockade assay to monitor the Anti–PD-L1 mAb ability to block PD-L1/PD-1 interaction.

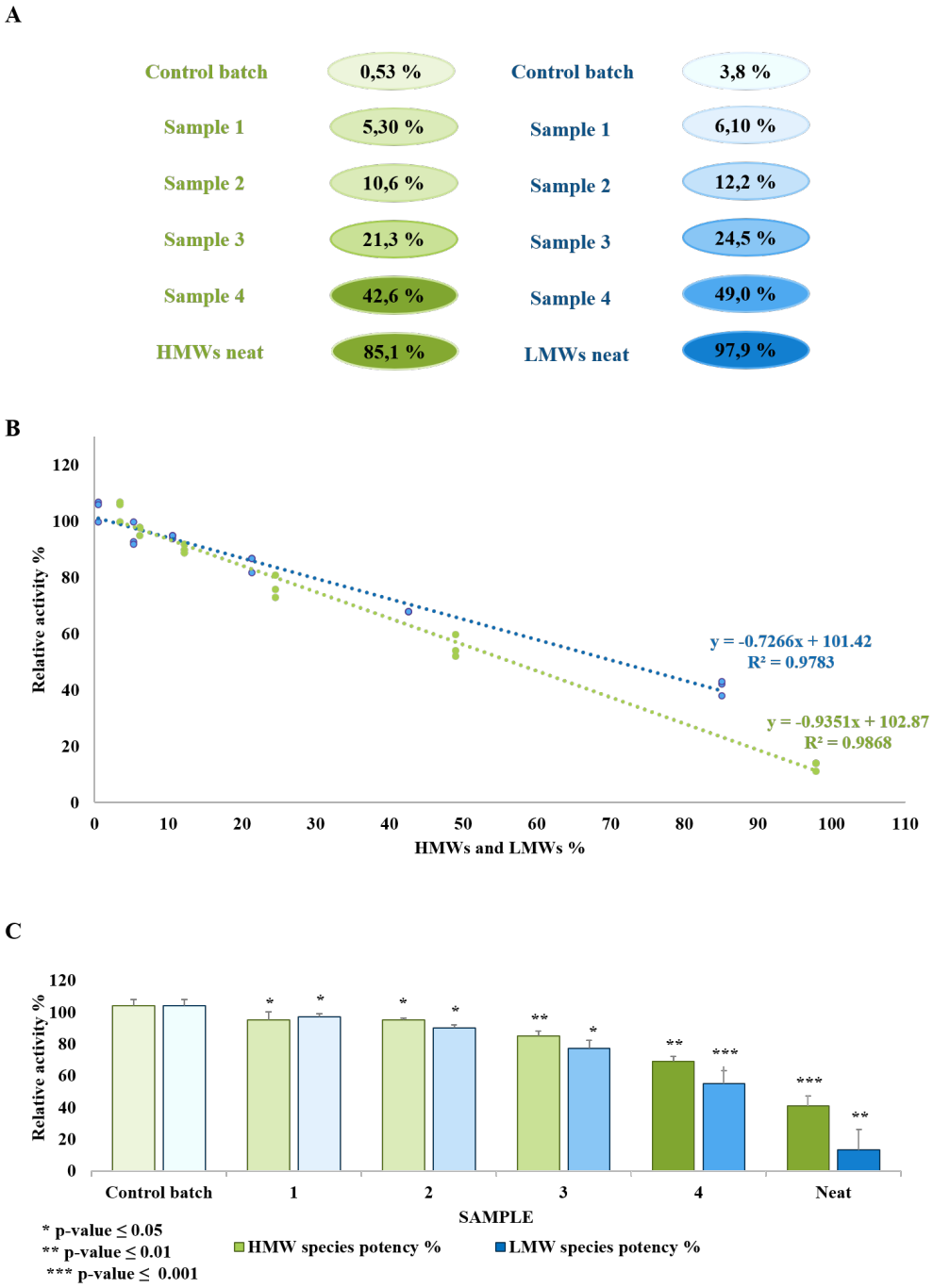

Figure 21 Structure-Activity relationship of Anti–PD-L1 mab HMWs/LMWs forms and biological activity

(A) HMWs and LMWs mixtures were prepared and tested by cell-based blockade assay for their ability to block PD-1/PD-L1 interaction. **(B)** Relative potencies results were generated and analyzed by linear analysis, resulting in a linear relationship among the increase of these species and a reduced biological activity. **(C)** Each relative potency value was compared head-to-head with that obtained testing the control batch. The difference in terms of relative activity was already significant when sample 1 was tested against control. However, a "real" negative effect of these species on the antibody function is more appreciable starting from sample 3.

In Figure 21 are reported the results obtained in terms of PD-L1/PD-1 blocking activity of Anti–PD-L1 mAb HMWs and LMWs native species tested. Firstly, it was demonstrated a clear relationship between these species and biological activity by linear regression analysis. Then, the several dilutions were analyzed head to head against the control batch by one-way ANOVA analysis. Results proved that biological activity was found statistically different from control batch starting from very low amount of these species (sample 1 and 2), even if a dramatic effect was obtained with mixture 3. As levels of HMWs and LMWs contained in samples 1 and 2 are usually those obtained during typical forced stressed conditions, it was assumed that at certain %, these species in combination with other types of structural modifications, may moderately contribute to the changes in biological activity.

3.6 Lack of core fucose and high mannosylation influence Anti–PD-L1 effector functions but does not affect its binding to PD-L1 and PK

As already defined in the introduction, ADCC is an Fc-mediated effector function that is typically part of Monoclonal antibody's Mechanism of Action (MoA). A mAb is able to trigger the ADCC activity by engaging through its Fc portion the FcγRIIIa (CD16, FcγRIIIa-158 V/F, Valine or phenylalanine polymorphism). FcγRIIIa is a receptor belonging to the FcγRs family, which is found widely expressed on several immune cells types, and more frequently, on Natural killer cells (NK). Anti-PD-L1 mAb, as IgG1-based antibody, exerts its therapeutic effect by leveraging this innate immune mechanism beyond targeting the transmembrane protein PD-L1 on tumor cells.

Anti–PD-L1 is an IgG-based mAb produced in CHO cells and has one Fc glycosylation site at Asn300. Beyond blocking PD-1/PD-L1 immune inhibitory pathway, a potent ADCC activity is also part of its mechanism of action. Like other therapeutic IgGs, ADCC activity depends on the quantity and complexity of the glycosylation patterns characterizing its structure. From literature it is known that the absence of core fucose in an IgG results in higher affinity binding to the FcγRIIIa allotypes F158 and V158 and increased ADCC activity (58). Other evidences demonstrated that, even if to a lesser extent, also high mannose species and galactosylation positively influence the binding to FcγRIIIa receptor and consequently the ADCC activity, while sialylation has an opposite effect (45). Finally, beyond the specific generation of such classes of glycans, the effect of the overall glycation of mAbs is also investigated during characterization studies, as it may occur during routine manufacturing and storage as well as during *in vivo* circulation (59). However, in most of published papers there are no particular reportable effects on Fab functionality, PK, FcγIIIa receptor and ADCC activity, so no major effects are expected for this stress (60).

Taking into consideration these assumptions, the following study aimed at defining a relationship between structural elements and functional properties of Anti–PD-L1 mAb, providing relevant data to support the current manufacturing process and define functional threshold limits in support of current product specifications. Through the application of tailored analytical strategy, it is possible to highlight potential differences in the product quality attribute profile that potentially affect safety and efficacy at certain levels.

In this study, the results obtained so far are related to the glycation, a-fucosylated and high mannose species. Experiments for evaluating the biological effect of galactosylated and sialylated variants are still ongoing and will be included in future works.

Anti–PD-L1 mAb samples were treated in order to increase the amount of overall glycation by incubating the samples with Glucose 1M. High mannose and a-fucosylation instead, were induced by adding Maduramycin ammonium and 2F-Peracetyl-Fucose (a Fucosyltransferase Inhibitor) in production medium. 2-AB peptide glycan mapping analysis was performed to quantify the total % of glycated, high mannosylated and a-fucosylated species. Results confirmed that treatments successfully modified Anti–PD-L1 mAb samples as shown in Figure 22, A-B. Afterwards, these species were qualitatively and quantitatively characterized by several *in vitro* platforms in terms of FcRn binding, Fab portion ability to block PD-1/PD-L1 interaction (target binding) and binding to the FcγRIIIa receptor (V158), Figure 22, C-D-E.

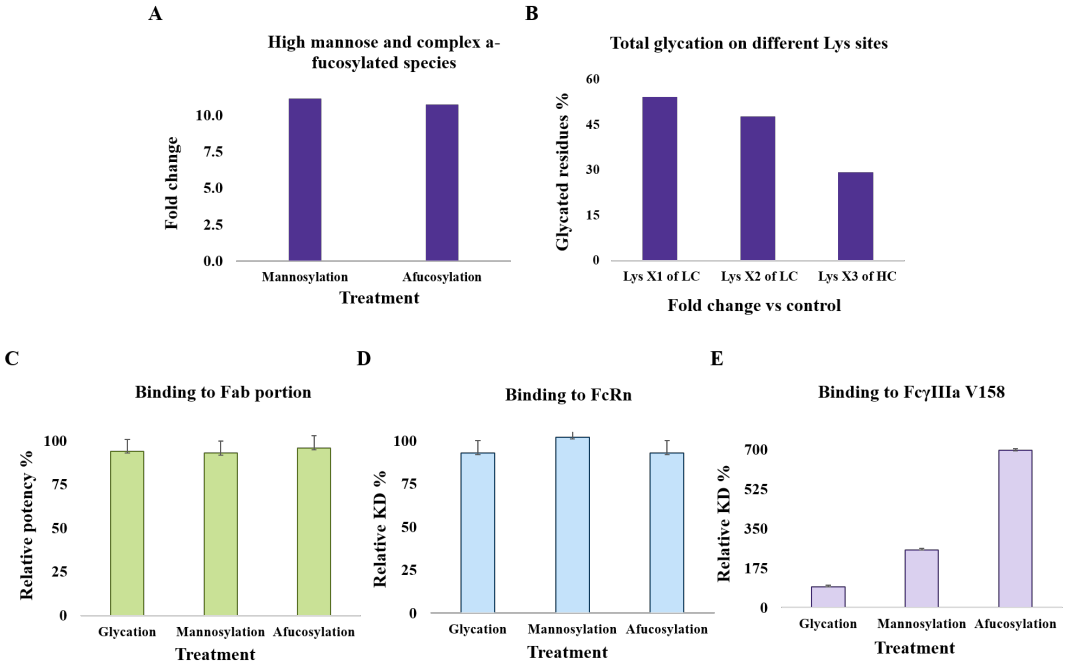

Figure 22 2-AB glycan mapping and biological results

2-AB glycan mapping analysis confirmed an increase of high mannosylated, A-fucosylated and glycated species. **A.** Total mannosylation and a-fucosylated glycans levels were quantified after being treated with specific enzymes. Results are expressed as fold change, given by the ratio of HM and AF forms of treated samples respect to those of untreated reference material. **B.** Three specific lysine residues were monitored as hot spots of glycation. Results were expressed as total % of glycation of critical lysine residues. **C, D, E.** Binding to Fab portion, FcRn and FcγIIIa receptor were monitored by blockade bioassay and SPR analysis. Results were expressed as relative potency % in the first case while FcRn and FcγIIIa receptor bindings were quantified as relative KD %. The Anti–PD-L1 mAb FcγIIIa binding was clearly affected by high mannosylation and a-fucosylated complex species.

As shown in Figure 22, 2-AB peptide mapping confirmed that treatments led to a strong increase of Anti–PD-L1 mAb high mannosylated, A-fucosylated complex and glycated species. In particular, mannosylation and a-fucosylation were increased of 11.1 and 10.7 folds (compared to the reference material) while glycation affected several critical lysine residues (Figure 22, A-B). The functional analysis of Anti–PD-L1 mAb confirmed some evidences found in literature for other similar drug products (Figure 22, C-D-E). Indeed, while Anti–PD-L1 Fab portion functionality and its binding to the FcRn were not affected at high level of these post translational modifications, the binding to the FcγIIIa receptor was significantly enhanced due to the presence of a-fucosylated complex (696 %) and high mannose species (256 %). Glycation instead, did not affect but neither enhanced Anti–PD-L1 mAb binding to the FcγIIIa receptor.

3.7 A-fucosylated and higly mannosylated variants significantly enhance Anti–PD-L1 mAb binding to FcγIIIa receptor and its ADCC activity

In order to understand up to which level complex a-fucosylation and mannosylation significantly enhance the binding to the FcγIIIa receptor and whether this activity correlates with antibody ADCC activity, a-fucosylated complex and highly mannosylated Anti–PD-L1 mAb mixtures were prepared and tested by reporter gene assay and SPR technology (Figure 23 A). These mixtures were generated by spiking several amounts of a control batch into samples containing high concentration of high mannose and a-fucosylated complex species. Results of these experiments were used to define a relationship between these biological activities and the levels of glycans tested. From a technical point of view, it is important to note that the presence of high mannose species within generated a-fucosylated complex samples was considered as having a negligible impact as their concentrations were low. Additionally, as reported in the literature and demonstrated by results of the current paragraph, the impact of mannosylated species on the ADCC activity and FcγIIIa receptor binding activity was relatively low, around those levels tested during this study. Regarding this latest consideration, M. Hutterer et al. (61) reported that values of about 5 % of high mannose species did not affect the FcγIIIa receptor binding or ADCC activity of their human IgG1-based mAb, a Trastuzumab biosimilar candidate. For these reasons, a potential cross-functional effect on ADCC caused by the concurrent presence of high mannose species in the tested a-fucosylated variants, should be negligible. Furthermore, the same considerations can be due for galactosylated and sialylated species, whose slight changes should not impact the ADCC activity overall.

The spiked a-fucosylated complex and high mannose species were then analyzed by reporter gene assay in order to monitor their ability in exerting ADCC. Specifically, dose response curves obtained were analyzed from a qualitative point of view (Figure 23, Figure 24).

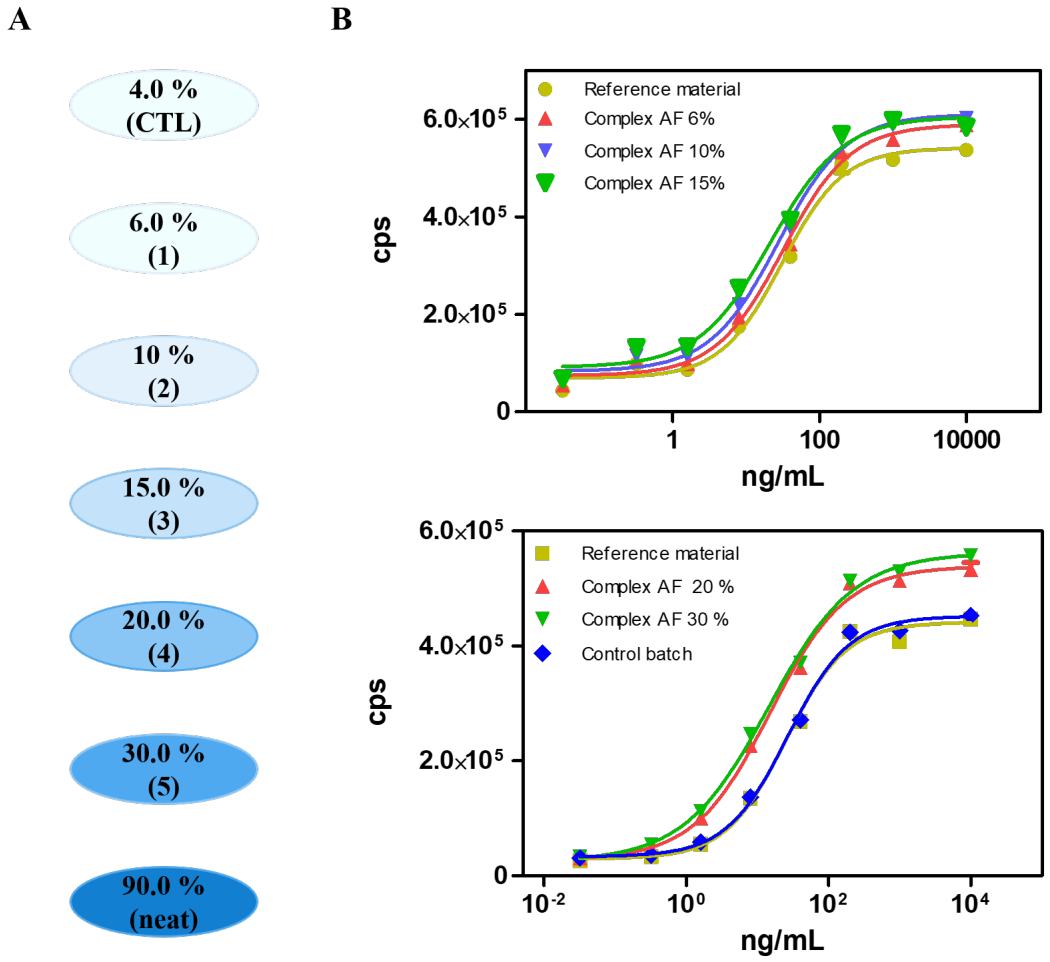

Figure 23 Qualitative evaluation of dose-response curves of AF complex species

A. Different mixtures of complex a-fucosylated forms were generated by spiking neat variants (about 90% of complex a-fucosylated species) with a control batch sample characterized by low levels of a-fucosylation % **B.** Exemplary dose-response ADCC curves of the reference material, control batch and the several a-fucosyalted mixtures. Curves were fitted with a 4 Parameter Logistic nonlinear regression model and compared to the reference material by F-test, in order to verify whether their biological behavior were comparable to the standard.

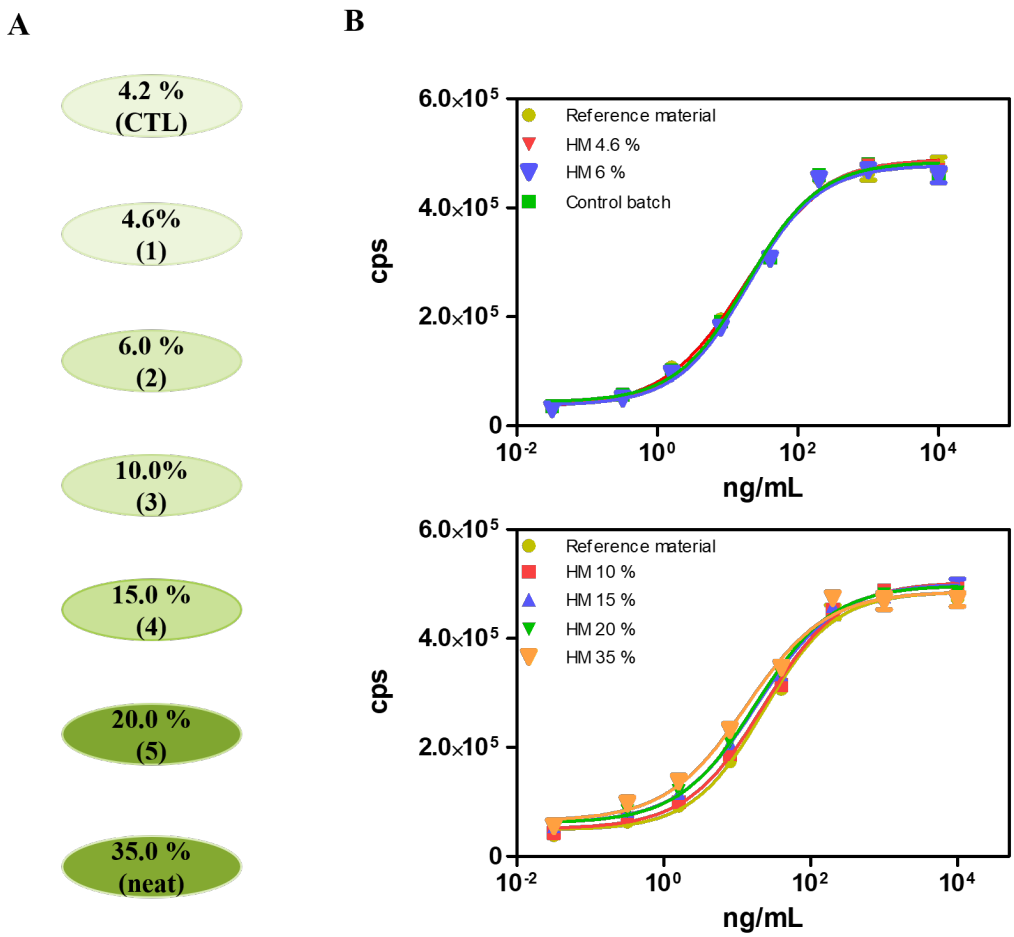

Figure 24 Qualitative evaluation of dose-response curves of HM species

A. Different mixtures of high mannose forms were generated by spiking neat variants (about 35 % of high mannose species) with a control batch sample characterized by low levels of high mannose % **B.** Exemplary dose-response ADCC curves of the reference material, control batch and the several high mannose mixtures. Curves were fitted with a 4 Parameter Logistic nonlinear regression model and compared to the reference material by F-test, in order to verify whether their biological behavior were comparable to the standard.

EC_{50} values were calculated from dose-response curves fitted with a 4 Parameter Logistic nonlinear regression model, while the comparison among the different dose-response curves against reference material was performed by F-test analysis. The qualitative analysis of dose-response curves obtained by testing these samples, proved that the biological behavior resulted comparable to the reference material up to 10 % of complex a-fucosylation and 35 % of high mannosylation. In particular, it is quite clear the differences highlighted to the top of the dose-response curves (maximum efficacy), where Anti–PD-L1 mAb a-fucosylated complex species

(15 %, 20 % and 30 %) were found statistically different respect to Anti–PD-L1 mAb reference material. However, the values of R^2 of all dose-response curves (data not shown) were found within the analytical procedure limits, meaning that the biological behavior was appropriately described, thus not lost due to the modification. Finally, due to the disproportionate biological response of the sample characterized by the highest level of a-fucosylation complex (about 90 %), it was not possible to fit the dose-response curve and to calculate a potency value.

The same a-fucosyalted complex type and high mannose samples reported above, were also analyzed by SPR, in terms of binding to FcγIIIa receptor (Figure 25 A-B). In the case of a-fucosylated complex species, the qualitative analysis was performed by fitting sensorgrams deriving from treated samples (red line) and control batch (green line). As shown in Figure 25 A, the sensorgrams of these samples resulted comparable to the reference material up to 10 %. At higher % levels instead, the differences in terms of association and dissociation of the Fc-FcγIIIa receptor complex were clearly appreciable. On the other hand (Figure 25 B) sensorgrams obtained from high mannose variants (green line) were qualitatively comparable to that of control batch up to 20 % of high mannose species (red line), while at 35 % it showed a different behavior in binding to FcγIIIa receptor.

A

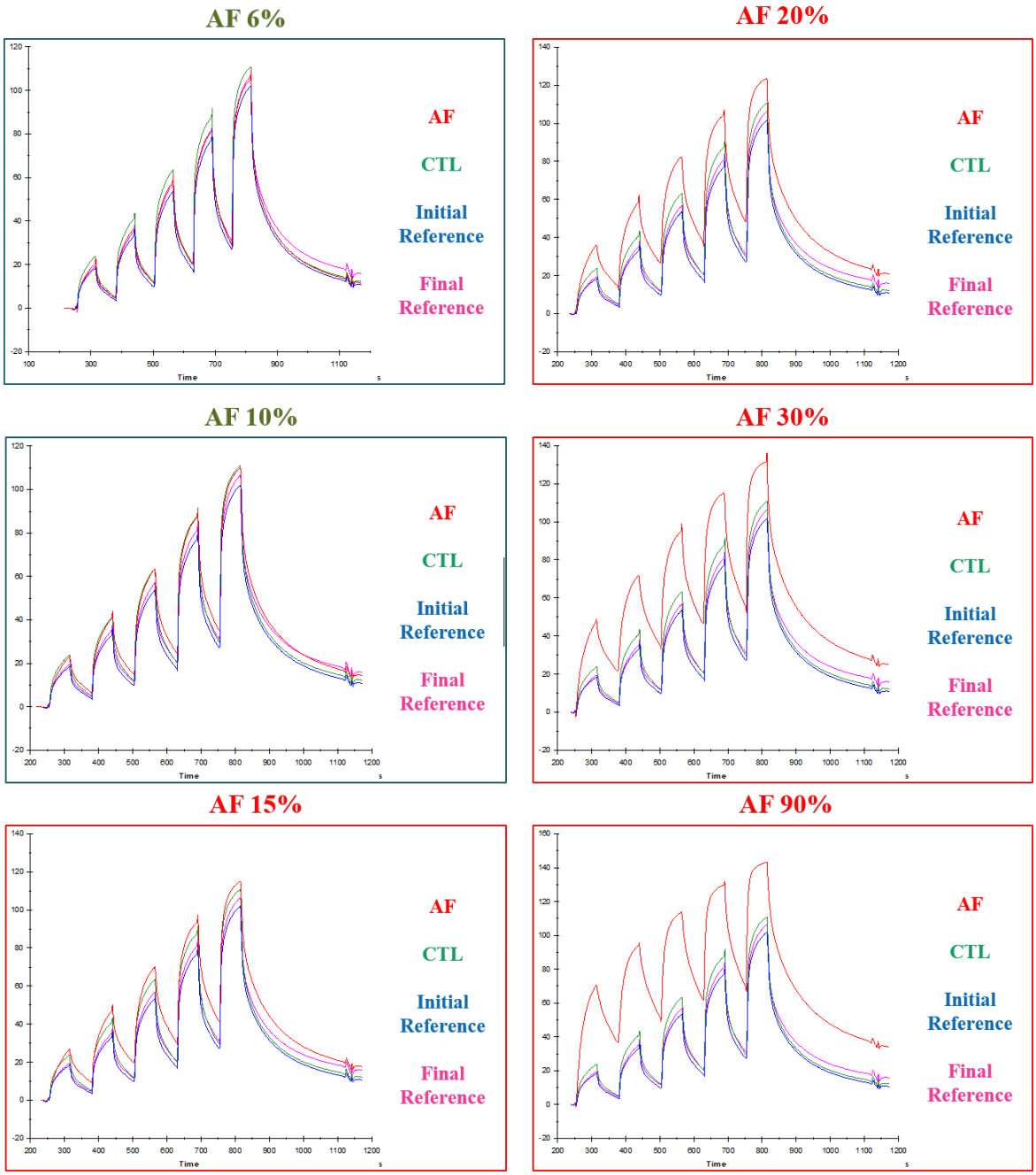
AF 6%
AF
CTL
Initial Reference
Final Reference
Time
s
AF 20%
AF
CTL
Initial Reference
Final Reference
Time
s
AF 10%
AF
CTL
Initial Reference
Final Reference
Time
s
AF 30%
AF
CTL
Initial Reference
Final Reference
Time
s
AF 15%
AF
CTL
Initial Reference
Final Reference
Time
s
AF 90%
AF
CTL
Initial Reference
Final Reference
Time
s

B

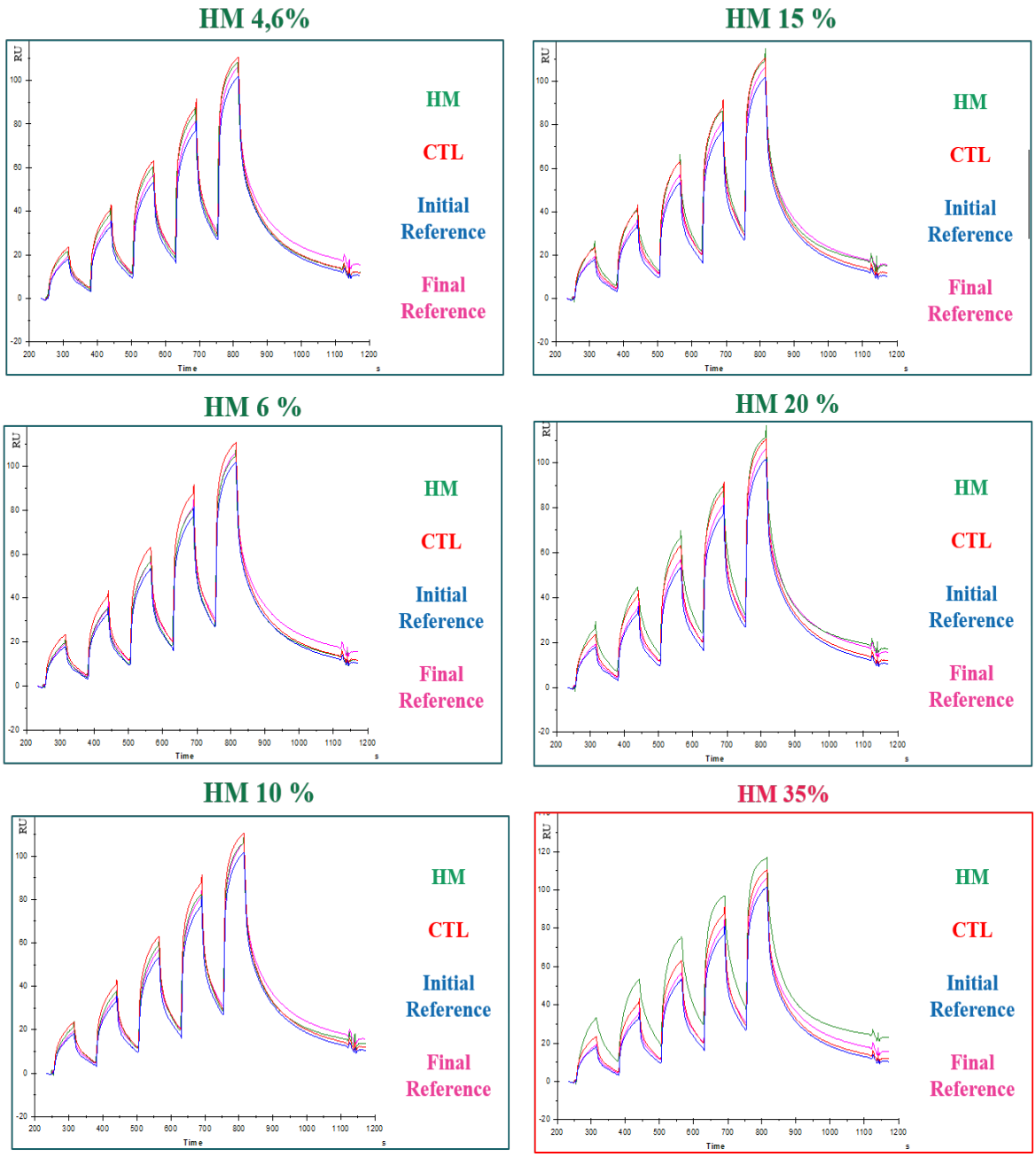

Figure 25 Sensorgrams analysis of AF and HM complex mixtures

A. Sensorgrams obtained from the analysis of different mixtures of a-fucosylated variant (green line) were compared from a qualitative point of view with reference material (pink line) and evaluated **B.** The same analysis was performed also for highly mannosylated species. In both experiments, a control batch was also run in parallel as internal control of the analysis and instrument performance.

In addition to a qualitative assessment, these samples were also analyzed from a quantitative point of view. Looking at Figure 26 A-B, it was demonstrated a direct correlation between high mannose and a-fucosylated complex type species with biological activity, in terms of both relative potency and KD %. Specifically, ADCC activity was directly correlated to the abundance of these species, and SPR analysis provided even more pronounced results in terms of binding affinity to the FcγRIIIa receptor. It is also to be mentioned that a-fucosylated complex samples 4 and 5 provided potency % values falling outside the analytical linear range of the method (set between 50-150 of relative potency % during method development and validation study), in which the potency estimation may result not accurate. Finally, due to the disproportionate biological response of the sample characterize by the highest level of a-fucosylation complex (about 90%), it was not possible to fit the dose-response curve and to calculate a potency value.

In addition to previous findings, while dose-response curves and sensorgrams indicated that qualitatively AF and HM species were comparable to the reference material up to 10% and 20% respectively, the relative potency % and relative KD % resulted affected at lower levels (Figure 26 A-B). In fact, potency data resulted statistically different from control sample at 10 % of total a-fucosylation complex and 15 % of total mannosylation. On the other hand, the binding to the FcγIIIa receptor resulted statistically different respect to reference material in presence of the 15 % of complex a-fucosylated species and 20 % of species characterized by high mannose.

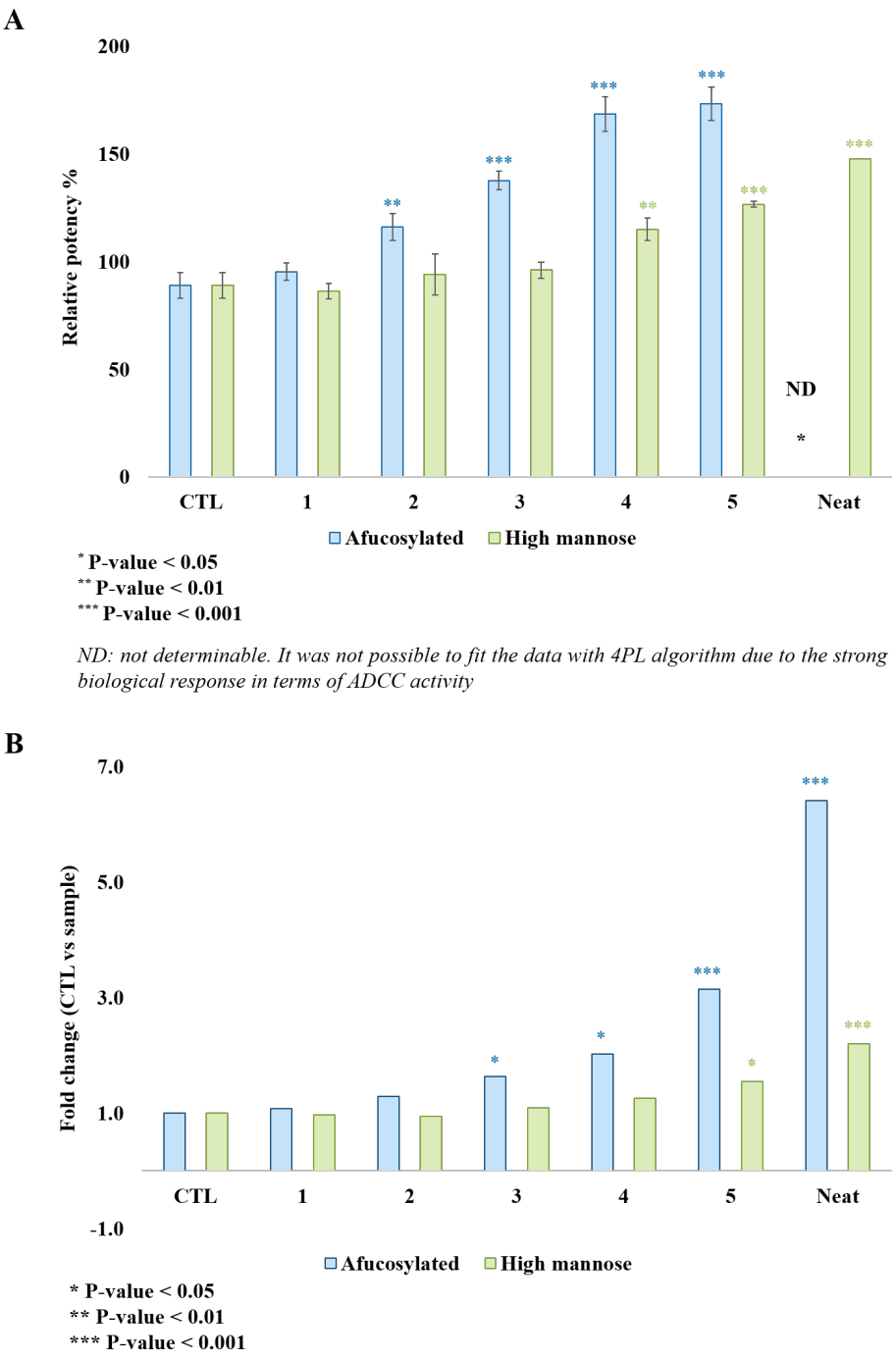

Figure 26 ADCC activity and FcγIIIa binding results

The different mixtures obtained from two variants at high a-fucosylation and high mannosylation % were analyzed by reporter gene assay and SPR analysis. **A.** Anti–PD-L1 mAb ADCC activity and affinity towards FcγIIIa receptor are positively correlated to increased % of mannosylation and a-fucosylation, in a linear and exponential manner respectively **B.** Reporter gene assay and SPR results were reported on a graph bar as relative potency % and fold change respectively. Each spiked sample was analyzed one-by-one with a control batch containing basal levels of each oligosaccharide form by one-way ANOVA analysis. The degree of significance was expressed considering different P-values levels.

As overall conclusion, taking into consideration both qualitative and quantitative analysis, the Anti–PD-L1 mAb binding activity to the FcγIIIa receptor and its ability to trigger ADCC activity, resulted significantly impacted when it brings the 10 % of complex a-fucosylated and 15 % of high mannose species.

3.8 Anti–PD-L1 ADCC activity is maintained down to low levels of a-fucosylation (complex forms) and high mannosylation

Considered data collected in the previous experiments, as a general rule it can be inferred that low or moderate levels of high mannosylation can be considered not such a critical attribute like a-fucosylated complex species. Many evidences found in literature indeed demonstrated that the effect of high mannose species on ADCC activity of several types of biotherapeutics is considerably less extended when compared to those caused by a-fucosylated complex species. M. Hutterer et al. (Amgen) reported that both values up to 5 % of high mannose species (61) did not affect the FcγIIIa receptor binding and ADCC activity of their ABP 980 human IgG1-based mAb, a Trastuzumab biosimilar candidate. Consideraing the data obtained and evidences in literature, the high mannose species are not critical in terms of ADCC activity and binding towards the FcγIIIa receptor down to the 4% of these species. In addition to the previous conclusions, as minimum amounts of a-fucosylated complex forms can significantly affect the aforementioned biological functions, the reverse could affect molecule properties as well. Indeed, even low levels of a-fucosylated complex forms may lead to an inefficacious ADCC activity. Maja Pučić and collegues, reported that in a population study, the fraction of neutral IgG glycans without the core fucose was found to vary between 19.3% and 1.3 %, where the lower value can negatively affect effector functions in individuals (62). For this reason, considering the criticality of this attribute to Anti-PD-L1 mAb structure, behavior and function, a subsequent study was performed to explore whether there is any lower a-fucosylation limit, below which, ADCC activity would no longer be therapeutically efficacious.

With the aim to deeply explore the relationship between very low amount of a-fucosylated samples and their biological activity, a new experiment has been designed. Specifically, it was used a new control batch containing almost the same levels of other oligosaccarides but lower levels of a-fucosylated complex forms respect the previous control batch. Starting from this sample, a new set of spiked samples was generated. The new mixtures were produced starting from the 15% of a-fucosylated complex species going down to the 3.3% (control batch).

Furthermore, since the control batch is characterized by the 3.3 % of a-fucosylated complex species, in addition to the classical linear regression analysis, it was performed also a predictive analysis in order to extrapolate the "theoretical" EC_{50} value when 2% of a-fucosylated complex glycan type is present into the sample. Indeed, one of the obejective of this activity was the determination of the biological activity of levels below the 3 %, which is difficult to reach in the current manufacturing process. At this aim, for the generation of these different mixtures, a new spiking experiement was performed using this new control batch and mixing it with the previous highly a-fucosylated sample. Since the reporter gene assay is fully representative of the ADCC mechanism of action and it is the assay used in routine for monitoring this activity, it was used to test the Anti–PD-L1 ADCC activity. However, biological assays are characterized by a general intrinsic variaibility that usually does not allow to really appreciate slight differences in terms of biological activity in relation to the presence of small ammounts of structural elements. For this reason, it was decided to perform a correlation analysis using EC_{50} values and % of a-fucosylated complex species, rather then analyze potencies of each sample one to one against the potency provided by a control batch. Furthermore, since the EC_{50} value is an absolute measure of biological efficacy, and it may depends on the physiological state of the cell culture used on the day of experiment, results were technically standardized by performing the entire analytical session (3 runs) in one single day. The scope to adopt such a technical expedient was to "normalize" as much as possible the basal activity levels of cells used, which depends on both their metabolic state and by the variability due to the manipulation from different operators. This modification allowed to test all different spikes side by side and to perform a qualitative comparison of all the dose response curves. Anyhow, each replicate was prepared independently to guarantee the requirement of the independence of technical replicates.

In Figure 27 are shown the several mixtures characterized by several amounts of a-fucosylated complex forms and results of the ADCC activity are reportered. The dose-response curves of the three experiments were compared one to one with that of reference material. Despite some differences in the top values, overall, the statistical F-test assessed that all curves obtained testing 3.3 % to 10 % of a-fucosylated complex species in each experiment were found to be comparable to the reference material. Furthermore, each curve resulted well-described (in terms of top, slope and bottom values) and showed a high value of the goodness of fit (greater than 0.98). However, as already observed in the previous SAR study, the dose-response curves obtained testing the mixtures containing 12 % and 15 % of a-fucosylated complex type species were statistically different respect to the dose-response curve of reference material. Typically,

the potency value generated by a dose-response curve which does not result to be statistically similar to that of reference material, is considered not comparable and cannot be calculated. In addition to the RGA analysis, the same samples were also tested by biacore platform in order to also monitor the Fc-FcγRIIIa binding. The qualified SPR procedure was applied as the technology allows the testing of up to 12 samples in the same analytical run, allowing a head to head comparison of all the tested samples. The EC_{50} results were obtained by analyzing the three runs performed on the same day. Similarly, SPR data were expressed as relative KD % obtained from three independent analytical runs.

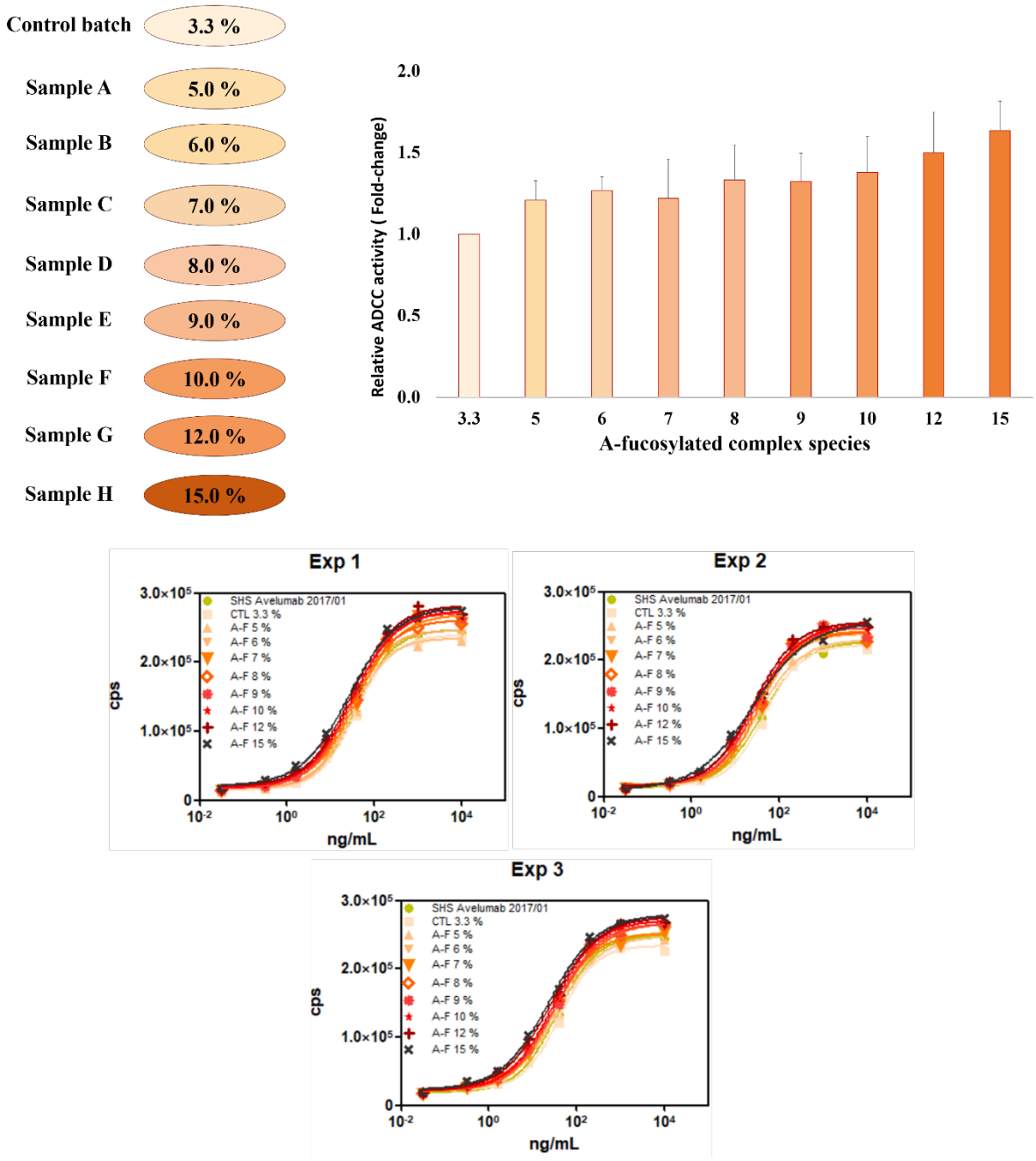

Figure 27 Experimental layout and dose-response curves

A. Several mixtures of the a-fucosylated variant previously used was mixed with a control batch containing low basal levels of a-fucosylated complex species. **B.** ADCC results are reported as fold-change given by EC_{50} of treated sample respect to that or reference material. Each mixture was loaded one time on three different plates (biological triplicate). **C.** In order to verify their biological behavior, curves were fitted with a 4 Parameter Logistic nonlinear regression model and compared to the reference material by F-test.

After that, these mixtures characterized by several levels of a-fucosylated complex species were further analyzed by linear regression analysis to define a theoretical functional threshold limit (Figure 28).

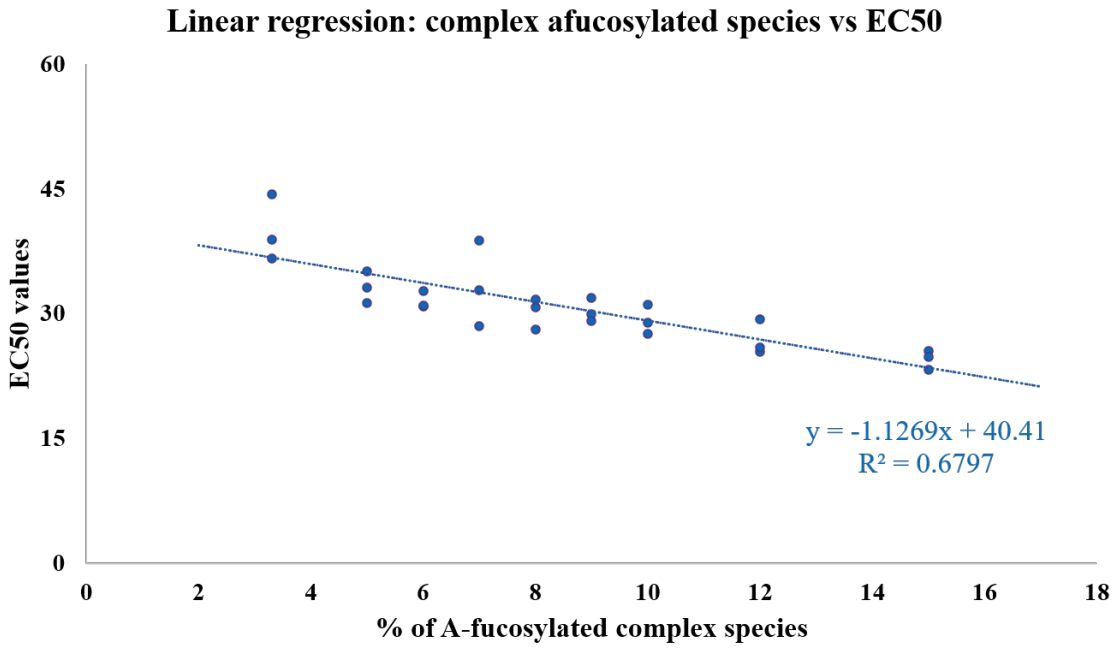

Figure 28 Linear regression and prediction analysis of low levels of complex a-fucosylated species

ADCC results expressed as EC_{50} values and the different levels of complex a-fucosylated species were plotted and analyzed by a regression analysis. The increased levels of a-fucosylation was linearly correlated to EC_{50} values and this linear relationship allowed to make reliable EC_{50} prediction down to low levels of a-fucosylated species.

The three EC_{50} values generated from these different runs, were plotted on a scatter graph and analyzed by linear regression. Overall, the check of the several parameters defining the goodness of this statistical model (not fully shown), led to the conclusion that it was enough representative in describing the biological relationship between a-fucosylated complex species and ADCC activity. In the end, also this analysis which started from the 15% of a-fucosylated species and went down to the 3.3 % showed a clear correlation among these species and ADCC activity. However, the main objective for which this regression was performed, was the fact that during the first study it was not possible to make any prediction of the biological activity

of samples not experimentally tested (specifically a “theoretical” EC_{50} at 2% of a-fucosylated complex type species). In other words, in the previous regression study there were no sufficient data points to create a reliable statistical linear regression model allowing a correct generation of relative potency values from samples showing not comparable top values (15%, 20% and 30% showed in Figure 23). In this new study, the use of the EC_{50} values was anyhow representative of the biological activity of the samples tested, but contextually, did not implied a preliminary comparison with a reference material to calculate a reliable relative potency value. Furthermore, this time 9 data points (9 different mixtures) useful to create a representative statistical model were available. As a consequence, it was performed a predictive analysis aimed at extrapolating a theoretical EC_{50} value of a sample bringing 2 % of a-fucosylated complex type species. The results in Figure 28 indicated that a possible EC_{50} value provided by a sample with 2 % of a-fucosylated complex forms could be about 38. Given that the average of the EC_{50} value obtained from dose-response curve of reference material was close to that value (data not shown), the two results can be considered comparable.

4 Discussion

The characterization of new biological entities is a mandatory practice that starts since the earlier stages of drug development and continues even after marketing authorization. This procedure is highly recommended by Health Authorities (which are responsible for reviewing the documental package for submission) and regulated by several international guidelines. Nowadays, biotech companies are even more prone to define well-tuned analytical strategies for the deep understanding of their biotherapeutic candidates. Among these strategies, several companies used to carry out dedicated structure-activity relationship studies to reach a deep molecule knowledge and improve final product understanding (32). These studies are conducted to complement the CQA assessment and bring out structural and functional features, with the final aim of ensuring the highest quality standards.

In this work, an advanced biological characterization of an Anti–PD-L1 mAb has been carried out by leveraging structure-activity relationship studies designed for this purpose. The results obtained so far clarified the role of several Anti–PD-L1 mAb degradation pathways on its binding properties, PK and ADCC activity while others are still under investigations. Starting from the accumulated knowledge on Anti–PD-L1 mAb mechanism of action, different experiments based on forced degradation studies and the generation of specific variants have been performed. Products generated by such stress were then characterized by an extended physico-chemical and functional analytical panel. Besides the mere characterization of this therapeutic antibody, it was also proposed an analytical strategy aimed at defining functional thresholds at which specific structural attributes can affect antibody biological activity. This latest experimental information has been obtained through dedicated structure activity relationship studies conducted for those attributes believed most critical for Anti–PD-L1 mAb functionality.

Firstly, in order to support functional data, a series of physico-chemical analysis were performed to highlight molecule structural modifications mainly induced by chemical and physical treatments. Among the several treatments undergone by the molecule, thermal stress had an impact on several attributes, resulting in an extended degradation profile. It is well-known indeed that such condition commonly induces antibody aggreagation and fragmentation. Although high temperature mainly favorites the formation of these degraded products, such condition can also induce deamidation of asparagine and glutamine residues, methionine oxidation, isomerization events as well as the generation of other minor degradation products

(48). Looking to the physico-chemical results reported in Figure 9, the overall deamidation of molecule was increased in all the four asparagine residues monitored. However, looking at Anti–PD-L1 mAb structure (not shown), despite Asn 1-2 are located on a Fab portion which is less involved in the antigen binding, they seem not having a main role in the interaction with PD-L1. In particular, the Asn 1 located in a loop of one of the CDRs, which could be partially involved in the binding to PD-L1, was found only moderately deamidated compared to reference material (8.0 % and 2.10 % respectively) after thermal stress. Regarding the Anti–PD-L1 mAb biological activity, monitored via cell-based assay and expressed as its ability in blocking the PD-L1/PD-1 interaction, it was considerably decreased over the weeks at +50°C (96 % at time zero and 84 % and 78 % after 2 and 4 weeks). Orthogonally, a Biacore analysis aimed at determining the binding affinity between Anti–PD-L1 mAb fab portion and its target PD-L1, was quite aligned with cellular results. Indeed, the relative K_D % decreased from 99 % of untreated sample to 93 % and 78 % after 2 and 4 weeks of exposure. From an in-depth analysis of the rate constants in PD-L1/PD-1 complex formation, it was noticed that these results were mostly impacted by an increased propensity to dissociate, more than a change in terms of association. Concerning this result, together with the post translational modifications following thermal stress, it should be considered that the presence of fragments or small and large aggregates could also contribute to the observed slight decrease of potency and binding affinity. In fact, while deamidation should not dramatically impact potency (based on deamidation % of Asn 1 and the criticality of this residue), simultaneous changes in HMWs and LMWs make it difficult to selectively address the impact to the deamidation only.

Concerning the effects on Anti–PD-L1 mAb incubated at high and low pH (Figure 10 A), as expected it was detected an increased at Asn 1 level (6.60 % versus 1.60 % of untreated sample). Also, while oxidation levels were substantially unchanged, size variants % were found moderately increased. On the other side, the acidic incubation did not provoke any significant impact in terms of post translational modifications, while an increase of size variants was detected according to the other stress applied (Figure 10 B). Despite these slight structurally changes, it was not highlighted significant effects on the mAb biological activity expressed as the ability to block PD-L1/PD-1 interaction (Figure 14 B-C). Both samples were also analyzed via Biacore technology in terms of binding affinity to the PD-L1, where a slight decrease of K_D % was observed. Similar results were also obtained following both forced oxidative and light stresses. Indeed, the moderate increase of Asn 1 deamidation %, were not sufficiently enriched to such an extent to significantly affect the potency, while the affinity for PD-L1 resulted

slightly decreased. This result is aligned with other stress conditions that have shown similar degradation profiles in terms of size variants.

Like observed with low and high pH stress, incubation under oxidative conditions and light exposure provided quite similar results in terms of modifications occurring on CDRs and size variants %. While the critical asparagine and methionine residues were basically unmuted, it was reported a noticeable increase of dimeric species and fragmentation following both treatments (Figure 11 A-B), particularly relevant following the light stress.

Considered all these evidences, it can be concluded that all the stress performed on the Anti–PD-L1 mAb did not significantly affect its biological activity in binding the PD-L1. However, as already mentioned above, some of the modifications and species generated under forcing conditions, caused the production of several secondary species like aggregates and fragments whose made difficult to selectively address the results specifically to a single structural attribute (63). Indeed, the slight loss of affinity for PD-L1, characterized by an increased dissociation rate of the Anti–PD-L1 mAb/PD-L1 complex, may be essentially due to the presence of the aforementioned species. As general rule, the presence of process derived size variants can affect in a negative way some of biological functions. In the frame of this work, a dedicated investigation concerning these species has been carried out and described in Figure 21. HMWs and LMWs species, showed a consistent decreased activity when tested by blockade bioassay, meaning that Anti–PD-L1 mAb activity was impaired by the formation of these degraded products. Neverthless, a 10 % of these forms caused only a slight decrease of biological activity, while a significative biological effect is clearly detectable around 20-25 % (Figure 21). Considering these assumptions and experimental evidences, the next step has been to evaluate how do oxidation and deamidation events alone, without the presence of secondary degraded products, affect Anti–PD-L1 ability to bind PD-L1. At this aim, in order to evaluate the impact of deamidation, it was conducted an in-depth analysis on a site-specific Anti–PD-L1 mAb mutant, characterized by an asparagine/aspartic acid substitution in a specific region of antibody's CDRs. The starting hypothesis was that this modification would potentially change the potency and binding affinity of antibody to PD-L1. Results shown in Figure 20 C, demonstrated that any of antibody's biological functions had been modified following the stress, although the structural stability profile resulted slightly different to the reference material (Figure 20 B). The effect of oxidation was also assessed in a similar way. First of all, a preliminary structural analysis of the molecule was carried out in order to figure out whether any methionine residues were exposed to the external environment and located in regions critical for epitope recognition (Figure 19 A). Indeed, methionine oxidation occurring in the

CDRs could potentially lead to a reduced binding to the target antigen and therefore lower biological activity (64). The analysis revealed that a total of 3 residues were present on the antibody CDRs. However, two of these were only partially exposed to the external environment, while a third was located in the inner part of the molecule. In order to confirm these evidences from an experimental point of view, it was also considered the data obtained during a previous study where an alternative cell-based assay had been used. The oxidized samples tested in that case, were generated by applying milder stress conditions (if compared to the present oxidation study), resulting in the production of a very small amount of size variants (data not shown). The analysis of the dose-response curves (Figure 19 B) showed that the biological behavior of the sample submitted to a forced oxidation, was fully comparable to that of reference material as well as its biological activity expressed in terms of EC_{50}.

In addition to above results, the impact of forced degradation study on the Fc-mediated biological functions has been also assessed. Among the post translational modifications occurring, Asn 3-4 and Met 3-4 were closely monitored as they are located in critical Fc region in proximity of FcγRIIIa and FcRn binding sites. For what concern the treatment at +50°C prolonged for 2 and 4 weeks, deamidation % on Asn 3 was found significantly increased after 2 weeks (30.6 %) and 4 weeks (52.2 %) of exposure. Since asparagine deamidation occurring in that region is known being critical for the binding to FcγIIIa and ADCC activity (51), stressed samples were tested for these biological functions. On the other side, only met 3 residue has experienced a change in terms of oxidation, while met 4 was substantially unmuted. As both are located in a region close to the FcRn binding site, they could potentially influence antibody PK profile. Finally, as already mentioned, antibody aggregation and fragmentation increased proportionally to the exposure time. As expected from high deamidation levels of asn 3, Anti–PD-L1 binding affinity towards the FcγIIIa was significantly reduced over the weeks, while the ADCC activity notably impaired (Figure 18). Regarding the latter indeed, it was not possible to determine a reliable potency result, as the dose-response curves of reference material and heat-stressed samples showed clear differences in terms of biological behavior. Furthermore, as already observed for other antibody functions, the effect of large aggregates, dimeric forms and fragments on biological activity cannot be excluded and should be considered to draw conclusions. Finally, the effect on FcRn binding was controversial. In fact, while at 2 weeks it was quite clear a decreased affinity towards this receptor, after 4 weeks of exposure the binding strongly rose up (Figure 14 A). Regarding this latest result, it could be related to the types of aggregates generated following thermal stress more than other modifications occurred to the sample, whose can affect in a conversely way the binding to the receptor (54). These species

indeed, are generally associated to a reduction of biological functions as demonstrated in a dedicated study on isolated HMWs and LMWs (Figure 21). Neverhtless, in certain circumstances, the generation of these forms can also challenge the analytical methods developed whose are surely able to detect changes in biological activity, but under particular conditions cannot provide exhaustive information for interpreting such differences. In this regards, it is well documented in literature that an avidity phenomenon may occur as a consequence of the presence of large aggregates in the sample (54). These species indeed, does not allow to make the classical consideration regarding the relationship between a single attribute and a given function. Such structural changes generate a kind of new species characterized by a "scrambled" high order structure profiles and new exposed "functional epitopes". While in most cases the loss of activity is expected and experimentally observed, in others the exposure of such regions make the antibody able to bind with a certain grade of affinity the target. As already mentioned, the nature of this binding depends on an avidity phenomenon more than an increased affinity towards the specific epitope. These formations are not fully predictable, but may change as a consequence of the stress conditions applied, protein concentration and presence of other substances preserving the sample stability. (55), (65).

In the second part of this thesis, the effect of several glycosylation patterns has been extensively characterized from a functional point of view. Specifically, being the ADCC part of Anti–PD-L1 mechnaism of action, the role of a-fucosylated complex type and high mannose type species at determined % were investigated by dedicated structure-activity relationship studies. Furthermore, as the presence of sugars in the manufacturing feed, drug's formulation and *in vivo* circulation, induces antibody glycation, the effect of this condition on the main Anti–PD-L1 mAb functions was also addressed. The investigation concerning the role of other events occurring on Fc N-linked oligosaccharides such as high sialylation and galactosylation, were instead not included in this study and will be address in future works.

The impact of core-fucose residues on N-linked oligosaccharides of CH_2 region has a central role in regulating the antibody mediated ADCC activity (66), (67), (68), (69), (70), (71). The enhancement of this function is attributed to improved affinity of non fucosylated IgGs for FcγRIIIa expressed on natural killer cells. As described by Ferrara and colleagues (72), the complex structure between fucosylated Fc and FcγRIIIa causes weakening of contacts as compared to a-fucosylated Fc, which explains the decreased affinity for the receptor. On the other side, the interaction with others Fcγ receptors remains substantially unaffected (73) while PK is known in most cases being not significantly affected by removal of fucose (74). Concerning high mannose species, these at certain concentrations may impact several fc-

mediated antibody functions, and among them, the ADCC activity. As seen in the case of a-fucosylation, the magnitude of this effect on the ADCC mechanism depends on the abundance of such forms beyond their types. On the other hand, glycation events occurring on known Anti–PD-L1 mAb lysine residues of both Fc and Fab portions were not expected to affect potency and PK, while a potential effect in terms of immunogenicity should be considered (75), (76).

In the current study, two Anti–PD-L1 mAb samples, characterized by a 90% of a-fucosylated complex type and 35% of high mannosylated species were generated by adding 2F-Peracetyl-Fucose and maduramycin ammonium in production medium. This procedure was followed in order to primarily increase the amount of such species, while maintaining quite unmuted other glycosylation patterns typical of a production batch. Furthermore, a glycated sample was also obtained by incubation in a glucose solution, for the evaluation of glycation events on mAb functionality. Following the treatments, these glycovariants have been analyzed by several techniques. As expected from previous knowledge in literature and preliminary data already available, SPR analysis confirmed the identical antigen-binding affinity to the PD-L1 of all samples tested, irrespective of oligosaccharide groups (Figure 22 C) and the same result was also obtained in terms of binding affinity to the FcRn (Figure 22 D). On the other hand, the FcγRIIIa binding activity of each sample estimated by SPR measurement, revealed that glycation did not affect this binding while it was found strongly enhanced by both a-fucosylation and high mannosylation treatments (Figure 22 E).

Once established that Anti–PD-L1 mAb binding to FcγRIIIa and ADCC activity were considerably affected by elevated levels of a-fucoysated complex type and high mannosyalted species, a more thorough investigation was conducted in order to determine at which levels these two glycosylation variants were able to induce such effect. For this purpose, by spiking the two variants into an Anti–PD-L1 mAb control batch, two mixtures at different % of a-fucosylated complex type and high mannosylated Anti–PD-L1 mAb forms were prepared and tested by reporter gene assay and SPR technology (Figure 23 A). Firstly, a qualitative analysis of ADCC activity and binding affinity to FcγRIIIa was carried out by comparing dose-response curves and sensorgrams of samples with that of reference material. Both were used to make useful assumptions as for as antibody biological behavior and Fc-FcγRIIIa complex affinity. Indeed, a p-value lower than 0.05 from F-test demonstrated that the dose-response curves of both samples were comparable to the reference material up to 15% of complex a-fucosylation and 35% of high mannosylation (Figure 23 A). After such levels, the differences highlighted were basically due to the maximal responses (top values) provided by highly glycosylated

variants compared to reference material (Figure 23 A). The same variants were then analyzed by SPR, in terms of binding affinity to FcγIIIa receptor (Figure 25 A-B). The qualitative analysis of the same variants were rather in line with that performed by reporter gene assay, showing comparable profiles up to 10 % and 20 % of a-fucosylated complex type and high mannose species (Figure 25 A-B).

Afterwards, results of these experiments were also analyzed from a quantitative point of view and then used to define a relationship between these biological activities and the levels of variants tested. It was clearly demonstrated a strong correlation of high mannose and a-fucosylated complex type species with potency and K_D % values (Figure 26 A). Then, in addition to previous findings, relative potency % and relative K_D % values were calculated, resulting statistically different from control sample at 10 % of total a-fucosylation complex and 15 % of total mannosylation (Figure 26 B). Considering the results of both analyses, it was concluded that the presence of up to 6 % of a-fucosylated complex type and 10 % of high mannose Anti–PD-L1 forms were enough to maintain the Anti–PD-L1 mAb binding affinity to the FcγRIIIa receptor and its ability to trigger ADCC activity. Beyond the determination of a potential high functional threshold, at which the ADCC activity should be maintained to ensure a certain grade of safety, a lower limit was also investigated. While during the first investigation it was possible to assess that at 4 % of high mannose species the biological activity was maintained, for a-fucosylation the establishment of a theoretical lower threshold limit was not immediate. The interest in exploring these lower ranges is related to the fact that low levels of a-fucosylated complex type species may potentially increase the risk of having an impaired therapeutic efficacy (62). Considered the criticality of this attribute, in this study were analyzed levels of a-fucosylation complex type forms down to the 4 % already tested in the previous experiment, in order to verify whether the biological activity was maintained. For this purpose, new mixtures were generated starting from the 15% of a-fucosylated complex species going down to the 3.3% (control batch). Furthermore, from linear regression analysis it was also possible to predict a theoretical EC_{50} value simulating the testing of a sample containing the 2% of a-fucosyalted complex type species. These samples were analyzed by reporter gene assay for their ADCC activity. As explained in the results section (Figure 27), to accomplish this task a modification of assay layout was needed and the use of EC_{50} instead of potency values were the only data available to draw conclusions.

From the analysis of dose-response curves, these resulted comparable with that of reference material from 3.3 % up to 10 %. However, as already seen in the previous spiking

study, the mixtures containing the 12 % and 15 % of a-fucosylated species showed statistically different top values respect to the dose-response curve of reference material. However, the use of EC_{50} values for this experiment made possible a quantitative other than qualitative analysis of data generated. In this case it was demonstrated that Anti–PD-L1 mAb characterized by the presence of 3.3 % of a-fucosylated complex type species, showed an ADCC activity comparable to the control batch and reference material. Furthermore, it was also assumed that at 2 % of complex a-fucosylation, the biological activity was not significantly altered by the reduction of these forms. However, this last finding represents just a theoretical result not experimentally tested but extrapolated with a reliable statistical model starting from a set of actual data. On the other side, the *in vitro* effect of such a level of a-fucosylated complex type forms is not fully predictable and would require the testing of a real sample to be confirmed.

In conclusion, the purpose of this work was the extended characterization of a new therapeutic Anti–PD-L1 mAb applying a tailored analytical strategy based on a series of structure-activity relationship studies. During the characterization task a huge amount of information was gained concerning the several major degradation pathways affecting molecule stability and as a consequence, its functionality. Most of these products, on the basis of a CQAs assessment, were considered being critical attributes affecting Anti–PD-L1 mAb biological activities, PK, immunogenicity and safety, and must be kept under control by a well-defined analytical strategy. A CQAs assessment workflow indeed, should be associated to a tailored and extended analytical monitoring of the selected attributes. Concerning the biological activity and efficacy, the testing carried out via a single method may not always provide all the relevant information for the in-depth characterization of a complex biological entity. This is the reason why here is emphasized how relevant could be the development of a holistic approach for an in-depth characterization of a drug candidate. The application of a well-defined analytical panel together with the use of orthogonal platforms, allow to bridge possible gap of information that may occur during the testing of heterogenous samples or in case of complex structural modifications, which can be difficult to interpret. In this regards, well designed structure-activity studies result very supportive during a thorough characterization task. Indeed, besides adding further pieces of information to the “knowledge package”, the typical spiking of an antibody variant specifically produced for a given attributes such as aggregates, fragments or a-fucosylated species, allow to make a direct correlation between the levels of such structural elements and biological functions. Moreover, in some cases, it is also possible to define a threshold value at which a specific structural modification of the molecule significantly affects

its biological activity. This approach leads to the prompt identification of critical attributes affecting molecule functionality and stability beyond improving drug product knowledge and it is recommended from different guidelines. The proposal to apply such a strategy since the early stages of drug development, leads to the identification of critical characteristics concerning the steps of a manufacturing process, materials or the molecule itself, allowing to the set-up of an appropriate control strategy, which translates into an ethical as well as economic impact.

5 Material and methods

The content of this chapter may be changed following an internal revision by Merck KGaA committee. The sharing of some information reported might be not disclosed despite the Industrial PhD agreement signed among Merck Serono S.p.A., Rome, Italy; an affiliate of Merck KGaA, Darmstadt, Germany and the University of Palermo.

Forced degradation study

Anti–PD-L1 mAb samples undergone to a series of stressing procedures aimed at forcing the generation of degraded products and exploring its main degradation pathways. The conditions applied are briefly described:

- High temperature at 50°C for 2-4-6 weeks
- Light stress, at 765 W/m^2 for 24 hours
- Treatment with Ammonium Bicarbonate 1.2M, pH 9.2 at room temperature for 1 week
- Treatment with hydrogen peroxide 0.1 % for 1 hour at room temperature

The pH stressed samples were buffer exchanged in Anti–PD-L1 mAb DS buffer, in order to minimize the matrix effect and allow the comparability with reference material.

Production and purification of Anti–PD-L1 mAb native HMW and LMW species

The Anti–PD-L1 mAb intermediate bulk (post capture material) was loaded on a chromatography column packed with CHT (Ceramic Hydroxyapatite). The elution was performed in 2 phases: in the elution 1 it was eluted the intact Anti–PD-L1 mAb form, while in the elution 2 the fraction of interest, which is called “Strip” and mainly contains a mixture of HMWs and LMWs. The strip was treated on a SEC-LC and the eluate was fractionated based on the chromatograms in HMWs, intact forms and LMWs. Fractions were concentrated on Amicon® Ultra centrifugal filters.

Generation of Anti–PD-L1 mAb glycosylation variants

For the generation of glycosylated forms, an anti–PD-L1 mAb representative production batch was chosen. High levels of a-fucosylation and high mannosylation were reached by adding Maduramycin ammonium and of 2F-Peracetyl-Fucose (a Fucosyltransferase Inhibitor) in production medium, while high glycation was obtained by incubating the antibody with Glucose 1M.

Cell Binding Assay (CBA)

In this method, the Fab biological activity was measured as the ability to bind the target PD-L1 specifically expressed on a HEK-293 (hPD-L1) cell line. Different concentrations of Anti–PD-L1 mAb were coated onto a Protein A coated 96well flat-white plate, through the binding of antibody Fc portion, for 30 minutes at room temperature under swirling. Then HEK-293 (hPD-L1) were added to the Anti–PD-L1 mAb coated plate and allowed to bind to the Anti-PDL1 mAb for 1 hour at 37°C 5%, CO2. The unbounded cells were then washed out, while the bounded cells incubated with the ATPlite 1 step reagent (an ATP monitor system). The final read-out is a luminescence emission expressed as counts per second (cps), detected by the Infinite pro 200 (Tecan). Cps were then plotted against the Log transformed Anti–PD-L1 mAb concentrations and elaborated using Magellano (by Tecan) or alternatively GraphPad prism software, applying the 4 Parameter Logistic (4PL) algorithm (Log10-transformed concentrations). For each data set, the concentration of Anti–PD-L1 able to bind PD-L1 at 50% of the maximum capacity (EC50) was calculated. The biological activity of a sample (Potency) was expressed as % of activity with respect to the reference material and calculated as follows:

$$Potency\ \% = \frac{EC50\ of\ reference\ material}{EC50\ of\ tested\ sample}\ x\ 100$$

The Potency was released as average of results coming from three independent assays.

Blockade Bioassay (BB)

The PD-1/PD-L1 Blockade Bioassay is a method able to monitor the Anti–PD-L1 mAb biological activity by measuring its ability to inhibit the PD-1/PD-L1 interaction expressed on two genetically engineered cell lines. Anti–PD-L1 aAPC/CHO-k1 were plated in 96well flat-

white plate and incubated at 37°C, 5% CO2 overnight. Next day, dose-response curves of reference material and Anti–PD-L1 mAb were diluted in assay medium and added onto the plate containing the CHO-k1 cells together with PD-1 Jurkat T effector. The plate was incubated at 37°C, 5% CO_2 for 6 hours. Luminescence emission derived from luciferase expression due to TCR activation was measured by adding Bio-Glo reagent to each well of the plate. The luminescence is proportional to the ability of Anti–PD-L1 mAb to block the PD-1/PD-L1 interaction. The signal expressed as cps were detected by Infinite pro 200 (by Tecan) and then plotted against the Log transformed Anti–PD-L1 mAb concentrations. Data were elaborated using Magellano (by Tecan) applying the 4 Parameter Logistic (4PL) algorithm (Log10-transformed concentrations). For each data set, the concentration of Anti–PD-L1 mAb able to induce luciferase expression at 50% of the maximum response (EC_{50}) was calculated. The biological activity of a sample (Potency) was expressed as % of activity with respect to the reference material and calculated as follows:

$$Potency\ \% = \frac{EC50\ of\ reference\ material}{EC50\ of\ tested\ sample}\ x\ 100$$

The Potency was released as average of results coming from three independent assays.

Reporter Gene Assay (RGA)

The ADCC Reporter gene assay allows to evaluate the ability of Anti-PDL-1 mAb to induce ADCC. The system exploits Hek-293 (hPD-L1) as target cells and engineered Jurkat effector cells stably expressing the FcγRIIIa receptor (V158, high affinity variant). In the latter model, a NFAT (nuclear factor of activated T-cells) response element driving expression of firefly luciferase is also expressed. The activation of gene transcription through the NFAT pathway in these effector cells provides an alternative readout at an earlier point in the ADCC MoA pathway. The ADCC activity therefore is quantified through the luciferase produced as a result of NFAT pathway activation. Hek-293 (hPD-L1) cells, Anti-PDL-1 mAb diluted in assay medium and 150,000 cells/well Jurkat cells, were prepared and then loaded in a 96 well flat-white plate. After 24 hours of incubation, 120 µL/well of the BioGlo Reagent was added to the plate. The plate was gently shaken and then the emitted luminescence read with a Luminescence counter (Infinite 200 pro, Tecan). The signal expressed as cps were then plotted against the Log transformed Anti–PD-L1 mAb concentrations. Data were elaborated using Magellano (by

Tecan), applying the 4 Parameter Logistic (4PL) algorithm (Log10-transformed concentrations). For each data set, the concentration of Anti–PD-L1 mAb able to induce an ADCC activity on the HEK-293 (PD-L1) cells at 50% of the maximum response (EC_{50}) was calculated. The biological activity of a sample (Potency) was expressed as % of activity with respect to the reference material and calculated as follows:

$$Potency\ \% = \frac{EC50\ of\ reference\ material}{EC50\ of\ tested\ sample}\ x\ 100$$

The Potency is released as average of results coming from three independent assays.

Surface Plasmon Resonance phenomenon and Biacore technology

Surface Plasmon Resonance (SPR) is a physical phenomenon which is usually exploited by several platforms for the analysis of protein-protein interactions. Biacore, is a SPR-based technology used to study the interaction between a ligand attached onto surface of a sensor chip and a ligand injected in solution through the flow cell. The sensor chip is composed by a glass slide coated with a thin layer of gold on which a matrix of carboxymethylated dextran is covalently attached. The gold is required for generation of the SPR response as at the interface between media of different refractive index the SPR phenomenon occurs. As the analyte binds to ligand and accumulates on the surface, the refractive index increases. This change is measured in real time and expressed as resonance units (RU) plotted versus time. These parameters are graphically represented as a *sensorgram*.

Interactions between the analyte and the ligand in SPR are observed in real time and provide various information about ***I)*** Kinetic: how fast the interaction is in both association and dissociation profile ***II)*** Affinity: how strong the interaction is.

Qualitative analysis of biacore data:

A sensorgram (SPR raw data) is a plot of response (Relative Unit, RU) against time, showing the progress of the interaction during both association and dissociation phases.

Schematic illustration of a typical sensorgram

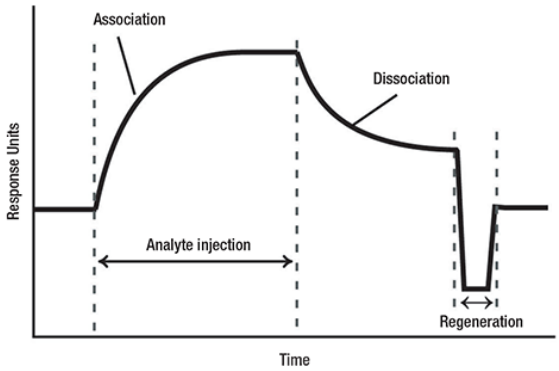

The BiaEvaluation software allows to obtain the overlay of sensorgrams generated by samples run in the same analytical session in order to provide a qualitative assessment in terms of interaction behavior in both association and dissociation phases. In order to focus on the biological behavior of the analyzed samples, the capture level (when foresees in the assay layout) and the regeneration phases are excluded and sensorgrams are reported normalized versus:

- the capture level: whereas the method foreseen a ligand capturing approach
- the baseline: whereas the method foreseen the direct immobilization of the ligand on the sensor chip
- the highest sample binding point in order to highlight, as for method purpose, the sample biological behavior in association and dissociation phase.

The qualitative assessment of the interaction profile via sensorgram overlay is carried out evaluating the shape of sensorgram generated by the sample in comparison with the shape of sensorgrams generated by the reference material run twice (beginning and ending position of the analytical sample session) and, if present, other reference samples. Differences in interaction profile are detected as distance of the sample sensorgram line respect to the line representing reference sensorgrams. In the evaluation the variability observed between sensorgrams generated by the reference material (or reference sample) run multiple times is considered.

Binding affinity to FcRγIIIa V158 via SPR

The interaction in terms of binding affinity between Anti–PD-L1 mAb and the FcγRIIIa V158 was measured in real time via Biacore T200. A tetra His Antibody was diluted in acetate buffer pH 4.5 to a defined concentration. For each flow cell (measurement and reference flow cells) were dispensed 200µL of NHS; 200µL of EDC; 200µL of EA, 200µL of Tetra His Antibody and 50mM NaOH. The Tetra His antibody was immobilized running a standardized software method. Then, the capture molecule FcγRIIIa V158 was prepared by resuspending it in HBS-EP+ to a defined working concentration. An Anti–PD-L1 curve (analyte) was prepared in HBS-EP+ to obtain a concentration in a defined range. The his-tagged FcγRIIIa V158/F158 was captured via anti-histidine mAb to the measurement flow cell of the sensor chip CM5 series S. Anti–PD-L1 mAb was then flown over both reference and measurement flow cells and bound onto the FcγRIIIa V158 captured on the sensor chip. The binding affinity was evaluated applying a "Two State Reaction" fitting model. Data evaluation was performed with Biacore T200 Evaluation software. Results were released as average of two independent analytical runs. Indeed, each Biacore assay is made of two different analytical runs where, in each run, the reference material is tested at the beginning and at the end of the run. Data were expressed as absolute affinity KD (M) and, as supporting information, the relative affinity KD (%) was also calculated according to the following formula:

$$KD\ \% = \frac{Average\ reference\ material\ (Absolute\ KD, initial\ and\ final)}{Sample\ (Absolute\ KD)}\ x\ 100$$

Binding affinity to FcRn via SPR

A detailed description of the platform, type of analysis and results that can be obtained with this technology, are detailed in paragraph "*Binding affinity to FcRγIIIa V158 via SPR*". The interaction, in terms of binding affinity, between Anti–PD-L1 mAb and the FcRn was measured in real time via Surface Plasmon Resonance (SPR) by Biacore T200. A huFcRn was diluted in acetate buffer pH 5.5 to obtain a defined concentration. For each flow cell (measurement and reference flow cell) were dispensed in 4 different 7mm plastic vials 200µL of NHS, 200µL of EDC, 200µL of EA, 200µL of huFcRn. HuFcRn was directly immobilized via amine coupling chemistry onto the Sensor CM4 Serie S. AntiPDL-1 curve was prepared in sample dilution buffer in a defined range. Anti–PD-L1 mAb was then flown over both reference

and measurement flow cells and bound onto the FcRn captured on the sensor chip. The binding affinity was evaluated applying a "Two State Reaction" fitting model. Data evaluation was performed with Biacore T200 Evaluation software. Results were released as average of two independent analytical runs. Indeed, each Biacore assay is made of two different analytical runs where, in each run, the reference material is tested at the beginning and at the end of the run. Data were expressed as absolute affinity KD (M) and, as supporting information, the relative affinity KD (%) was also calculated according to the following formula:

$$KD\ \% = \frac{Average\ reference\ material\ (Absolute\ KD, initial\ and\ final)}{Sample\ (Absolute\ KD)}\ x\ 100$$

SEC-MALLS

Size exclusion chromatography coupled with Multi angle laser light scattering (MALLS), is a technique that determines the molecular weight and size of complex proteins or oligomers. In this work it was used to detect and determine the molar mass of aggregates generated as a consequence of the several forced stresses performed. The output signals from the different detectors were imported into Astra 7® software for data processing. HPLC (UV/VIS) data analysis was performed and Astra 7.1.3 was used for analyzing the MALLS data. The analysis was carried out according to an internal procedure

Reducing peptide mapping analysis by LC-MS

Reducing Peptide Mapping by LC-MS/MS of Anti–PD-L1 mAb samples was performed to monitor the relative distribution of post translational modifications (PTMs) of Anti–PD-L1 mAb samples. The analysis was carried out according to an internal procedure.

2-AB Glycan Mapping

The glycan mapping analysis is based on the enzymatic release of the N-glycan species from the polypeptide moiety using N-glycosidase F (PNGase F). The released glycans are labeled with a fluorescent marker 2-aminobenzamide (2-AB), and then separated and detected by chromatography coupled with a fluorescence detector. The analysis and data processing were carried out according to an internal procedure.

Non reducing capillary electrophoresis – Sodium dodecyl sulphate (NR/RE-CE-SDS)

The method was applied for the determination of purity of Anti–PD-L1 mAb samples. The instrument was a PA800, P/ACE MDQ and PA8000 plus (Beckman coulter) with a PDA detector. Samples were incubated under reducing conditions with 2-mercaptoethanol, acetate buffer and SDS (4%). An electropherogram obtained under non-reducing analysis generally show a series of peaks corresponding to the following species: Internal reference at 10 kDa, Light chain (LC), Heavy chain (HC), 2 heavy chains (2HH), 2 heavy chains and a light chain (2H1L), non-glycosylated monomer (NG), monomer (IgG). This analysis is performed for the determination of fragmentation level of the molecule and the result is expressed as the total % of the low molecular weight fragments (LMWs). Samples analyzed are in both cases analyzed respect to the Anti–PD-L1 mAb reference material. The analysis and data processing were carried out according to an internal procedure.

Thermal analysis by Nano DSF

Nano DSF is a technology used for detecting small changes in the fluorescence of tryptophan and tyrosine residues. Generally, tryptophan is in the hydrophobic core of proteins. When structural modifications occur, the conformational changes cause the exposure of this residue to the aqueous solvent, causing a modified fluorescence emission. In these analyses, the intrinsic tryptophan and tyrosine fluorescence were monitored at the emission wavelengths of 330 nm and 350 nm. The fluorescence ratio (F350/F330) was measured respect to the increment of temperature and it was monitored changes in fluorescence intensity as well as tryptophan specific shift of the maximum fluorescence emission. The thermal denaturation curve provides two different parameters: *I*) The inflection point (IP), represents the temperature at which 50% of the protein is denatured. It was determined by detecting the maximum of the first derivative of the fluorescence ratio (F350/F330 nm) and it gave an indication on the thermodynamic stability of the protein. *II*) The temperature of onset (T_{onset}). *e.g.* the temperature at which the protein starts to denature. It provided a further indication about the thermodynamic stability of the protein. In fact, at equal inflection points, the protein with lower Tonset shows the lower stability. The analysis was carried out with nano DSF Prometheus NT Plex supplied by Nano Temper Technologies. The experiment was performed according to an internal procedure.

Generation of the three-dimensional (3D) model of Asn deamidation mutant and its interaction network

The three-dimensional (3D) model carrying the site-specific Asn substitution, was generated starting from X-ray structure of Fab domain. The tool used was "Protein builder", available in Molecular Operating Environment (MOE) package v. 2019.01 (77). After a local energy minimization run, it led to a new Fab structure: variant 1 (Asn -> Asp). Then, the analysis of substituted Asn interaction network was investigated by computing the number and type of hydrogen bonds (H-bonds) between Asn/Asp and near residues according to the Baker-Hubbard criterion and considering only H-bonds occurring with a frequency equal or major of 10 % of the simulated time (structural data not shown).

SAR statistical analysis of A-fucosylated and high mannose species

EC_{50}, relative potencies % and relative KD % data were plotted and fitted to a linear regression model using Minitab 19 software, MS excel or GraphPad prism depending on the specific experiment. EC_{50} and relative potencies were analyzed as average of three analytical runs while Biacore data as average of two analytical runs. Error bars indicate corresponding standard deviations or CV % depending on the specific analysis. A one-way analysis of variance (ANOVA) was also performed on relative potency % and KD % data.

6 References

1. *The PD1:PD-L1/2 Pathway from Discovery to Clinical Implementation.* Kankana Bardhan, Theodora Anagnostou and Vassiliki A. Boussiotis. 7, s.l. : Frontiers in Immunology, 2016, Vol. 12.

2. *Immune Checkpoint Inhibitors: Basics and Challenges.* Bin Li, Ho Lam Chan, Pingping Chen. 17, s.l. : Current Medicinal Chemistry, 2019, Vol. 26.

3. ICH. ICH Q8 (R2) Pharmaceutical development. [Online] 01 05 2006. [22 06 2017.] https://www.ema.europa.eu/en/documents/scientific-guideline/international-conference-harmonisation-technical-requirements-registration-pharmaceuticals-human-use_en-11.pdf.

4. *Fcγ Receptors: Old Friends and New Family Members.* Falk Nimmerjahn, Jeffrey V. Ravetch. 1, s.l. : Immunity, 2006, Vol. 24.

5. *Pharmacokinetics of monoclonal antibodies and Fc-fusion proteins.* Liu, Liming. 1, s.l. : Protein & Cell, 2018, Vol. 9.

6. *Cell culture processes for monoclonal antibody production.* Feng Li, Natarajan Vijayasankaran, Amy Yijuan Shen, Robert Kiss, Ashraf Amanullah. 5, s.l. : MAbs, 2010, Vol. 2.

7. J. Posner P, Barrington T, Brier A, Datta-Mannan. Monoclonal Antibodies: Past, Present and Future. *Handbook of Experimental Pharmacology.* 2019, Vol. 260, p. 81-141.

8. *Antibody drug conjugates: lessons from 20 years of clinical experience.* W.Tolcher. 12, s.l. : Elsevier, 2016, Annals of Oncology, Vol. 27, p. 2168-2172.

9. *Therapeutic monoclonal antibodies.* Breedveld, FC. 9205, 2000, Lancet, Vol. 355, p. 735-740.

10. *IgG subclass profiles in normal human sera of antibodies specific to five kinds of microbial antigens.* Astrid Hjelholt, Gunna Christiansen, Uffe S. Sørensen, Svend Birkelund. 3, s.l. : Pathogens and Disease, 2013, Vol. 67. 206–213.

11. *IgG subclasses and allotypes: from structure to effector functions.* Gestur Vidarsson, Gillian Dekker and Theo Rispens. 2014, Frontiers in Immunology, Vol. 5.

12. *Increased aggregation propensity of IgG2 subclass over IgG1: role of conformational changes and covalent character in isolated aggregates.* Heather Franey, Stephen R Brych, Carl G Kolvenbach, Rahul S Rajan. 9, s.l. : Protein Science, 2010, Vol. 19. 1601-15.

13. *Human anti-mouse antibodies.* Klee, G G. 6, s.l. : Archives of Pathology & Laboratory Medicine, 2000, Vol. 124. 921-3.

14. *Molecular engineering of antibodies for therapeutic and diagnostic purposes.* Frédéric Ducancel, Bruno H Muller. 4, 2012, MAbs, Vol. 4, p. 445–457.

15. *Antibodies to watch in 2019.* Hélène Kaplon, Janice M Reichert. 2, 2019, Vol. 11. 219-238.

16. The Antibody Society. In: Approved antibodies. *https://www.antibodysociety.org/tag/approved-antibodies/.* [Online] Antibody society, 2019. [06 01 2020.] https://www.antibodysociety.org/tag/approved-antibodies/.

17. P.Riggs. *Brenner's Encyclopedia of Genetics (Second Edition).* s.l. : Elsevier, 2013, p. 134-135.

18. *Nanobodies: Chemical Functionalization Strategies and Intracellular Applications.* Dominik Schumacher, Jonas Helma, Anselm F L Schneider, Heinrich Leonhardt, Christian P R Hackenberger. 57, s.l. : Wiley, 2018, Angewandte Chemie (International Ed. in English), Vol. 9, p. 2314–2333.

19. *Bi- and Tri-Specific T Cell Engager-Armed Oncolytic Viruses: Next-Generation Cancer Immunotherapy.* Zong Sheng Guo, Michael T Lotze, Zhi Zhu, Walter J Storkus, Xiao-Tong Song. 7, 2020, Biomedicines, Vol. 8, p. 204.

20. *FcγRs Modulate the Anti-tumor Activity of Antibodies Targeting the PD-1/PD-L1 Axis.* Rony Dahan, Emanuela Sega, John Engelhardt, Mark Selby, Alan J Korman, Jeffrey V Ravetch. 3, 2015, Cancer Cell, Vol. 28, p. 285-295.

21. *A novel method for determining antibody-dependent cellular phagocytosis.* Kamen L, Myneni S, Langsdorf C, Kho E, Ordonia B, Thakurta T, Zheng K, Song A, Chung S. 2019, Journal of Immunological Methods, Vol. 468, p. 55-60.

22. Jantine E Bakema, Marjolein van Egmond. Fc Receptor-Dependent Mechanisms of Monoclonal Antibody Therapy of Cancer. *Fc Receptors.* s.l. : Springer, 2014, p. 373-392.

23. Bice Perussia, Matthew J. Loza. Assays for Antibody-Dependent Cell-Mediated Cytotoxicity (ADCC) and Reverse ADCC (Redirected Cytotoxicity) in Human Natural Killer Cells. Kerry S. Campbell Marco Colonna. *Natural Killer Cell Protocols - Cellular and Molecular Methods.* s.l. : Humana press, 2000.

24. *Regulation of antibody-mediated complement-dependent cytotoxicity by modulating the intrinsic affinity and binding valency of IgG for target antigen.* Bo Wang, Chunning Yang, Xiaofang Jin, Qun Du, Herren Wu, William Dall'Acqua, Yariv Mazor. 1, 2020, mAbs, Vol. 12.

25. *The PD1:PD-L1/2 Pathway from Discovery to Clinical Implementation.* Bardhan, Kankana. 550, 2016, Frontiers in Immunology, Vol. 7.

26. FDA. Food and Drug Administration: Development & Approval Process (Drugs). [Online] FDA, 28 10 2019. [22 11 2020.] www.fda.gov/drugs/developmentapprovalprocess.

27. *Development of an in vitro activity assay as an alternative to the mouse bioassay for Clostridium botulinum neurotoxin type A.* Reuven Rasooly, Paula M Do. 14, 2008, Applied and Environmental Microbiology, Vol. 74, p. 09-13.

28. *Best practices in bioassay development to support registration of biopharmaceuticals.* John R White, Marla Abodeely, Sammina Ahmed, Gaël Debauve, Evan Johnson, Debra M Meyer, Ned M Mozier, Matthias Naumer, Alessandra Pepe, Isam Qahwash, Edward Rocnik, Jeffrey G Smith, Elaine Se Stokes, Jeffrey J Talbot, Pin Ye. 3, 2019, Biotechniques, Vol. 67, p. 126-137.

29. *Quality by Design: Development of the Quality Target Product Profile (QTPP) for Semisolid Topical Products.* Namjoshi S, Dabbaghi M, Roberts MS, Grice JE, Mohammed Y. 3, 2020, Pharmaceutics, Vol. 12, p. 287.

30. development, ICH guideline Q8 (R2) on pharmaceutical. Q8 (R2) Step 5 Pharmaceutical Development. [Online] ICH, 22 06 2017. [25 11 2020.] https://www.ema.europa.eu/en/documents/scientific-guideline/international-conference-harmonisation-technical-requirements-registration-pharmaceuticals-human-use_en-11.pdf.

31. Development, Quality Guideline Q8(R2) Pharmaceutical. The International Conference on Harmonisation of Technical Requirements for Registration of Pharmaceuticasl in Human Use. 2009.

32. *A cross-industry forum on benchmarking critical quality attribute identification and linkage to process characterization studies.* Sarah Demmona, Swapnil Bhargavab, Doreen Ciolekc,

Jennifer Halleyd, Nomalie Jayab, Marisa K. Jouberte, Edward Koepff, Phillip Smithg, Melody Trexler-Schmidth, Philip Tsaib. 9-20, s.l. : Biologicals Elsevier, 2020, Vol. 67.

33. *The practice of structure activity relationships (SAR) in toxicology.* McKinney JD, Richard A, Waller C, Newman MC, Gerberick F. 1, 2000, Toxicological Sciences, Vol. 56, p. 8-17.

34. ICH Q5E Biotechnological/biological products subject to changes in their manufacturing process: comparability of biotechnological/biological products. [Online] ICH, 01 06 2005. [2020 11 23.] https://www.ema.europa.eu/en/documents/scientific-guideline/ich-q-5-e-comparability-biotechnological/biological-products-step-5_en.pdf.

35. *Impact of mAb Aggregation on Its Biological Activity: Rituximab as a Case Study.* Rohit Bansal, Rozaleen Dash, Anurag S Rathore. 9, s.l. : Journal of Pharmaceutical Sciences, 2020, Vol. 109. 2684-2698.

36. *Glycan engineering reveals interrelated effects of terminal galactose and core fucose on antibody-dependent cell-mediated cytotoxicity.* Qingchun Zhang, Marisa K Joubert, Alla Polozova, Ronandro De Guzman, Kamala Lakamsani, Francis Kinderman, Dong Xiang, Andrew Shami, Nahira Miscalichi, Gregory C Flynn, Scott Kuhns. 6, 2020, Vol. 36. 3045.

37. *Glycation of antibodies: Modification, methods and potential effects on biological functions.* Wei B, Berning K, Quan C, Zhang YT. 4, 2017, MAbs, Vol. 9, p. 586-594.

38. *Fc Glycan-Modulated Immunoglobulin G Effector Functions.* Lünemann, Isaak Quast & Jan D. s.l. : Journal of Clinical Immunology, 2015, Vol. 34.

39. *Surface Glycans of Candida albicans and Other Pathogenic Fungi: Physiological Roles, Clinical Uses, and Experimental Challenges.* Masuoka, James. 2, 2004, Clinical Microbiology Reviews, Vol. 17, p. 281–310.

40. *The challenge and promise of glycomics.* Richard D Cummings, J Michael Pierce. 21, s.l. : Chemistry & Biology, 2014, Vol. 16.

41. *Impact of Glycosylation on Effector Functions of Therapeutic IgG.* Teillaud, Riad Abès and Jean-Luc. 1, s.l. : Pharmaceuticals (Basel), 2010, Vol. 3.

42. *Effects of N-Glycosylation on the Structure, Function, and Stability of a Plant-Made Fc-Fusion Anthrax Decoy Protein.* Yongao Xiong, Kalimuthu Karuppanan, Austen Bernardi, Qiongyu Li, Vally Kommineni, Abhaya M. Dandekar, Carlito B. Lebrilla, Roland Faller, Karen A. McDonald, Somen Nandi. s.l. : Frontiers in Plant Science, 2019.

43. *Effects of N-Glycan Composition on Structure and Dynamics of IgG1 Fc and Their Implications for Antibody Engineering.* Hui Sun Lee, Wonpil Im. 1, s.l. : Scientific Reports - Nature, 2017, Vol. 7.

44. *Variable domain N-linked glycosylation and negative surface charge are key features of monoclonal ACPA: Implications for B-cell selection.* Katy A Lloyd, Johanna Steen, Khaled

Amara, Philip J Titcombe, Lena Israelsson, Susanna L Lundström, Diana Zhou, Roman A Zubarev, Evan Reed, Luca Piccoli, Cem Gabay, Antonio Lanzavecchia, Dominique Baeten , Karin Lundberg, Daniel L Mueller, Lars Klares. 6, s.l. : European Journal of Immunology, 2018, Vol. 48. 1030-1045.

45. *Influence of N-glycosylation on effector functions and thermal stability of glycoengineered IgG1 monoclonal antibody with homogeneous glycoforms.* Ryuta Wada, Makoto Matsui, and Nana Kawasaki. 2, s.l. : MAbs, 2019, Vol. 11. 350–372.

46. *Challenges of glycosylation analysis and control: an integrated approach to producing optimal and consistent therapeutic drugs.* Peiqing Zhang, Susanto Woen , Tianhua Wang, Brian Liau, Sophie Zhao, Chen Chen, Yuansheng Yang, Zhiwei Song, Mark R Wormald, Chuanfei Yu, Pauline M Rudd. 5, s.l. : Drug Discovery Today, 2016, Vol. 21. 740-65.

47. *Using bispecific antibodies in forced degradation studies to analyze the structure–function relationships of symmetrically and asymmetrically modified antibodies.* Adam R. Evans, Michael T. Capaldi, Geetha Goparaju, David Colter, Frank F. Shi, Sarah Auber, Lian-Chao Li, Jingjie Mo, Michael J. Lewis, Ping Hu,Pedro Alfonso & Promod Mehndiratta. 6, s.l. : MAbs, 2019, Vol. 11.

48. *Forced degradation of recombinant monoclonal antibodies: A practical guide.* Christine Nowak, Jason K Cheung, Shara M Dellatore, Amit Katiyar, Ram Bhat, Joanne Sun, Gomathinayagam Ponniah, Alyssa Neill, Bruce Mason, Alain Beck, Hongcheng Liu. 8, s.l. : MAbs, 2017, Vol. 9. 1217-1230.

49. *Identification and characterization of asparagine deamidation in the light chain CDR1 of a humanized IgG1 antibody.* Vlasak J, Bussat MC, Wang S, Wagner-Rousset E, Schaefer M, Klinguer-Hamour C, Kirchmeier M, Corvaïa N, Ionescu R, Beck A. 2, s.l. : Analytical Biochemistry, 2009, Vol. 392.

50. *Understanding the Impact of Methionine Oxidation on the Biological Functions of IgG1 Antibodies Using Hydrogen/Deuterium Exchange Mass Spectrometry.* Jingjie Mo, Qingrong Yan, Chi Kwong So, Tam Soden, Michael J. Lewis and Ping Hu. 19, s.l. : Analytical Chemistry, 2016, Vol. 88.

51. *Characterization of IgG1 Fc Deamidation at Asparagine 325 and its impact on Antibody-dependent Cell-mediated Cytotoxicity and FcγRIIIa binding.* Xiaojun Lu, Lee Ann Machiesky , Niluka De Mel, Qun Du, Weichen Xu, Michael Washabaugh, Xu-Rong Jiang, Jihong Wang. 1, 2020, Scientific Reports - Nature Research, Vol. 10, p. 383.

52. *Best practices in bioassay development to support registration of biopharmaceuticals.* John R White, Marla Abodeely, Sammina Ahmed, Gaël Debauve, Evan Johnson, Debra M Meyer, Ned M Mozier, Matthias Naumer, Alessandra Pepe, Isam Qahwash, Edward Rocnik, Jeffrey G Smith, Elaine SE Stokes, Jeffrey J Talbot & Pin Yee Wong. 3, s.l. : Biotechniques, 2019, Vol. 67.

53. *EC50 estimation of antioxidant activity in DPPHradical dot assay using several statistical programs.* Zheng Chen, Riccardo Bertin, Guglielmina Froldi. 1, 2003, Food Chemistry, Vol. 1, p. 414-420.

54. *Effect of protein aggregates on characterization of FcRn binding of Fc-fusion therapeutics.* Adriana Bajardi-Taccioli, Andrew Blum, Chongfeng Xu, Zoran Sosic, Svetlana Bergelson, Marina Feschenko. 2, 2015, Molecular Immunology, Vol. 67, p. 616-624.

55. *Therapeutic protein aggregation: mechanisms, design, and control.* Roberts, Christopher J. 7, 2014, Trends in Biotechnology, Vol. 32, p. 372-8.

56. *A novel approach to investigate the effect of methionine oxidation on pharmacokinetic properties of therapeutic antibodies.* Jan Stracke, Thomas Emrich, Petra Rueger, Tilman Schlothauer, Lothar Kling, Alexander Knaupp, Hubert Hertenberger, Andreas Wolfert, Christian Spick, Wilma Lau, Georg Drabner, Ulrike Reiff, Hans Koll, Apollon Papadimitriou. 5, 2014, mAbs, Vol. 6, p. 1229–1242.

57. *Formation of multimeric antibodies for self-delivery of active monomers.* Yaron Dekel, Yossy Machluf, Tal Gefen, Gennady Eidelshtein, Alexander Kotlyar, Yaron Bram, Ehud Shahar, Farah Reslane, Elina Aizenshtein, Jacob Pitcovski. 1, 2017, Drug Delivery, Vol. 24, p. 199-208.

58. *Defucosylated anti-CCR4 monoclonal antibody (KW-0761) for relapsed adult T-cell leukemia-lymphoma: a multicenter phase II study.* Takashi Ishida 1, Tatsuro Joh, Naokuni Uike, Kazuhito Yamamoto, Atae Utsunomiya, Shinichiro Yoshida, Yoshio Saburi, Toshihiro Miyamoto, Shigeki Takemoto, Hitoshi Suzushima, Kunihiro Tsukasaki, Kisato Nosaka, Hiroshi Fujiwara, Kenji Ishitsuka, Hiroshi Inag. 8, 2012, Journal of Clinical Oncology, Vol. 30, p. 837-42. 837-42.

59. *Rates and impact of human antibody glycation in vivo.* Andrew M Goetze, Y Diana Liu, Thomas Arroll, Lily Chu, Gregory C Flynn. 2, s.l. : Glycobiology, 2012, Vol. 22. 221-34.

60. *Glycation of antibodies: Modification, methods and potential effects on biological functions.* Wei, Bingchuan. 4, 2017, MAbs, Vol. 9, p. 586-594.

61. *Assessing Analytical and Functional Similarity of Proposed Amgen Biosimilar ABP 980 to Trastuzumab.* Katariina M Hutterer, Alla Polozova, Scott Kuhns, Helen J McBride, Xingxiang Cao, Jennifer Liu. 5, 2019, BioDrugs, Vol. 33, p. 321-333.

62. *High Throughput Isolation and Glycosylation Analysis of IgG–Variability and Heritability of the IgG Glycome in Three Isolated Human Populations.* Maja Pučić, Ana Knežević, Jana Vidič, Barbara Adamczyk, Mislav Novokmet, Ozren Polašek, Olga Gornik, Sandra Šupraha-Goreta, Mark R. Wormald, Irma Redžić, Harry Campbell, Alan Wright, Nicholas D. Hastie, James F. Wilson, Igor Rudan,. 10, 2011, Vol. 10.

63. *Structure and function of purified monoclonal antibody dimers induced by different stress conditions.* Rajsekhar Paul, Alexandra Graff-Meyer, Henning Stahlberg, Matthias E Lauer, Arne C Rufer, Hermann Beck, Alexandre Briguet, Volker Schnaible, Thomas Buckel, Sabine Boeckle. 8, s.l. : Pharmaceutical Research, 2012, Vol. 29.

64. *Oxidation in the complementarity-determining regions differentially influences the properties of therapeutic antibodies.* Tetyana Dashivets, Jan Stracke, Stefan Dengl, Alexander

Knaupp, Jan Pollmann, Johannes Buchner and Tilman Schlothauer. 8, s.l. : MAbs, 2016, Vol. 8. 1525–1535.

65. *Identification of IgG1 variants with increased affinity to FcγRIIIa and unaltered affinity to FcγRI and FcRn: Comparison of soluble receptor-based and cell-based binding assays.* Yanmei Lu, Jean-Michel Vernes, Nancy Chiang, Qinglin Ou, Jiabing Ding, Camellia Adams, Kyu Hong, Bao-Tran Truong, Domingos Ng, Amy Shen, Gerald Nakamura, Qian Gong, Leonard G Presta, Maureen Beresini, Bob Kelley, Henry Lowman, Wai Lee Wong, Y Gloria Men. 1-2, s.l. : Journal of immunological methods, 2010, Vol. 365. 132-41.

66. *Comparison of biological activity among nonfucosylated therapeutic IgG1 antibodies with three different N-linked Fc oligosaccharides: the high-mannose, hybrid, and complex types.* Yutaka Kanda, Tsuyoshi Yamada, Katsuhiro Mori, Akira Okazaki, Miho Inoue, Kazuko Kitajima-Miyama, Reiko Kuni-Kamochi, Ryosuke Nakano, Keiichi Yano, Shingo Kakita, Kenya Shitara, Mitsuo Satoh. 1, s.l. : Glycobiology, 2007, Vol. 17. 104-118.

67. *Lack of fucose on human IgG1 N-linked oligosaccharide improves binding to human FcγRIII and antibody-dependent cellular toxicity.* Shields RL, Lai J, Keck R, O'Connell LY, Hong K, Meng YG, Weikert SH, Presta LG. s.l. : Journal of Biological Chemistry, 2002, Vol. 277. 26733-26740.

68. *The absence of fucose but not the presence of galactose or bisecting N-acetylglucosamine of human IgG1 complex-type oligosaccharides shows the critical role of enhancing antibody-dependent cellular cytotoxicity.* Shinkawa T, Nakamura K, Yamane N, Shoji-Hosaka E, Kanda

Y, Sakurada M, Uchida K, Anazawa H, Satoh M, Yamasaki M, et al. s.l. : Journal of Biological Chemistry, 2003, Vol. 278. 3466-3473.

69. *Enhancement of the antibody-dependent cellular cytotoxicity of low-fucose IgG1 Is independent of FcgammaRIIIa functional polymorphism.* Rinpei Niwa, Shigeki Hatanaka, Emi Shoji-Hosaka, Mikiko Sakurada, Yukari Kobayashi, Aya Uehara, Haruhiko Yokoi, Kazuyasu Nakamura, Kenya Shitara. 10, s.l. : Clinical Cancer Research, 2004, Vol. 15. 6248-55.

70. *Fucose removal from complex-type oligosaccharide enhances the antibody-dependent cellular cytotoxicity of single-gene-encoded antibody comprising a single-chain antibody linked the antibody constant region.* Akito Natsume, Masako Wakitani, Naoko Yamane-Ohnuki, Emi Shoji-Hosaka, Rinpei Niwa, Kazuhisa Uchida, Mitsuo Satoh, Kenya Shitara. 1-2, s.l. : J Immunological Methods, 2005, Vol. 306. 93-103.

71. *Glycosylation of recombinant antibody therapeutics.* Jefferis, R. 2005, Vol. 21. 11-16.

72. *Unique carbohydrate-carbohydrate interactions are required for high affinity binding.* Claudia Ferrara, Sandra Grau, Christiane Jäger, Peter Sondermann, Peter Brünker, Inja Waldhauer, Michael Hennig, Armin Ruf, Arne Christian Rufer, Martine Stihle, Pablo Umaña, Jörg Benz. 31, s.l. : Sciences, Proceedings of the National Academy of Sciences, 2011, Vol. 108. 12669–12674.

73. *Glycoengineering of Therapeutic Antibodies Enhances Monocyte/Macrophage-Mediated Phagocytosis and Cytotoxicity.* Sylvia Herter, Martina C. Birk, Christian Klein, Christian

Gerdes, Pablo Umana, Marina Bacac. 5, s.l. : The journal of Immunology, 2014, Vol. 192. 2252–2260.

74. *Superior In vivo Efficacy of Afucosylated Trastuzumab in the Treatment of HER2-Amplified Breast Cancer.* Teemu T. Junttila, Kathryn Parsons, Christine Olsson, Yanmei Lu, Yan Xin, Julie Theriault, Lisa Crocker, Oliver Pabonan, Tomasz Baginski, Gloria Meng, Klara Totpal, Robert F. Kelley and Mark X. Sliwkowski. 11, s.l. : Cancer research, 2010, Vol. 70.

75. *Advanced glycation end-product (AGE)-damaged IgG and IgM autoantibodies to IgG-AGE in patients with early synovitis.* Marianna M Newkirk, Raphaela Goldbach-Mansky, Jennifer Lee, Joseph Hoxworth, Angie McCoy, Cheryl Yarboro, John Klippel, Hani S El-Gabalawy. 2, 2003, Vol. 5. 82-90.

76. *Immunological studies on glycated human IgG.* Saman Ahmad, Moinuddin, Asif Ali. 25-26, s.l. : Life sciences Elsevier, 2012, Vol. 90. 980-7.

77. ULC, Chemical Computing Group. [Online] Molecular Operating Environment (MOE); 1010 Sherbrooke St. West, Suite #910, Montreal, QC, Canada, H3A 2R7, 2019.